Lightning NO_x emissions and the impact on the effect of aircraft emissions - Results from the EU-Project TRADEOFF

V. Grewe*
DLR-Institut für Physik der Atmosphäre Oberpfaffenhofen, Germany

Keywords: Aircraft NO_x, Lightning, global modelling, ozone

ABSTRACT: The intercomparison of upper troposphere and lower stratosphere NO_x measured on board of commercial aircraft with results of the chemistry-climate model E39/C revealed an underestimation of summertime simulated NO_x concentrations. A further investigation of the causes within the EU-project TRADEOFF, using new satellite data, indicated a deficiency in the lightning parameterisation. A new parameterisation has been developed, which is based on the convective massflux. The effect of individual emissions on the NO_x and ozone concentration is shown. Tropical lightning emissions have the potential to enhance the mid-latitude NO_x concentration via transport through the lowermost stratosphere. This transport process enhances ozone at mid-latitudes to the same magnitude as mid-latitude lightning. Compared to the previous formulation of lightning the impact of air traffic is reduced when applying the new lightning parameterisation, although the absolute amount of emitted NO_x by lightning was not affected, but the horizontal and vertical location of the emitted NO_x. The contribution of air traffic to the NO_x budget in the northern upper troposphere is reduced from 30%-40% to 20%-30% and the contribution to ozone is reduced from 3%-4% to 2.5%.

1 INTRODUCTION

The impact of aircraft NO_x emissions on the chemical composition of the atmosphere was investigated on the basis of 6 chemistry transport and chemistry climate models for 1999 IPCC assessment report (IPCC, 1999). Besides that all models showed an ozone increase caused by air traffic, the pattern of the ozone change was quite different from one model to another. One aim of the EU project TRADEOFF was to better understand those differences and in case of an identification of deficiencies, to enhance the model's quality based on intercomparison with observational data. A comprehensive model-observation intercomparison had been performed by Brunner et al. (2003). Prior to that an intercomparison was performed between NO_x and ozone measurements on board a commercial aircraft (NOXAR-data) with the climate chemistry model E39/C (Grewe et al., 2000), which clearly indicated too low NO_x values in the mid-latitude summer tropopause region and a weak seasonal cycle. In principle, there are two processes leading to this deficiency: (1) Underestimated vertical transport of NO_x emitted at the surface or (2) underestimated lightning NO_x emissions. Although satellite data of the occurrence of convective systems are available, almost no data are available, which are suitable to validate vertical convective mass fluxes. On the other hand, new observational data are available to get more insights into the occurrence of lightning. One result was that mid-latitude lightning is underestimated in summer and that the seasonal cycle is too weak in that region, which gives reasons for the discrepancy of the mid-latitude upper troposphere NO_x budget. Based on those data an intercomparison was performed and a new lightning parameterisation was derived yielding much better agreements with observations (Grewe et al, 2001; Kurz and Grewe, 2002) than in the previous version. After a short description of the climate chemistry model E39/C, the lightning parameterisation and the NO_x emissions from lightning are introduced. Section 4 describes how tropical lightning contributes to the mid-latitude NO_x budget, which then alters the effect of aircraft NO_x emissions. How the new

* *Corresponding author:* Volker Grewe, DLR-Institut für Physik der Atmosphäre, Oberpfaffenhofen, D-82205 Wessling, Germany. Email: volker.grewe@dlr.de

lightning parameterisation, which does not change the total amount of emitted NO_x, alters the ozone increase caused by air traffic is given in section 6.

2 THE CLIMATE-CHEMISTRY MODEL E39/C

The coupled climate-chemistry model E39/C (**E**CHAM4, **39** levels up to 10 hPa, chemistry module **C**HEM, Hein et al., 2001) is based on the spectral general circulation model (GCM) ECHAM4 (Roeckner et al., 1996) with increased vertical resolution from 19 to 39 levels (Land, 1999), i.e., from around 2 km to 700 m at tropopause altitudes. The chemical module CHEM (Steil et al., 1998) has already been coupled to ECHAM3 and used in a variety of studies regarding tropospheric and stratospheric chemistry (Dameris et al., 1998; Grewe et al., 1999, 2001). It includes stratospheric heterogeneous and homogeneous ozone chemistry and tropospheric NO_x-CH_4-CO-HO_x-O_3-chemistry with 107 photochemical reactions and 37 species. An upper boundary condition for NO_y and ClO_y is applied to account for CFC and N_2O photolysis above 10 hPa.

Surface NO_x emissions (industry, traffic, soils, biomass burning) of 33.1 TgN per year, and aircraft NO_x emissions of 0.56 TgN per year are included in the E39/C model, respectively. The lightning parameterisations generate NO_x interactively with the convection scheme according to Grewe et al. (2001). Details are given below. Wash-out is calculated interactively with the cloud schemes.

The model has been validated with respect to a variety of species and processes (Hein et al., 2001, Grewe et al., 2001, Stenke and Grewe, 2003; Lauer et al., 2002, Shine et al., 2003).

3 LIGHTNING NOX EMISSION

The lightning parameterisation (Grewe et al., 2001) is based on a correlation between model's convective mass flux (Tiedke, 1989) and flash frequency. This correlation has been derived from an observed correlation between flash frequencies and convective cloud top heights (Price and Rind, 1992, PR92) and a correlation between the simulated cloud top heights and simulated convective mass fluxes, which then directly relate the simulated mass fluxes with flash frequencies. The correlation between flash frequencies and convective cloud top heights, derived by PR92 was only valid for continental thunderstorms. Ocean storms have similar cloud top heights but only less lightning and lower mass fluxes (DelGenio and Kovari, 2002). Since E39/C is able to simulate different mass fluxes for ocean and land conditions also the lightning intensity of ocean thunderstorms is significantly lower than over land, which makes an artificial differentiation between land and ocean lightning obsolete. Summertime continental mid-latitude lightning is much better represented in absolute amounts and patterns compared to the PR92 parameterisation based on OTD satellite data (Kurz and Grewe, 2002). Therefore a better representation of mid-latitude upper troposphere NO_x can be expected.

This parameterisation provides a horizontal distribution of lightning. Additionally a parameterisation for intra-cloud and cloud-to-ground separation depending on the „cold cloud area", which is the thickness of the cloud with temperatures below 0°C, is applied (Price and Rind, 1993). Intra-cloud flashes are assumed to be 10 times less energy efficient than cloud-to-ground flashes and therefore produce 10 times less NO_x. The NO_x emissions are then vertically distributed from the ground to the cloud top using C-shape profiles (Pickering et al., 1998). The resulting NO_x emission is shown in Figure 1. The centres of the lightning emissions are clearly separated from air traffic corridors. However, transport mixes those airmasses.

4 THE IMPACT OF TROPICAL LIGHTNING NOX EMISSIONS ON OZONE

The mixing of airmasses owning lightning characteristics with airmasses owning air traffic characteristics is manifold. At mid-latitudes upper troposphere airmasses will definitely be mixed with airmasses, which experienced lightning in the mid-latitudes. In contrast, lower stratosphere airmasses (where also aircraft fly) are much less effected by mid-latitude lightning, since vertical

mixing is less effective (Holton et al., 1995; Grewe and Dameris, 1996; Schoeberl and Morris, 2002; Grewe et al., 2002a). However, tropical lightning has the potential to emit NO_x at much higher altitudes. Those airmasses can be transported to mid-latitudes, which has been shown by aircraft measurements (Hoor et al., 2002), and contribute to the NO_y and NO_x budgets. E39/C model simulations suggest that this transport significantly contributes to the NO_x budget in the mid-latitude tropopause region. It also affects the ozone budget because ozone is produced in the tropical mid and upper troposphere and also on the way through the lowermost stratosphere. There, the simulated ozone production is small compared to the tropics, but the residence times of air masses are much larger than in the upper troposphere, which leads to a significant contribution of ozone produced in the lowermost stratosphere by lightning NO_x from tropical origin. E39/C simulations show that the lightning induced ozone increase at mid-latitudes in the tropopause region is caused by 50% by tropical lightning (Figure 2; Grewe et al., 2002a).
In July (Figure 3), this leads to a contribution of lightning to the ozone budget of 30% in the tropics and southern hemisphere and around 15% to 20% in the northern troposphere, where also other sources are of importance. Aircraft effects are mainly restricted to the northern hemisphere troposphere. Although, air traffic in the southern hemisphere also leads ozone changes there, and tropical air traffic can lead to ozone increase in the lowermost stratosphere similar to the transport-chemistry interaction discussed above. On the other hand air parcels emitted in the tropopause region of the northern hemisphere rarely have the chance to be transported to higher altitudes. Trajectory analysis of E39/C model data showed that air parcels from the tropopause region of the northern mid-latitudes only have the chance to be transported to the southern lowermost stratosphere by upward lifting in the tropical troposphere (Figure 4).

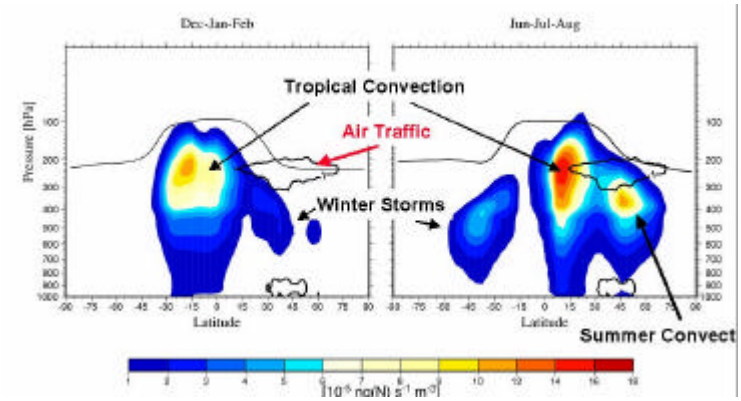

Figure 1. Zonal mean lightning NO_x emissions simulated with the chemistry-climate model E39/C [10^{-5} ng(N) s^{-1} m^{-3}]. The thin black line indicates the simulated tropopause and the heavy line the air traffic NO_x emissions [10^{-5} ng(N) s^{-1} m^{-3}]. Main centres of lightning emissions are marked.

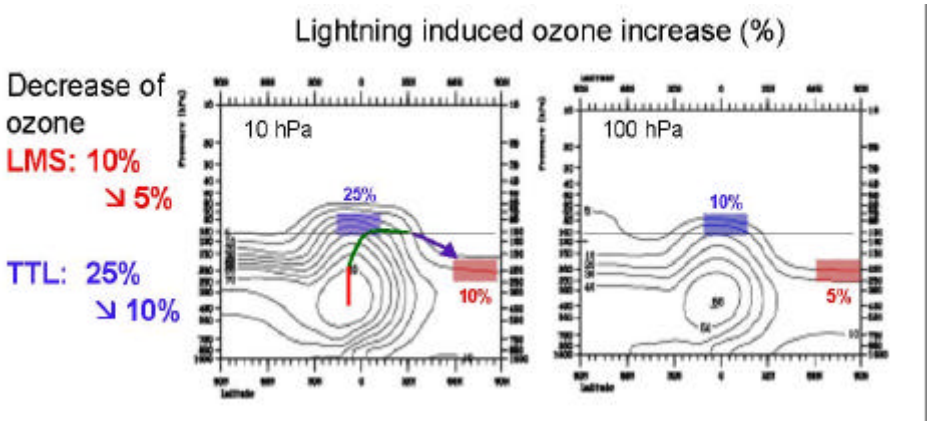

Figure 2. Annual mean ozone increase [%] caused by lightning NO_x emissions calculated with the E39/C climate-chemistry model using the standard version (left) and applying a NO_y upper boundary at 100 hPa (right). The horizontal line indicates the location of the lowered upper boundary. The isolines are 5%, 10%, 20%, 50%, 60%, 70%, and 80%. Areas are shaded for better intercomparison.

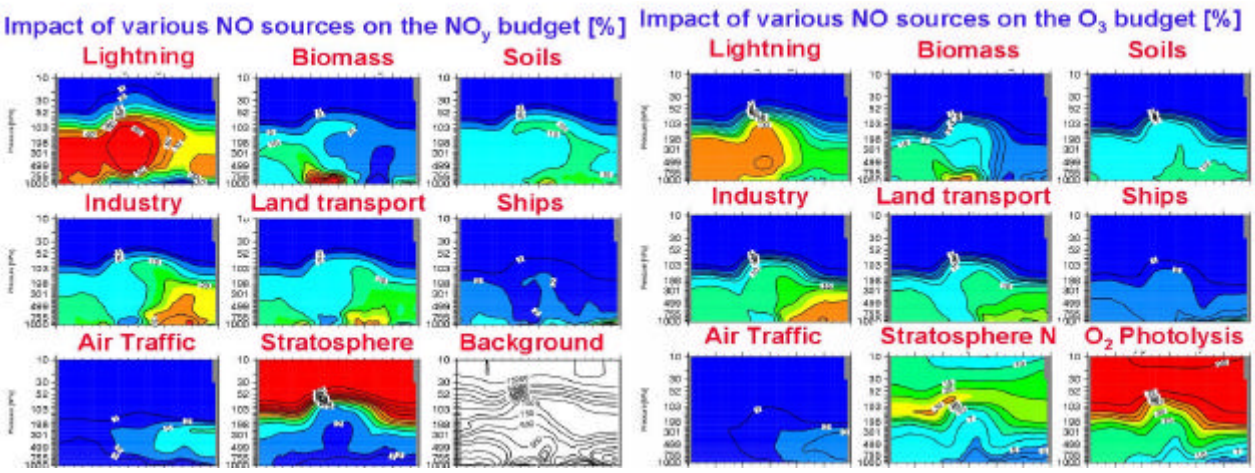

Figure 3. Impact of various NO_x sources to the NO_y (left) and ozone (right) budget [%] for an individual simulated July. Isolines are 1%, 2%, 5%, 10%, 20%, 30%, 40%, 50%, and 60% for Noy and 1%, 2%, 3%, 4%, 5%, 7%, 10%, 15%, 20%, 30%, 50%, 70%, 90% for ozone. Note: Here contributions are presented, whereas Figure 2 shows enhancements.

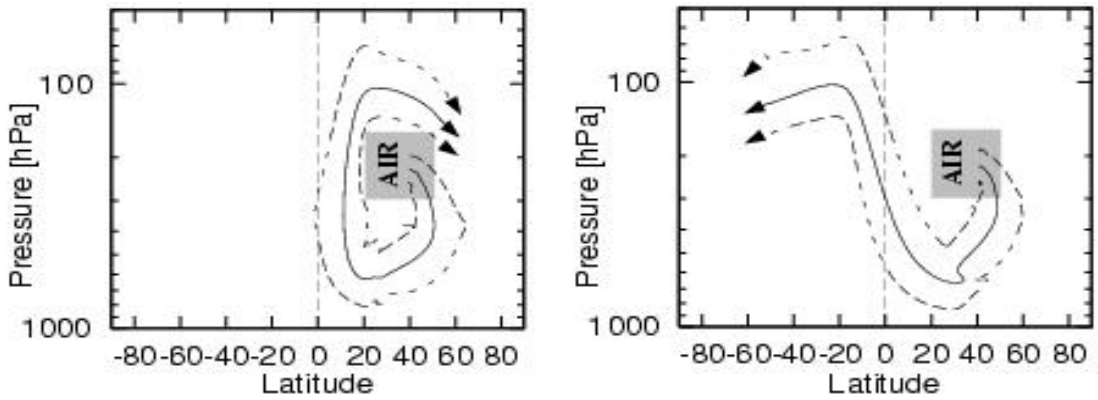

Figure 4. Pathways of air parcels from the upper troposphere (air traffic corridor) to the lower-most stratosphere.

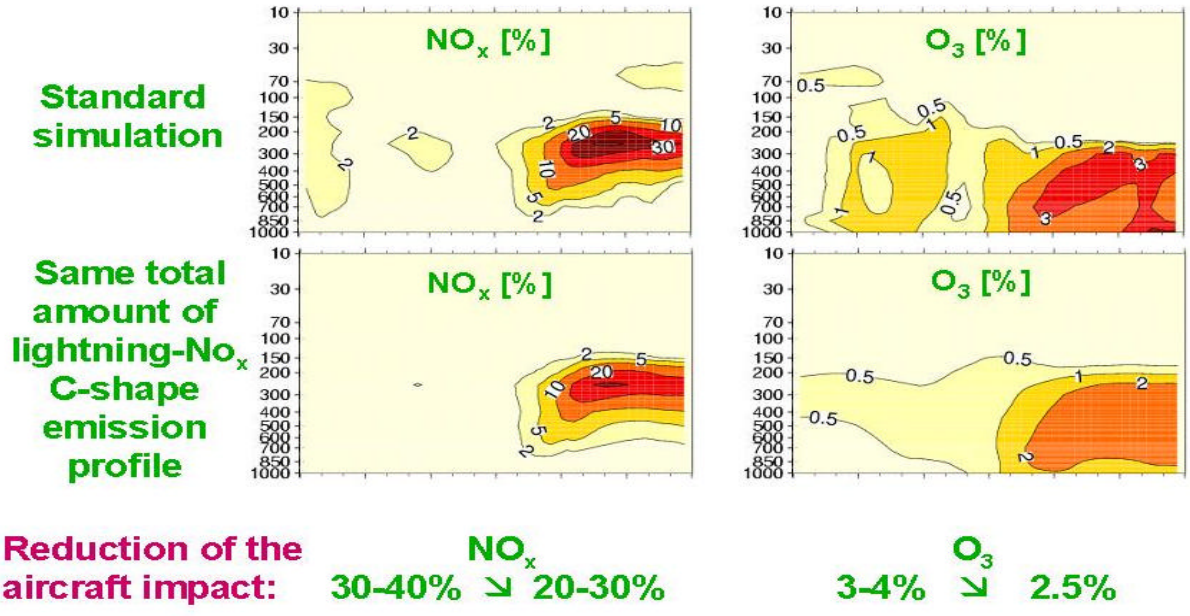

Figure 5. Annual mean contributions [%] of air traffic emissions to the atmospheric burden of NO_x (left) and ozone (right) in the standard E39/C simulation (top) and a simulation with a new lightning parameterisation (bottom).

5 THE IMPACT OF LIGHTNING NOX EMISSIONS ON THE EFFECT OF AIR TRAFFIC

The new lightning parameterisation leads to higher background NO_x concentrations in the upper troposphere especially in July (see discussion above). This affects the ozone production efficiency of a NO_x molecule emitted by an aeroplane, which is reduced from 3.5 to 2.6 10^8 kg per year in the main perturbation region (20°N to 70°N; 500 to 200 hPa) (Grewe et al., 2002b). It therefore reduces the impact of air traffic on ozone. Figure 5 shows these effects for NO_x and ozone in the case of the ‚old' lightning parameterisation and the ‚new' parameterisation. The NO_x enhancement cause by air traffic is reduced from 30% to 40% down to 20% to 30%. The ozone increase is reduced from 3%-4% to 2.5%.

6 CONCLUSIONS

The EU-project TRADEOFF aimed at a better understanding of the effect of aircraft NO_x emissions on the atmospheric composition. Based on the outcome of a comparison of upper troposphere and lower stratosphere measurements with the climate-chemistry model E39/C, the model's quality has been enhanced by developing a new lightning parameterisation (Grewe et al., 2001). The effect of lightning has been investigated. Tropical lightning has the potential to contribute significantly to the mid-latitude NO_x and ozone concentration at tropopause altitudes, by transport through the lowermost stratosphere (Grewe et al., 2002a), which has been also observed by aircraft measurements (Hoor et al., 2002).

Since the new lightning parameterisation enhances the UTLS NO_x concentration the effect of air traffic on the ozone production is reduced and also the contribution to the NO_x and ozone budget. Simulations with the coupled climate-chemistry model E39/C showed a reduction of the air traffic NO_x contribution from 30%-40% to 20%-30% and a reduction of the ozone contribution from 3%-4% to 2.5% (Grewe et al., 2002b).

The study clearly showed that upper troposphere and lower stratosphere data of chemical species are of outstanding importance for the evaluation of climate-chemistry models, if they provide seasonal climatologies and frequency distributions (see also Grewe et al., 2001), like data from the NOXAR and MOSAIC projects. Further, the study implied that lightning effects the ozone concentration globally, so that the knowledge of tropical storm systems and lightning is of importance also for the understanding of mid-latitude effects, like air traffic. EU-projects like TROCCINOX and HIBISCUS will help to reduce uncertainties linked to tropical lightning.

REFERENCES

Brunner, D., J. Staehelin, H.L. Rogers, M.O. Köhler, J.A. Pyle, D. Hauglustaine, L. Jourdain, T.K. Berntsen, M. Gauss, I.S.A. Isaksen. E. Meijer, P. van Velthoven, G. Pitari, E. Mancini, V. Grewe, and R. Sausen, 2003: An evaluation of the performance of chemistry transport models by comparison with research aircraft observations. Part 1: Concepts and overall model performance. *Atmos. Chem. Phys. Discuss. 3*, 2499-2545.

Dameris, M. , Grewe, V., Köhler, I., Sausen, R., Brühl, C., et al., 1998: Impact of Aircraft NOx-Emissions on Tropospheric and Stratospheric Ozone. Part II: 3-D Model Results.. *Atmos. Environ. 32*, 3185-3200,

Del Genio, A, and W Kovari, 2002: Climatic properties of tropical precipitating convection under varying environmental conditions, *J. Climate 15*, 2597-2615.

Grewe, V., Dameris, M., 1996: Calculating the Global Mass Exchange between Stratosphere and Troposphere.. *Ann. Geophys. 14*,. 431-442.

Grewe**,** V., M. Dameris, R. Hein, I. Köhler, and R. Sausen, 1999: Impact of future subsonic aircraft NO_x emissions on the atmospheric composition. *Geophys. Res. Lett. 26***,** 47–50.

Grewe, V., Grenfell, J.L., Shindell, D.T., Dameris, M., Hein, R., et al. 2000: Origin and Variability of Upper Tropospheric Nitrogen Oxides and Ozone at Northern Mit-Latitudes. Quadrennial Ozone Symposium 2000, Hokkaido University, Sapporo, Japan, 3-8 July 2000, 781-782.

Grewe, V., Brunner, D., Dameris, M. , Grenfell, J.L., Hein, R., et al. 2001: Origin and Variability of Upper Tropospheric Nitrogen Oxides and Ozone at Northern Mid-Latitudes. *Atmos. Environ. 35*, 3421-3433.

Grewe, V., Dameris, M., Fichter, C., Sausen, R. 2002a: Impact of Aircraft NOx Emissions. Part 1: Interactively Coupled Climate-ChemistrySimulations and Sensitivities to Climate-Chemistry Feedback, Lightning and Model Resolution. *Meteorol. Z. 11*, 177-186.

Grewe, V., Reithmeier, C., Shindell, D.T., 2002b: Dynamic-Chemical Coupling of the Upper Troposphere and Lower Stratosphere Region. *Chemosphere 47*, 851-861.

Hein, R., Dameris, M., Schnadt, C., Land, C., Grewe, V., et al. 2001: Results of an Interactively Coupled Atmospheric Chemistry-General Circulation Model: Comparison with Observations. *Ann. Geophys. 19*, 435-457.

Holton J.R., Haynes, P.H., McIntyre, M.E., Douglass, A.R., Rood, R.B., and Pfister, L., 1995. Stratosphere-troposphere exchange, *Reviews of Geophysics 33*, 403-439.

Hoor, P., Fischer, F., Lange, L., Lelieveld, J., Brunner, D., 2002. Seasonal variations of a mixing layer in the lowermost stratosphere as identified by the CO-O_3 correlation from in-situ measurements, *J. Geophys. Res.*, .107, DOI 10.1029/2000JD000289.

IPCC - Intergovernmental Panel on Climate Change, 1999. Aviation and the global atmosphere, eds. J.E. Penner, D.H. Lister, D.J. Griggs, D.J. Dokken, M. McFarland, Cambridge University Press, Cambridge, U.K.

Kurz, C., Grewe, V., 2002: Lightning and Thunderstorms, Part 1: Observational Data and Model Results. *Meteorol. Z. 11*, 379-393.

Land, C. (1999) Untersuchungen zum globalen Spurenstofftransport mit dem Atmosphärenmodell ECHAM4.L39(DLR), *Ph.D. Thesis*, Fakultät für Physik, Ludwig-Maximilians-Universität München, Germany.

Lauer, A., Dameris, M., Richter, A., Burrows, J.P. 2002: Tropospheric NO2 Columns: A Comparison between Model and Retrieved Data from GOME Measurements. *Atmos. Chem. Phys.* 2, 67-78,

Pickering, K.E., Yansen, W., Wei-Kuo, T., Price, C. Muller, J.-F. 1998: Vertical distributions of lightning NO_x for use in regional and global chemical transport models, *J. Geophys. Res. 103*, 31,203-31,216.

Price, C., Rind, D. 1992: A simple lightning parameterization for calculating global lightning distributions, *J. Geophys. Res. 97*, 9919-9933.

Price, C., Rind, D. 1993: What determines the cloud-to-ground lightning fraction in thunderstorms?, *Geophys.l Res. Lett. 20*, 463-466.

Roeckner, E., Arpe, K., Bengtsson, L., Christoph, M., Claussen, M., Dümenil, L., Esch, M., Giorgetta, M., Schlese, U., Schulzweida, U. 1996: The atmospheric general circulation model ECHAM4: Model description and simulation of present-day climate, *MPI-Report* 218, ISSN 0937-1060, Max-Planck-Institut für Meteorologie, Hamburg, Germany.

Schoeberl, M.R., Morris, G.A., 2000. A Lagrangian simulation of supersonic and subsonic aircraft exhaust emissions, *J. Geophys. Res. 105*, 11,833-11,839.

Shine, K.P., Bourqui, M.S., Forster, P.M. de, Hare, S.H.E., Langematz, U., et al.:2003 A Comparison of Model Simulated Trends in Stratospheric Temperatures. *Q. J. R. Met. Soc. 129*, 1565-1588.

Stenke, A., Grewe, V., 2003: Impact of Ozone Mini-Holes on the Heterogeneous Destruction of Stratospheric Ozone. *Chemosphere 50*, 177-190.

Steil, B., Dameris, M., Brühl, C., Crutzen, P.J., Grewe, V., et al. 1998: Development of a Chemistry Module for GCMs: First Results of a Multiannual Integration. *Annales Geophysicae 16*, 205-228.

Tiedke, M. 1989: A comprehensive mass flux scheme for cumulus parameterization in large-scale models. *Mon. Wea. Rev. 117*, 1779-1800.

Impact of Aircraft NOx Emissions: Effects of Changing the Flight Altitude

M. Gauss*, I. Isaksen
Department of Geophysics, University of Oslo, Norway

V. Grewe
Institute for Atmospheric Physics, DLR Oberpfaffenhofen, Wessling, Germany

M. Köhler
Centre for Atmospheric Science, University of Cambridge, United Kingdom

D. Hauglustaine
LSCE, CNRS-CEA, Gif-sur-Yvette, France

D. Lee
Manchester Metropolitan University, Manchester, United Kingdom

Keywords: model study, aircraft NOx emissions, impact on ozone, cruising altitude

ABSTRACT: Within the framework of the European TRADEOFF project, model studies have been performed to investigate the altitude dependence of the impact of NOx emissions from aircraft on the chemical composition of the atmosphere. Here we present results for present (year 2000) conditions from two chemical transport models and two coupled climate-chemistry models. We consider five different aircraft emissions scenarios, which were developed for TRADEOFF. Effects of changes in flight altitude and concomitant changes in fuel consumption are investigated separately.

1 INTRODUCTION

Aircraft are operated at or near the boundary between the troposphere and the stratosphere, i.e. two atmospheric regions with highly different physical and chemical characteristics. E.g. wash-out processes of water-soluble species such as HNO3 are common in the upper troposphere while they are negligible in the lower stratosphere. In the lower stratosphere, the high vertical stability allows pollutants to accumulate much more efficiently than in the troposphere. For these reasons lower emission heights of NOx will result in shorter residence times of aircraft NOx in the atmosphere. In addition, chemical processes controlling ozone depend on altitude. E.g. the importance of the ozone production cycle through oxidation of methane and other hydrocarbons decreases with height while ozone loss cycles involving NOx become more efficient.

Therefore, it has been suggested that a change in flight altitude can reduce the impact of aircraft emissions. In this study, which was performed for the EU FP5 project TRADEOFF, we have used four models to calculate the aircraft impact for three different cases: 1) a standard case assuming normal cruise altitudes, 2) aircraft cruising 2000 ft higher, and 3) aircraft cruising 6000 ft lower. Due to the altitude dependence of combustions and fuel and efficiency both an increase and a decrease in flight altitude will result in higher NOx emissions. By considering additional scenarios where the total NOx emission is normalized to the base case, we have separated the effect of changing cruise altitudes and concomitant increases in fuel consumption.

In sections 2 and 3 the models and emission scenarios used in this study are briefly described, while the results are presented in section 4.

* *Corresponding author:* Michael Gauss, University of Oslo, Department of Geosciences, PO 1022 Blindern, 0315 Oslo, Norway. Email: michael.gauss@geo.uio.no

2 THE MODELS AND EMISSION SCENARIOS USED IN THIS STUDY

Brief descriptions of the four models applied in this study (two chemistry transport models and two coupled climate chemistry models) are given in the following sections.

2.1 *The TOMCAT model (CTM)*

TOMCAT is a global chemistry transport model that integrates a tropospheric chemistry scheme on 31 hybrid pressure levels from the surface to 10 hPa. The chemistry scheme includes methane oxidation with additional reactions for ethane and propane degradation. The species are transported on a T21 horizontal grid (i.e. 5.6° by 5.6 °) using an advection scheme that conserves second-order moments (Prather, 1986). A description of the model has been given by Law et al. (2000).

2.2 *The UiO model (CTM)*

The Oslo CTM-2 (**UiO**) is a comprehensive chemistry transport model that includes non-methane hydrocarbon chemistry and stratospheric O_3 production/destruction chemistry. The model is operated on a T21 resolution over 40 vertical levels between the surface and 10 hPa. The meteorology is taken from ECMWF forecast data for 1997. Advection is based on the Prather (1986) Second Order Moments scheme, and photodissociation coefficients are calculated on-line once every hour. Chemistry in aircraft plumes is included following Kraabøl et al. (2002). A recent description has been given by Gauss et al. (2003).

2.3 *The DLR model (GCM)*

ECHAM.L39(**DLR**)/CHEM (Hein et al., 2001) is based upon the German community climate model, ECHAM 4 (Roeckner et al., 1996; Land et al., 1999). It is operated on a T30 resolution over 39 vertical levels. The stratospheric/tropospheric chemistry scheme includes 37 species, grouped into families, which are transported using a semi-Lagrangian advection scheme. The chemistry computations have been configured to feedback on the dynamics of the coupled atmosphere/ocean model. In addition, the ECHAM.L39 model has been used to calculate contrail coverage and radiative forcing/temperature responses as described by Ponater et al. (2002).

2.4 *The IPSL model (GCM)*

LMDz-INCA (**IPSL**) couples the LMDz GCM on-line to the chemistry and aerosol model INCA. The version of the GCM used for this study is based on prescribed SSTs and relaxed winds towards ECMWF (re)analysis. The model includes 45 tracers and is operated for chemical computations on a regular grid (3.75°longitude × 2.5° latitude) over 19 vertical levels. It incorporates tropospheric O_3 chemistry from CH_4, NO_x and CO represented by 100 chemical reactions. At present, the chemical scheme does not feed back onto the dynamical part (Hauglustaine et al., in preparation, 2003).

3 AIRCRAFT EMISSION SCENARIOS

Aircraft emission scenarios were provided on a basic 1º × 1º latitude/longitude grid with a vertical resolution of 2,000 feet (610 m), evenly spaced. Emission calculations were made with the FAST model based upon the ANCAT/EC2 movements database (i.e. for 1991/1992). Thus, as in ANCAT, the data were for months 1, 4, 7 and 10 (January, April, July, October). Scenario 1 is the standard scenario for the year 2000 with ‘normal’ cruise altitudes. Scenarios 3 and 5 are for reduced (-6 kft) and enhanced (+2 kft) cruising altitude, respectively. A summary of the aircraft emission scenarios used in this study is given in Table 1. In the ‘b’ scenarios, changes in fuel consumption were taken into account, while the ‘a’ scenarios are normalized, i.e. the total fuel consumption is the same as in scenario 1.

The meteorology for the year 1995 was used for TOMCAT, while UiO used the year 2000. For the GCM simulations, an appropriate 1990’s meteorology was used.

Table 1. Year 2000 aircraft emission scenarios used in this study.

Abbr.	Description	Fuel consumption	NO_x emission
0	no aircraft	-	-
1	Tradeoff standard case (standard flight altitudes)	151.9 Tg/year	0.59 Tg(N)/year
3a	Lower cruise altitude (-6000ft), normalized	151.9 Tg/year	0.59 Tg(N)/year
3b	Lower cruise altitude (-6000ft), enhanced	160.8 Tg/year	0.62 Tg(N)/year
5a	Higher cruise altitude (+2000ft), normalized	151.9 Tg/year	0.59 Tg(N)/year
5b	Higher cruise altitude (+2000ft), enhanced	151.2 Tg/year	0.60 Tg(N)/year

4 RESULTS

Figure 1 shows zonal-mean perturbations in the TRADEOFF base case scenario 1 with respect to the 'no aircraft' scenario. Both the TOMCAT and the UiO models calculate clear ozone enhancements due to aircraft in the upper troposphere and lower stratosphere in Northern mid- to high latitudes. The TOMCAT model has a higher peak perturbation at the North Pole. Also at other locations, especially in the tropical tropopause, perturbations are larger compared to the UiO simulation. Some of the difference can be explained by chemical processes in aircraft plumes in the UiO model, which have the effect of reducing the NOx impact (see Kraabøl et al. 2002).

Figures 2 to 5 show zonal-mean perturbations in July 2000 due to changes in flight altitude, i.e. with respect to the standard scenario 1. The models agree in regard to the spatial pattern of changes. However, the magnitudes differ. In the lower stratosphere, the UiO decrease in ozone change due to a reduction in flight altitude is largest while the corresponding DLR decrease is smallest. The tropospheric ozone increase is largest in the UiO and TOMCAT models, while it is smallest in the IPSL model. For an increase in flight altitude (case 5) the three participating models calculate an increase, with UiO yielding the largest increase, but spatially more confined than in the other models.

The maximum zonal-mean ozone perturbation with respect to the 'no aircraft' case is plotted for the UiO model in Figure 6 as a function of season. The perturbations as well as the differences in perturbations are largest in the summer season, mainly as a result of solar radiation.

The separate effect of changes in total NOx emissions resulting from a change in flight altitude is shown for the TOMCAT model in Figure 7. For the case of reduced flight altitude the increased total NOx output results in an upward shift of the level of zero-change (see Figure 3). In the case of enhanced flight altitude, about one third of the increase in the ozone perturbation at the high Northern latitude tropopause is due to the enhanced NOx output. In the UiO model (not shown) the importance of changes in total NOx output is less important.

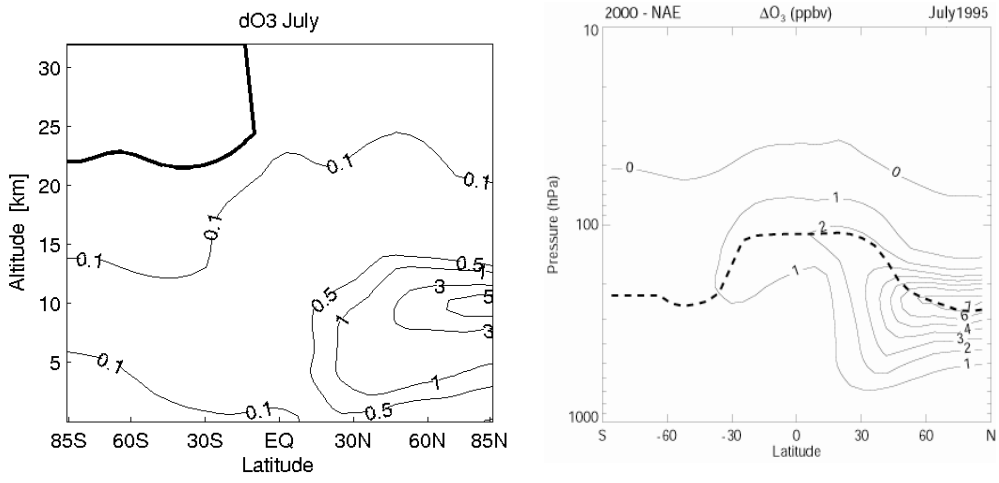

Figure 1: Zonal-mean ozone change due to aircraft in July 2000 (scenario 1 minus scenario 0) calculated by the UiO (left) and the TOMCAT (right) models. Unit: ppbv.

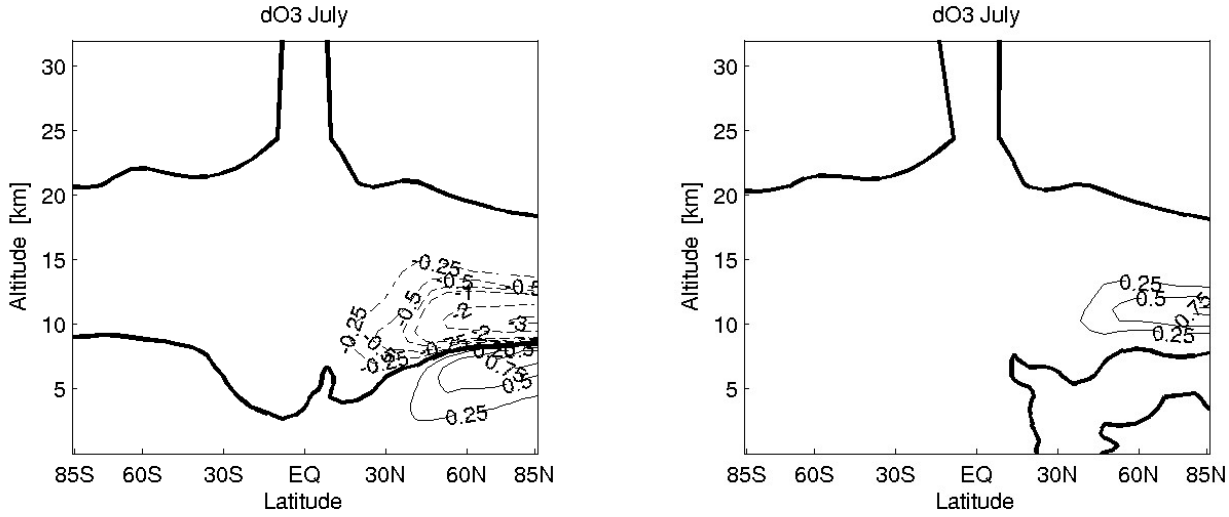

Figure 2: Effect of a change in cruise altitude on the aircraft-induced zonal-mean ozone perturbation in July 2000 calculated by the UiO model. Left panel: '3b minus 1', i.e. the effect of reducing the flight altitude. Right panel: '5b minus 1', i.e. the effect of increasing the flight altitude. Unit: ppbv.

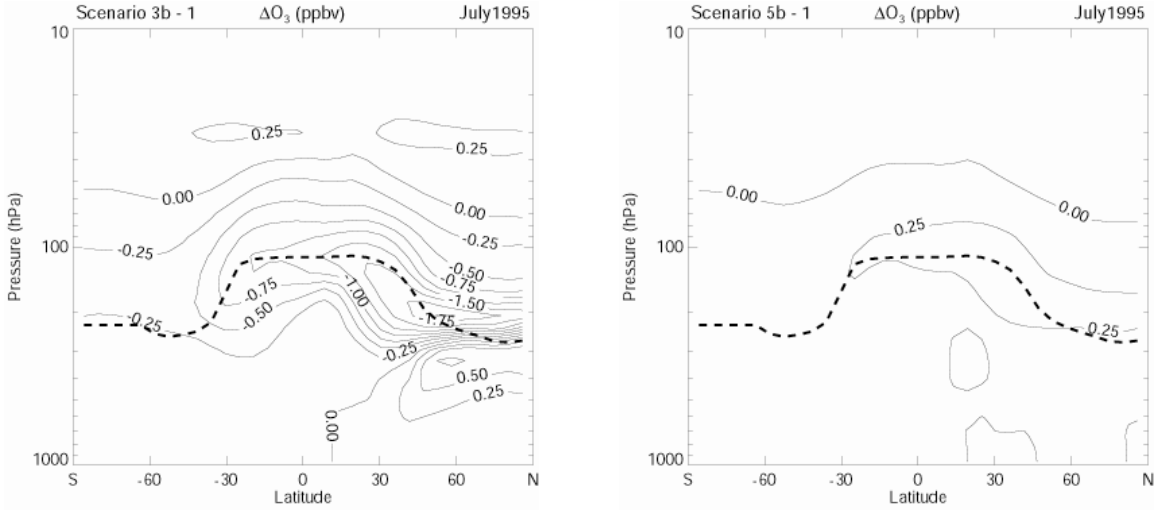

Figure 3: As Figure 2, but with results from the TOMCAT model. Left: '3b minus 1', right: '5b minus 1'.

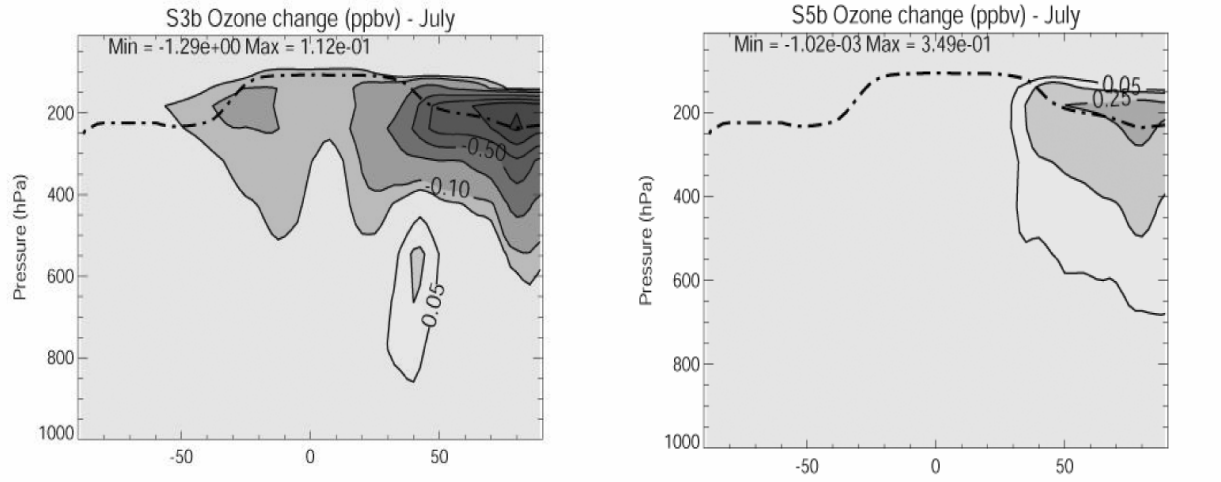

Figure 4: As Figure 2, but with results from the IPSL model. Left: '3b minus 1', right: '5b minus 1'.

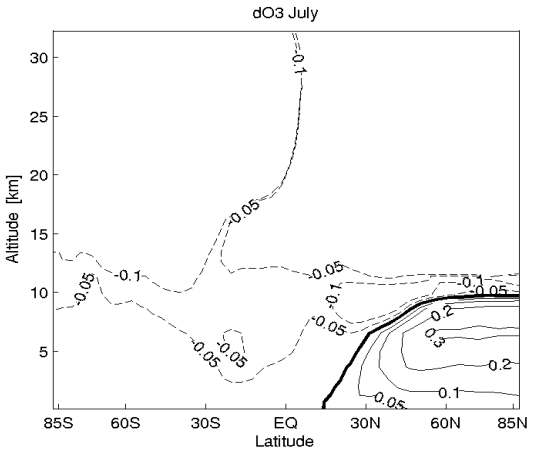

Figure 5 (left panel): '3b minus 1', i.e. the effect of lowering the flight altitude, calculated by the DLR model. Unit: ppbv. The Figure has to be compared with the left panels of Figures 2, 3, and 4. (The DLR model did not participate in the case 5 study.)

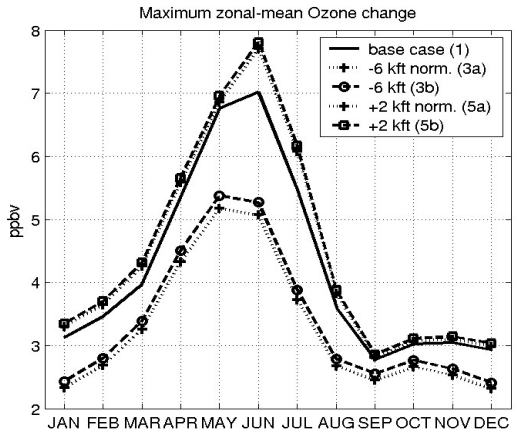

Figure 6 (right panel): Maximum zonal-mean ozone perturbation as a function of season, calculated by the UiO model for the different TRADEOFF scenarios considered in this study.

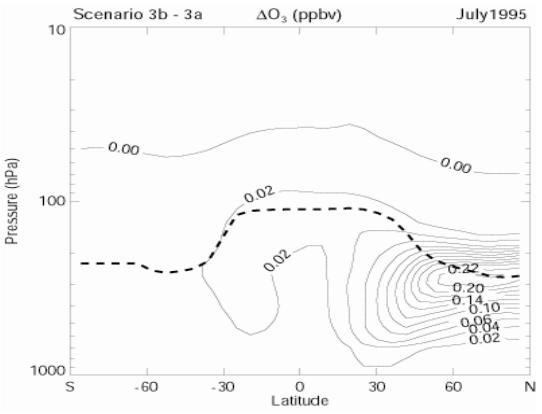

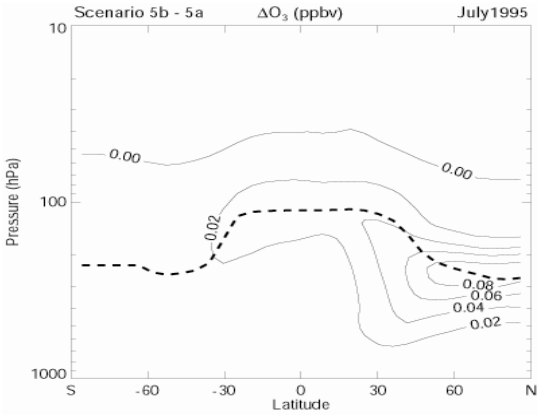

Figure 7: Effect of fuel consumption and increased NOx output due to a change in flight altitude, calculated by the TOMCAT model. Left: '3b minus 3a', right: '5b minus 5a'. Unit: ppbv.

Finally, Figure 8 shows the impact on the tropospheric and stratospheric ozone columns. The impact is strongly dependent on season. In case 3b there is a high degree of cancellation between the positive tropospheric change and the negative stratospheric change. However, the negative change dominates in most times of the year, especially at low latitudes, due to the weakening of the positive tropospheric change by wash-out processes. The contrary is true for case 5 where a positive change in the total ozone column is modelled at nearly all locations throughout the year, except for winter at high Northern latitudes.

5 CONCLUSIONS

This model study has investigated the impact of changes in flight altitude on aircraft-induced changes in ozone and has found the modifications in the ozone impact to be strongly dependent on height and season. A reduction in flight altitude is likely to result in a reduction of the aircraft-induced total ozone column increase in most times of the year.

It has to be stressed, however, that only changes in ozone were investigated. Other issues such as the impact on cirrus cloud formation are beyond the scope of this paper but will be addressed in

other publications of the TRADEOFF project. Also, radiative forcing calculations are being made based on the calculated perturbations in ozone and will be published in the near future.

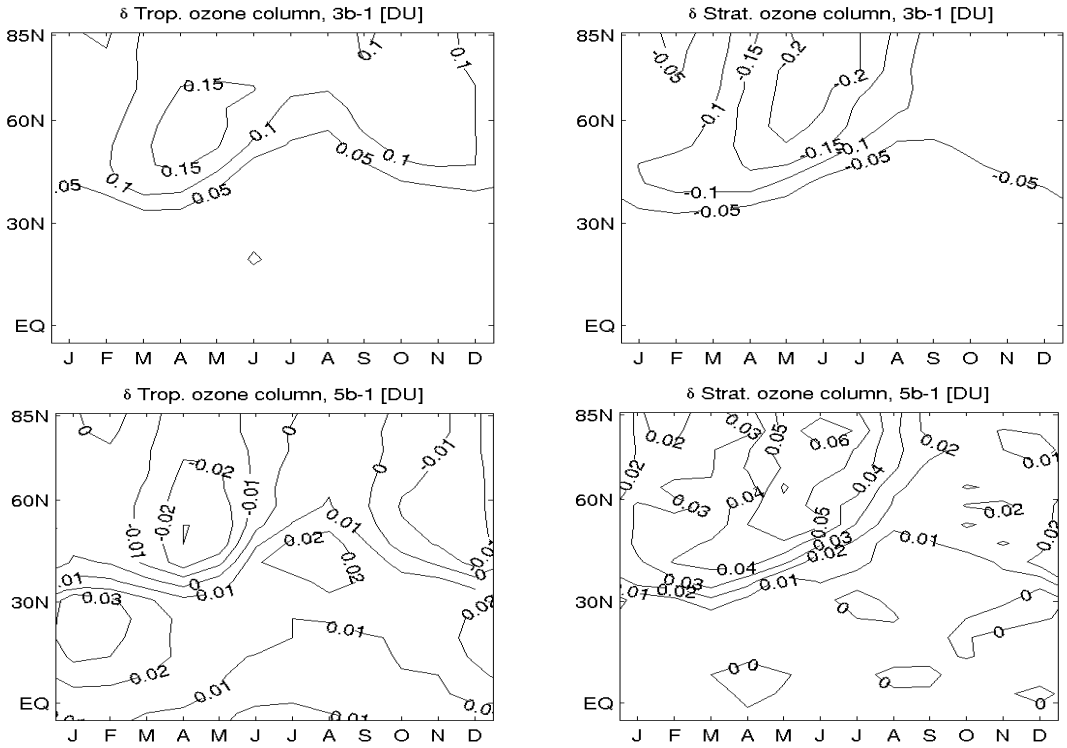

Figure 8: Ozone column change due to changes in flight altitude, calculated by the UiO model.

REFERENCES

Gauss, M., I. S. A. Isaksen, S. Wong, and W.-C. Wang, 2003: Impact of H_2O emissions from cryoplanes and kerosene aircraft on the atmosphere, *J. Geophys. Res.*, 108(0), XXXX, doi:10.1029/2002JD002623.

Hauglustaine, D., F. Hourdin, L. Jourdain, M.-A. Filiberti, S. Walters, J.-F. Lamarque, 2003: Interactive chemistry in the Laboratoire de Météorologie Dynamique General Circulation Model : description and background tropospheric chemistry evaluation, in preparation.

Hein R., M. Dameris, C. Schnadt, C. Land, V. Grewe, I. Köhler, M. Ponater, R. Sausen, B. Steil, J. Landgraf, C. Brühl, 2001: Results of an interactively coupled atmospheric chemistry – general circulation model: Comparison with observations, *Annales Geophysicae* 19, 435-457.

Kraabøl A.G., F. Stordal. T. Berntsen, and J.Sundet. 2002: Impacts of NOx emissions from subsonic aircraft in a global 3-D CTM including plume processes. *J. Geophys. Res*., 10.1029/2001JD001019.

Land, C., M. Ponater, R. Sausen, E. Roeckner, 1999: The ECHAM4.L39(DLR) atmosphere GCM, Technical description and climatology, DLR-Forschungsbericht 1991-31, 45 pp., ISSN 1434-8454, Deutsches Zentrum für Luft- und Raumfahrt, Köln, Germany.

Law et al. 2000: Comparison between global chemistry transport model results and measurements of ozone and water vapor by airbus in-service aircraft (MOZAIC) data. *J. Geophys. Res.* 105(D1), 1503-1525.

Ponater, M., S. Marquart, and R. Sausen, 2002: Contrails in a comprehensive global climate model: parameterisation and radiative forcing results, *J. Geophys. Res.*, 107 (D13), 4164, doi:10.1029/2001JD000429.

Prather M. J., 1986: Numerical advection by conservation of second-order moments. *J. Geophys. Res.* 91, 6671–6681.

Roeckner, E., K. Arpe, L. Bengtsson, M. Christoph, M. Claussen, L. Dümenil, M. Esch, M. Giorgetta, U. Schlese, U. Schulzweida, 1996: The atmospheric general circulation model ECHAM4: Model description and simulation of present-day climate, MPI-Report 218, ISSN 0937-1060, Max-Planck-Institut für Meteorologie, Hamburg, Germany.

Improved Mass Fluxes in a Global Chemistry-Transport Model: Implications for Upper-Tropospheric Chemistry

E.W. Meijer*, P.F.J. van Velthoven, A. Segers, B. Bregman
Royal Netherlands Meteorological Institute, De Bilt, Netherlands

D. Brunner
Institute for Atmospheric and Climate Science, ETH Zurich, Switzerland

Keywords: atmospheric chemistry, modelling, hydroxyl, ozone, ozone production, aviation

ABSTRACT: A new method that solves the imbalance between the mass transport and the surface pressure tendency, a problem existing in most global chemistry-transport models, has been evaluated by comparing model results with observations of the age-or-air and trace gases, such as CO and ozone. Furthermore we have investigated the implications for upper-tropospheric chemistry by comparing the modelled and observed hydroxyl reaction rates. The model reproduced these rates reasonably well. On average the modelled ozone production was 20% larger than the observed one, if samples exposed to recent convection and lightning were excluded from the analysis.

1 INTRODUCTION

Calculating the impact of aircraft emissions is a particularly difficult task, since the largest fraction of these emissions occurs in the upper troposphere and lowermost stratosphere (UTLS). Global chemistry-transport models have great difficulties to simulate trace gas concentrations in this region that is characterised by strong cross-tropopause concentration gradients and mixing between the stratosphere and the troposphere. Thus model results for this region are very sensitive to errors in the mass fluxes. Yet it is near the tropopause where radiative forcing is most sensitive to the greenhouse gas perturbations.

One source of error in the mass fluxes arises from an imbalance between the surface pressure tendency and the vertically integrated mass change. This imbalance exists in most global chemistry-transport models (CTMs) and models have to be corrected for this. Previous corrections, proposed amongst others by Heimann and Keeling (1989), proved to be unsatisfactory in recent studies on ozone in the lowermost stratosphere (Bregman et al., 2001). However, recently one of us (Segers et al., 2002) has developed a new solution by calculating the mass fluxes from wind fields in a spherical harmonical form (divergence and vorticity) rather than in grid coordinates, thus mimicking the physics of the weather forecast model (ECMWF) as closely as possible.

In this study we evaluated how this solution for the mass-imbalance problem improved the ability of our CTM to simulate the composition and chemistry of the tropopause region, and consequently its ability to quantify the impact of aviation. First the new method was evaluated in more general terms by comparing model results with observed age-of-air and ozone concentrations. This will show that this new method gives significantly better simulated age-of-air and ozone fields than previous approaches (Bregman et al., 2003). Secondly we investigated modelled trace gas concentrations with observations from the TRADEOFF database (Brunner et al., 2003; website http://www.lapeth.ethz.ch/~dominik/tradeoff/). This database was especially compiled in order to evaluate the performance of global CTMs with respect to the effects of aviation on the atmospheric composition. In this work we restrict our results to comparison with the 5-minute averaged observations of the SONEX campaign that were included in this database. The completeness of the SONEX data set allows analysis of the implications of our new method for upper-tropospheric chemistry by comparing modelled chemical rates for hydroxyl (OH) with observed rates from the

* *Corresponding author:* Ernst Meijer, Royal Netherlands Meteorological Institute, P.O. Box 201, 3730 AE De Bilt, Netherlands. Email: meijere@knmi.nl

SONEX. We will show that there is a small but significant improvement in the modelling of the OH chemistry.

The next section gives a brief description of our CTM along with the old and new method of processing the mass fluxes, followed by a section stating the results for the age-of-air experiments and the comparison with observed ozone fields. These two sections (2 and 3) form basically a summary of the work of Bregman et al. (2003), except for the application of ECMWF 40-years reanalysis (ERA40) data in one of the age-of-air calculations. Section 4 describes the comparison with the SONEX observations, followed with a discussions section about the CTM's ability to quantify the effects of aviation on ozone. Section 6 summarises the conclusions.

2 MODEL DESCRIPTION

The global Tracer Model Version 3 (TM3) used in this study is a 3D-CTM, originally developed by Heimann (1995). TM3 is driven by 6-hourly meteorological fields from the forecast model of the European Centre for Medium-range Weather Forecasts (ECMWF). Detailed model descriptions can be found elsewhere (i.e. Houweling et al., 1998; Meijer et. al., 2001; Bregman et al., 2001; and references therein).

In the old method the mass-imbalance was adjusted by adding small horizontal correction fluxes to the vertically integrated mass fluxes (details in Segers et al., 2002). This method introduced errors in the mass fluxes, since these corrections lack physical grounds. Furthermore, the mass fluxes were derived from the ECMWF spectral data, gridded on 1^ox1^o resolution, followed by interpolation to the desired grid, adding multiple interpolation errors.

The new processing method solves these problems. The mass balance is much better maintained by taking the divergence, vorticity, and the surface pressure into account. The new processing method is performed in the ECMWF spherical harmonics representation, thereby avoiding interpolation errors. Again, details can be found in Segers et al. (2002).

3 EVALUATION OF THE NEW MASS FLUX PROCESSING METHOD

We have performed two tracer studies to evaluate the new processing method for the mass fluxes: one age-of-air experiment to assess the large-scale effects and one ozone tracer experiment to assess the effects on shorter time-scales.

3.1 *Age-of-air experiments*

The age spectrum, formally developed by Hall and Plumb (1994), is the probability distribution function of transit times from a source region to the sample region. With a tracer model the age spectrum is directly obtained from a passive tracer simulation with a small source region where the mass mixing ratio is a delta-function in time. The response is then simply the age spectrum. In order to include all transit time-scales into the age-spectrum, the simulation was continued for 20 years, using ECMWF 1996 meteorology repeatedly. The results of the age-of-air simulations were compared with the age-of-air at 20 km altitude, derived from in situ observations of CO_2 (Andrews et al., 2001). Figure 1 shows the observed mean age-of-air at 20 km together with the zonally averaged simulated age-of-air. The results for the new method constitute a significant improvement with respect to the old method, but the mean age of air remains too young in the extra-tropics. An additional run based on ECMWF ERA40 meteorology with the aim to improve results further, revealed anomalously large vertical transport. The simulation was performed at a lower resolution and compared with ECMWF operational data (OD) at a similar resolution. In both cases the mass fluxes were processed with the new method.

3.2 *Ozone tracer experiment*

Next we performed simulations with TM3 containing an ozone tracer with prescribed loss rates from a 2-D stratospheric model (Pitari et al., 1993) constrained by an ozone climatology down to 50 hPa, scaled with total ozone column data from the Global Ozone Monitoring Experiment (GOME) for 1996. Figure 2 shows the seasonally averaged ozone mean mixing ratios ± 1s from simulations

with the old and new mass fluxes, compared with data from MOZAIC flights routes Frankfurt–New York (FRA-NEW) and Vienna–Tokyo (VIE-TOK) (Marenco et al., 1998). The new mass flux processing method shows an excellent overall agreement. The large overestimate in all seasons, except for summer, has disappeared. Even in summer the observed variability is well represented by TM3.

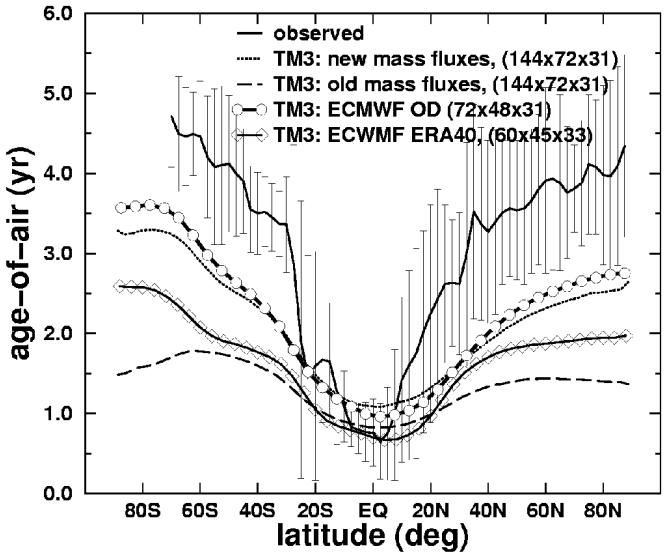

Figure 1. Simulated and observed mean age of air at 20 km altitude as a function of latitude.

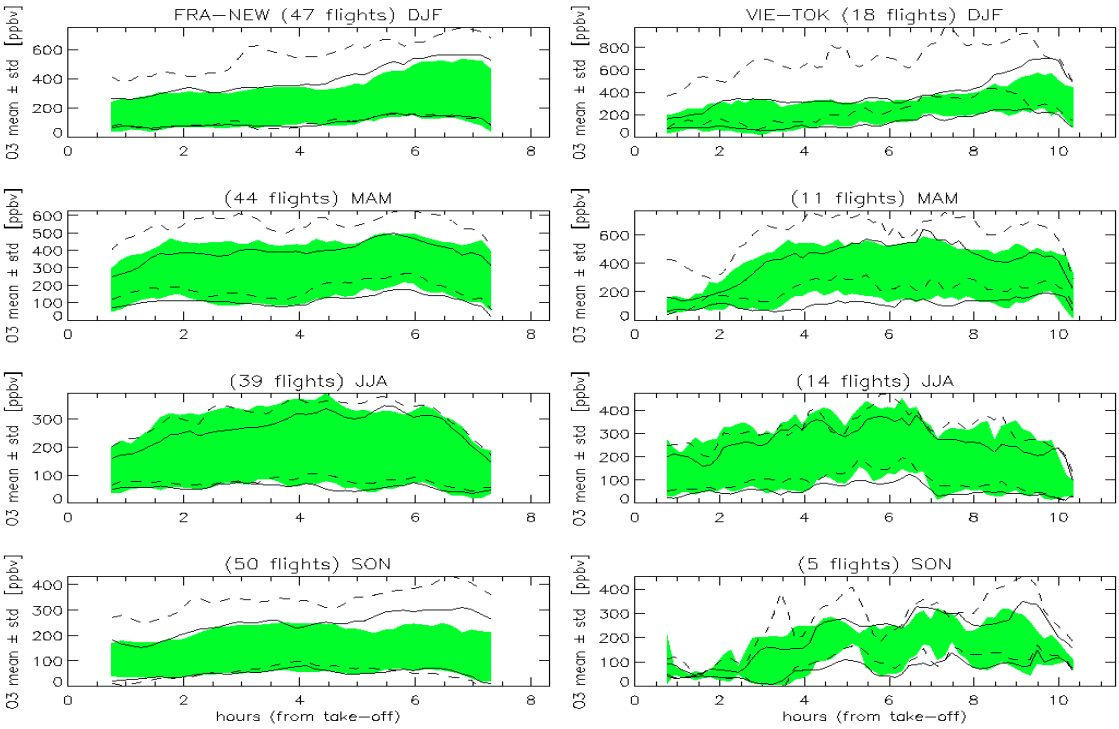

Figure 2. Seasonal mean ozone mixing ratios (ppbv) (±1s) as observed during the MOZAIC project (filled grey) and simulated with TM3 using the old (dashed) and new (solid) mass flux processing method.

4 IMPLICATIONS FOR UPPER-TROPOSPHERIC CHEMISTRY

Next we applied the full tropospheric chemistry version of TM3 and compared the results with the observations made during the SONEX campaign (Singh et al, 1999). These observations are very complete, allowing a detailed analysis of the chemistry and are representative for cruise flight conditions. The model output was interpolated to the positions of the 5-minute averaged observations. Table 1 summarises the results for the species CO, ozone, OH, and HO_2 by stating the correlations and overall biases (the relative mean difference) between observed and modelled (with the old and new method) concentrations. Differences in the mass fluxes affect primarily the concentrations of the long-lived tracers, such as CO and ozone, which ultimately cause changes in concentrations of OH and HO_2. The correlations for all tracers, except for CO, are reasonably good (>0.6) regardless of the mass flux processing method. The biases on the other hand are quite large. Nevertheless the overall bias improves for CO and ozone, and OH with the new method. The bias for HO_2 is not affected significantly. Considering the central role of OH in driving tropospheric chemistry, the new method has a positive effect on chemistry.

Table 1. Correlations and overall biases (%) between observed and modelled (using the old and new mass flux processing methods) trace gas concentrations of the SONEX campaign.

	O_3		CO		OH		HO_2	
Method	Old	New	Old	New	Old	New	Old	New
Correlation	0.72	0.68	0.53	0.56	0.57	0.69	0.76	0.78
Bias	33%	29%	35%	15%	-32%	-25%	27%	29%

Next we investigated the upper-tropospheric chemistry in more detail by comparing the modelled with the observed reaction rates that produce or destroy OH. Again the comparison occurred by interpolation to the locations of the observations. Figure 3 shows the modelled and observed rates, averaged over all samples between 150 and 300 hPa. The most important production and loss reactions are $NO+HO_2$? NO_2+OH and $CO+OH$? CO_2+H, respectively, which were underestimated by TM3. Other large differences between model and observations exist, but do not contribute significantly to the OH concentration (i.e. the photolysis of H_2O_2). Furthermore the differences between the results with the old and new method are small.

However, removal of the samples that were influenced by continental convection and/or lightning improved the comparison considerably for the simulation based on the new mass method (see Fig. 4). Elevated NO_x/NO_y concentration (>0.5) ratios and NO_y concentrations (>500 pptv) over large spatial scales (>20 km) were interpreted as resulting from the continental boundary layer or recent lightning activity (Jaeglé et al., 2000 and references therein). In our analysis about 30% of the samples fitted this criterion. Without these samples the model results for the new method are in much better agreement with the observations. Furthermore, application of the new mass flux processing method improved the model results for all considered chemical rates.

5 DISCUSSION

Previously, we investigated the contributions of different NO_x sources to the composition of the North-Atlantic flight corridor (Meijer et al., 2000). This study demonstrated that the aircraft contributions to the total NO_x concentration could be quantified for moderate cases without recent influence from convection or lightning. Ozone perturbations could not be attributed to specific sources due to the large natural variability of this tracer in the tropopause region.

Taking into account that the ozone production is approximately equal to the rate of reaction $NO+HO_2$? NO_2+OH, there is evidence that TM3 with the new mass flux processing method is now capable to calculate the ozone perturbation due to aviation with a moderate accuracy for cases without recent influence from convection and lightning. The modelled rate of this reaction was

about 20% higher than the observed rate for all SONEX observations without convective/lightning influence (and about 30% lower for all points).

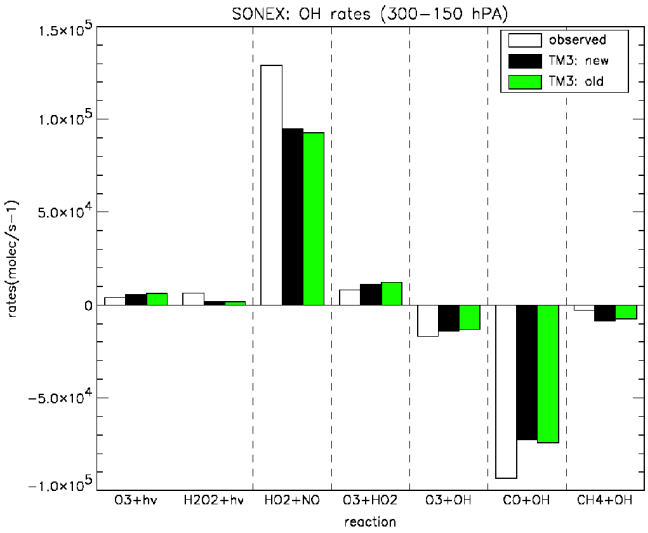

Figure 3. The most important production and loss rates of OH, averaged for all observation points between 150 and 300 hPa compared with modelled rates, using the new and old method. The model results are also averages of model output that interpolated to the observation points.

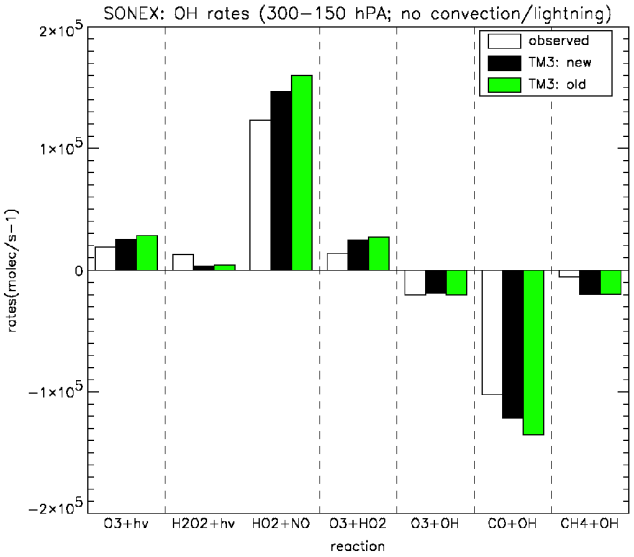

Figure 4. As in Figure 3, but averaged over samples not influenced recently by convection and lightning (samples with NO_x/NO_y>0.5 and NO_y>500 pptv).

6 CONCLUSIONS

We have investigated a new method for processing the mass fluxes for the TM3 model that solves earlier reported mass-imbalance problems. The model improvement was demonstrated by the comparison of age-of-air calculations and ozone tracer simulations with observations. Application of ERA40 data of ECMWF revealed anomalously large vertical circulation in this data set.

The new method improves the model results for long-lived tracers, such as ozone and CO, in the upper troposphere and lowermost stratosphere. This ultimately has a positive effect on the OH concentration, as indicated by point-by-point comparison with SONEX observations. Analysis of the important chemical rates that produce or destroy OH showed that TM3 is capable of simulating the upper-tropospheric chemistry well, if samples exposed to recent convection or lightning were

excluded from the analysis. The approximate ozone production from the simulations was 20% higher than the observed. This is an indication that the model is also capable to calculate the aircraft-induces ozone perturbations for these cases, given the fact that the model simulates aircraft-induced NO_x perturbations reasonably well.

With all samples included, the approximate ozone production from the simulations was 30% lower than observed, and there was a small improvement with the new mass flux processing method. Application of the on-line convective mass fluxes from ECMWF ERA40 might improve the model results further (Olivié, submitted). This is now under investigation.

REFERENCES

Andrews, A., Boering, K. ,Daube, B., Wofsy, S, Loewenstein, M., Jost, H., Podolske, J., Webster, C., Herman, R., Scott, D., Flesh, G., Moyer, E., Elkins, J., Dutton, G., Hurst, D., Moore, F., Ray, E., Romanshkin, P., and Strahan, S.: Mean ages of stratospheric air derived from in situ observations of CO_2, CH_4, and N_2O, J. Geophys. Res., 106, 32295-32314, 2001.

Bregman A., Krol. M., Teyssèdre, H., Norton, W., Chipperfield, M. Pitari, G., Sundet, J., and Lelieveld, J.: Chemistry-transport model comparison with ozone observations in the midlatitude lowermost stratosphere, J. Geophys. Res., 106, 17479-17496, 2001.

Bregman A., Segers, A., Krol M., Meijer E., and van Velthoven, P.: On the use of mass-conserving wind fields in chemistry-transport models, Atmos. Chem. Phys., 3, 447-457, 2003.

Brunner D., Staehelin J., Rogers, H.L., Köhler, M.O., Pyle, J.A., Hauglustaine, D., Jourdain, L., Berntsen, T.K., Gauss, M., Isaksen, I.S.A, Meijer, E., van Velthoven, P., Pitari, G., Mancini, E., Grewe, V., and Sausen, R.: An evaluation of the performance of chemistry transport models by comparison with research aircraft observations. Part 1: Concepts and overall model performance, Atmos. Chem. Phys. Discuss., 3, 2499-2545, 2003.

Hall, T. and Plumb, R.: Age as a diagnostic of stratospheric transport, J. Geophys Res., 99, 1059-1070, 1994.

Heimann, M.: The global atmospheric tracer model TM2: DKRZ TM2 model documentation, Techn. Rep., 10, Max-Planck-Inst. für Meteorol., Hamburg, Germany, 1995.

Heimann, M. and Keeling, C: A three-dimensional model of atmospheric CO_2 transport bases on observed winds, 2: Model description and simulated tracer experiments, Geophys. Mon., 55, 237-257, 1989.

Houweling, S. M., Dentener, F., and Lelieveld, J.: The impact of nonmethane hydrocarbon compounds on tropospheric chemistry, J. Geophys. Res., 103, 10,673-10.696, 1998.

Jaeglé, L., Jacob, D.L., Brune, W.H., Faloona, J. Tan, D., Heikes, G., Kondo, Y., Sachse, G.W., Anderson B., Gregory, G.L., Singh, H.B., Pueschel, R. Ferry, G., Blake, D.R., and Shetter E.R, Photochemistry pf HO_x in the upper troposphere at northern midlatitudes, J. Geophys. Res. 105, 3833-3850, 2000.

Marenco, A., Thouret, V., Nedelc, P., Smit, H. Helten, M., Kley D., Karcher, F., Simon, P., Law, K., Pyle, J., Poschmann, G., von Wrede, R., Hume, C., and Cook, T.: Measurements of ozone and water vapor by Airbus in-service aircraft: the MOZAIC airborne program, an overview: J. Geophys. Res., 103, 25631-25642, 1998.

Meijer E.W., van Velthoven, P.F.J., Thompson, A.M., Pfister, L., Schlager, H., Schulte, P., and Kelder H.: Model calculations of the impact of NO_x from air traffic, lightning, and surface emissions, compared with measurements, J. Geophys. Res. 105, 3877-3892, 2000.

Meijer, E.W., van Velthoven, P.F.J., Brunner, D.W., Huntrieser H., and Kelder, H.: Improvement and evaluation of the parameterisation of nitrogen oxide production by lightning, Phys. Chem. of the Earth 26**,** 557-583, 2001.

Olivié, D., van Velthoven, P.F.J., Beljaars, A.C.M., and Kelder, H.M.: Comparison between archived and off-line diagnosed convective mass fluxes in the chemistry transport model TM3, submitted to J. Geophys. Res., 2003.

Pitari, G., Rizi, V., Ricciardulli, L., and Visconti, G.: High-speed civil transport impact: Role of sulfate, nitric acid trihydrate, and ice aerosols studied with a two-dimensional model including aerosol physics, J. Geophys. Res. 98, 23141-23164, 1993.

Segers, A., van Velhoven P., Bregman, B, and Krol, M.: On the computation of mass fluxes for Eulerian transport models from spectral meteorological fields, in: Proc. of the 2002 Intern. Conf. on Computational Science, Lecture Notes in Computer Science (LNCS), Spinger Verlag, 1769-1770, 2002.

Singh, H.B., Thompson, A.M., and Schlager, H.: SONEX airborne mission and coordinated POLINAT-2 activity: overview and accomplishments, Geophys. Res. Lett., 26, 3053-3056, 1999.

Activities of NASA's Global Modeling Initiative (GMI) in the Assessment of Subsonic Aircraft Impact

J. M. Rodriguez*
Rosenstiel School of Marine and Atmospheric Science, University of Miami, Miami, FL., USA

J. A. Logan
Harvard University, Cambridge, MA, USA

D. A. Rotman, D. J. Bergmann
Lawrence Livermore National Laboratory, Livermore, CA

S. L. Baughcum
Boeing Company, Seattle, WA, USA

R. R. Friedl
Jet Propulsion Laboratory, Pasadena, CA, USA

D. E. Anderson
NASA Headquarters, Washington, DC USA

Keywords: Aircraft, impact, ozone, troposphere

ABSTRACT: The Intergovernmental Panel on Climate Change (Penner et al., 1999) estimated a peak increase in ozone ranging from 7-12 ppbv (zonal and annual average, and relative to a baseline with no aircraft), due to the subsonic aircraft in the year 2015, corresponding to aircraft emissions of 1.3 TgN/year. This range of values presumably reflects differences in model input (e.g., chemical mechanism, ground emission fluxes, and meteorological fields), and algorithms. The model implemented by the Global Modeling Initiative allows testing the impact of individual model components on the assessment calculations. We present results of the impact of doubling the 1995 aircraft emissions of NOx, corresponding to an extra 0.56 TgN/year, utilizing meteorological data from NASA's Data Assimilation Office (DAO), the Goddard Institute for Space Studies (GISS), and the Middle Atmosphere Community Climate Model, version 3 (MACCM3). Comparison of results to observations can be used to assess the model performance. Peak ozone perturbations ranging from 1.7 to 2.2 ppbv of ozone are calculated using the different fields. These correspond to increases in total tropospheric ozone ranging from 3.3 to 4.1 Tg/O_3. These perturbations are consistent with the IPCC results, due to the difference in aircraft emissions. However, the range of values calculated is much smaller than in IPCC.

1 INTRODUCTION

The emission of trace gases and particles by subsonic aircraft can lead to changes in the chemical composition of the atmosphere which in turn could affect Earth's radiative balance. Concern has been raised about the impact of emission of greenhouse gases (CO_2), ozone precursors (NO_x, non-methane hydrocarbons), soot, and sulfate particles, as well as the direct and indirect effects of contrail formation, modification of cirrus cloud coverage and properties, and changes in the lifetime of greenhouse gases such as CH_4 (Penner et al., 1999). In particular, the potential increase in upper tropospheric NO_x from aircraft emissions can lead to increases in O_3 production and abundances in the corridor region. At the same time, increases in NO_x can also lead to decreased OH abundances and longer lifetimes for methane.

The latest assessment of these effects by IPCC (Penner et al., 1999) indicated ozone increases of 7-12 ppbv in the upper troposphere, and a decrease in the methane lifetime of 1.6-2.9%, due to NO_x

* *Corresponding author:* Jose M. Rodriguez, RSMAS/MAC, University of Miami, 4600 Rickenbacker Causeway, Miami, FL 33149 USA. Email: jrodriguez@rsmas.miami.edu

aircraft emissions of 1.3 TgN/year for 2015 conditions. The almost factor of 2 range in the estimated impacts reflect the different algorithms, chemical mechanisms, ground emission fluxes, lightning contribution, meteorological fields, and assumptions in the models utilized. Because each of these models includes a large number of processes, it is difficult to ascertain the reason for the above variability.

We present here preliminary results from calculations carried out by NASA's Global Modeling Initiative (GMI) of the impact of doubling the 1996 aircraft NO_x emissions, while keeping all model inputs and components constant except for the meteorological fields. Our results indicate a smaller variability in the ozone calculated ozone perturbations, with magnitudes consistent with previous assessments.

2 DESCRIPTION OF CALCULATIONS

We utilize the GMI chemistry-transport model (Rotman et al., 2001), modified for tropospheric calculations. The modular architecture of this model allows for simulations that keep all model components the same except for a chosen one, thus permitting a more accurate assessment of the impact of a particular process. For the simulations presented here, we have chosen to change the input meteorological data. For this, we have utilized three set of meteorological fields: a) assimilated data for 1996 conditions, provided by the NASA/Goddard Data Assimilation Office (DAO), but utilized as a "perpetual" year; b) meteorological data from the Goddard Institute for Space Studies (GISS) general circulation model, version II' (D. Rind, private communication; c) meteorological data from the Middle Atmosphere Community Climate Model, version (MACCM3).

Although these fields extend from the boundary later to the mesosphere, only tropospheric chemistry is included in these calculations. The tropospheric chemical mechanism is the same as that utilized in Harvard's GEOS-CHEM model (Bey et al., 2001), and the numerical solver for the chemistry is the SMVGEAR-II (Jacobson, 1995). Stratospheric ozone fluxes are simulated by incorporating an ozone synthetic tracer (SYNOZ; MacLinden et al., 2000), with a source in the tropical stratosphere corresponding to 475 TgO_3/year. This approach guarantees the same total flux of ozone through the tropopause for all simulations, although the spatial distribution will depend on the meteorological field. A similar approach was utilized for NO_x fluxes from the stratosphere. The tropopause was diagnosed to occur at SYNOZ concentrations of approximately 150 ppbv.

Aircraft emissions were interpolated to the year 1995 based on previously published inventories of aircraft emissions for scheduled flights for 1992 (Baughcum, et al., 1996), 1999 (Sutkus, et al., 2001), and projected to 2015 (Baughcum, et al., 1998), as well as unscheduled traffic (Mortlock, et al., 1998). Annual emissions of NO_x by aircraft were 0.56 TgN/year. Other natural and anthropogenic surface emissions were updated and scaled from those used in the GEOS-CHEM model (Bey et al., 2000). Emission of NO_x by lightning was fixed at 5 TgN/year for all three simulations. The spatial distribution was also fixed for all simulations,using the parameterization of Price and Rind (1992), with corrections to the vertical distribution (Pickering, private communication).

Simulations were carried out for a "base" scenario approximating 1995-1996 conditions, and one for which the aircraft simulations described above were doubled. Both baseline and perturbation calculations were carried for 18 model years, of which the last 12 months were analyzed. Since there were no other changes in other boundary conditions or meteorology in the double aircraft scenario, the results presented here are not to be interpreted as a "future" prediction, but rather as a study of the sensitivity of the results to increases in aircraft emissions using different meteorological inputs.

3 RESULTS AND CONCLUSIONS

3.1 *Validation of baseline calculations*

The baseline results have been compared to ozone-sonde climatologies (Logan, 1999), CO and O_3 observations at surface sites, radionucleide observations, and data from different tropospheric

aircraft campaigns. These and other validation efforts are being summarized in a series of manuscripts in preparation. The ultimate purpose of these comparisons is to develop a methodology to document and assess model performance when utilizing different meteorological (and other) inputs. Ideally, such evaluation of model performance would lead to the selection of a series of inputs that best fit data. However, the current evaluation does not clearly point to a preferred set of meteorological input in the context of agreement with observations. Thus, the results presented below can be seen as reflecting the existing uncertainty due to the different meteorological assumptions represented by the fields adopted.

An example of how the model results compare with observations is presented in Figure 1, where calculated ozone mixing ratios at three tropospheric levels are shown along with the ozone sonde climatology, for stations situated in the Northern Hemisphere at high to mid-latitudes. In this particular instance, only the DAO fields seem to compare reasonably to the observations at 300 and 500 hPa, while all three fields perform reasonably well at lower altitudes. Part of the disagreement at high altitudes may reflect the limitations of the SYNOZ approach in reproducing the spatial distribution of the stratospheric ozone flux. It would be tempting to prefer the DAO results to those of other fields when predicting aircraft perturbations. However, such decision cannot be based on a limited comparison. For example, the calculated lifetimes of CH_3CCl_3 against removal by tropospheric OH are 4.9 years for DAO and MACCM3 fields, and 5.5 years for GISS fields, which points to the GISS fields as performing better under this criterion. Further work is needed by the modeling community to identify measurements that best constrain model results in the context of a particular assessment.

3.2 *Aircraft perturbation results*

Our calculated perturbations to NOx and O3 are shown in Figures 2. Peak changes in NOx mixing ratios for the month of July range from about 20 pptv using DAO meteorological fields, to about 45 pptv in calculations using MACCM3 fields. As seen in Figure 2 the NOx accumulation between the three meteorological fields is strikingly different, although the changes in ozone (right column) are more similar. These should be compared to changes ranging from 60-150 pptv calculated by the models participating in the IPCC assessment, for 2015 conditions Penner et al., 1999). Although the relative spread in NOx perturbations is similar for both IPCC and our calculations, our results are smaller than those of IPCC. This can be easily understood if we compare the increase in aircraft emissions in both instances, 1.3 Tg/year for IPCC vs. 0.56 TgN/year in our calculations.

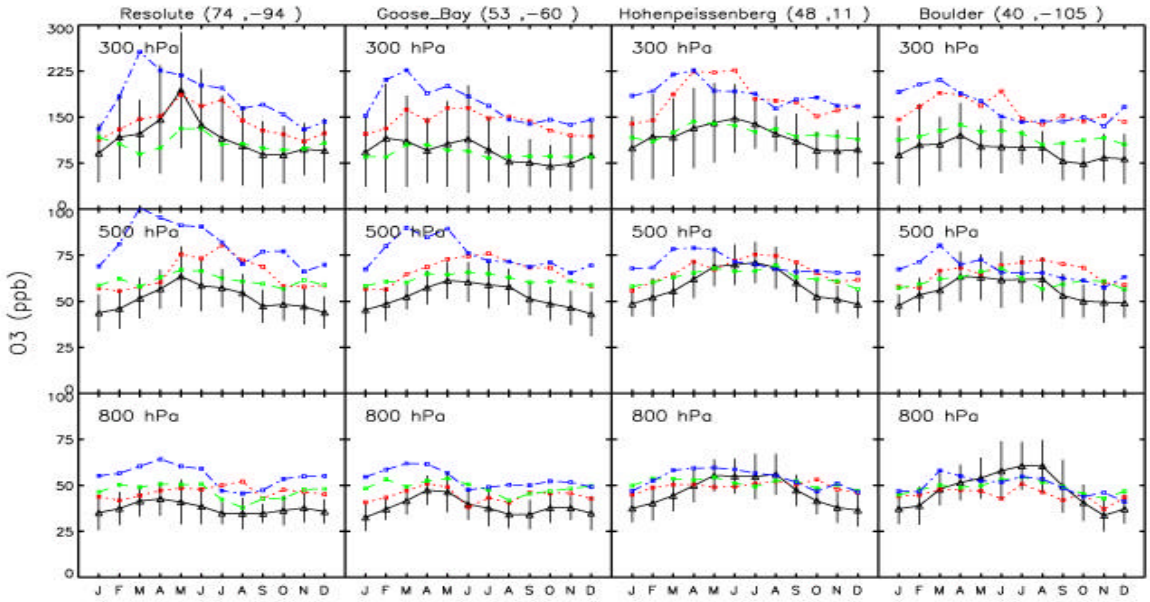

Figure 1. Calculated ozone mixing ratios utilizing DAO (green line), GISS (blue line), and MACCM3 (red line) meteorological fields. Climatological data from ozonesondes (Logan, 1999) with their standard deviation are also shown for comparison.

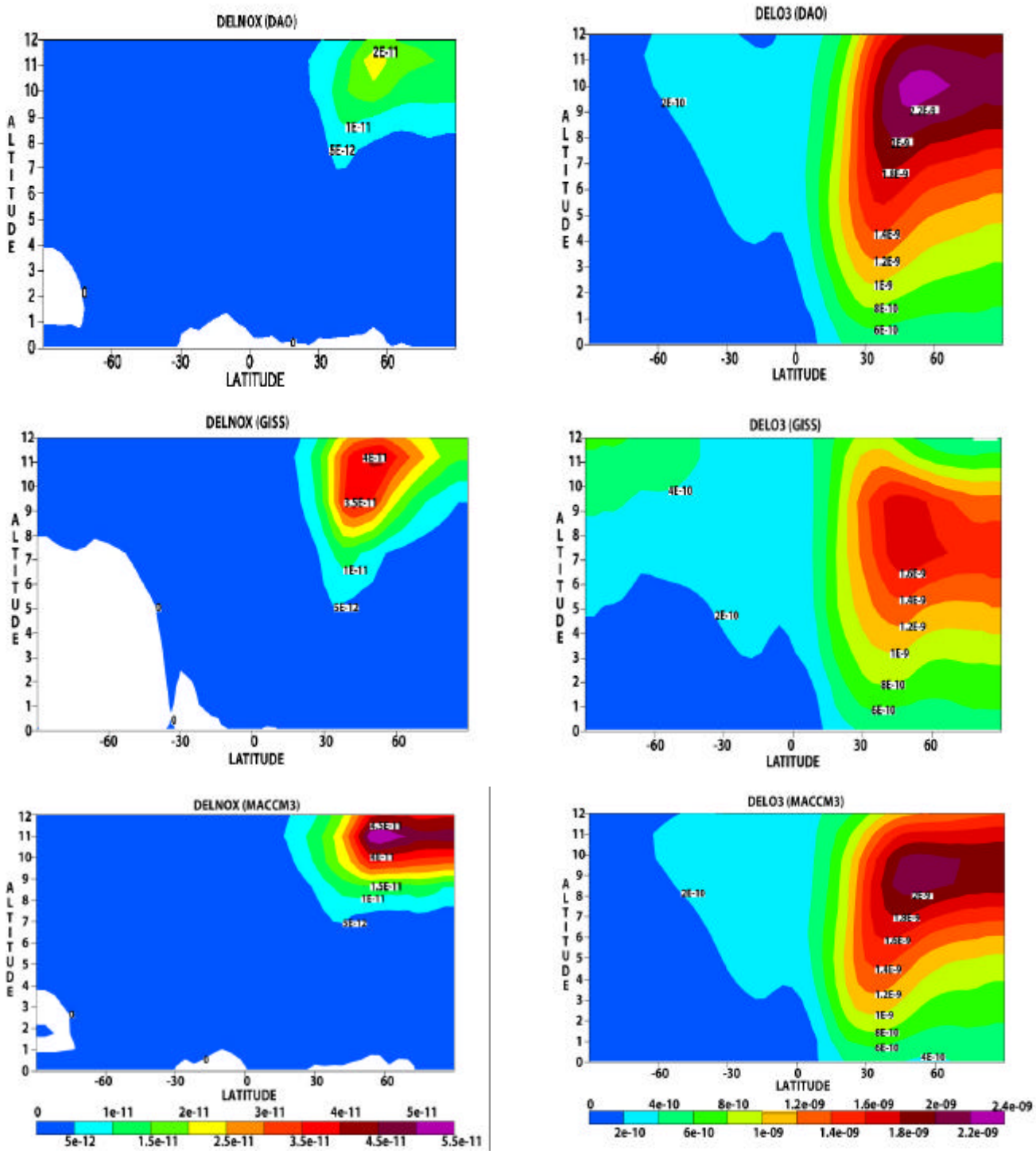

Figure 2 Calculated change in NOx (left column) and O3 mixing ratios using meteorological fields from the DAO, GISS, and MACCM3 models. The NOx calculations are for the month of July, while the O3 results denote annual averages. The altitude scale has been calculated from a standard atmosphere

In contrast to the NO_x results, the ozone perturbations shown in Figure 2 exhibit a much smaller variability in the magnitude of the perturbation. Peak ozone perturbations range from 1.8 ppbv using GISS fields to 2.2 ppbv with DAO fields. These peak perturbations are consistent with the lower limit of the perturbations calculated by IPCC, ie., 7-12 ppbv, were we to assume simple scaling of the perturbation with NO_x emissions by aircraft. A better comparison to IPCC results is obtained if we examine the total increases in tropospheric ozone, which are: 4.1, 3.3 and 3.7 Tg/O_3 for calculations utilizing DAO, GISS, and MACCM3 fields, respectively. The IPCC report showed increases in tropospheric O_3 ranging from about 4-8 Tg/O_3 for the 1992 scenario, whose aircraft emission (0.5 TgN/year) is similar to our adopted increase. Thus, our calculated ozone

perturbations are consistent with the lower range of the IPCC results. We note, however, that the range in ozone perturbations using three meteorological fields is smaller than that obtained by the IPCC models.

Our simulations also obtained increases in tropospheric OH. This led to reductions in the atmospheric lifetime of methane by 0.95% for DAO fields, 0.76% for GISS fields, and 1 % for MACCM3. These reductions are somewhat smaller than those calculated by IPCC for the 1992 scenario, which ranged from 1.2 to 1.4%.

For convenience, we summarize our results in Table 1, and compare them to those shown in the IPCC report, whenever possible.

Table 1: Comparison of GMI Simulations with those of IPCC*

	IPCC	GMI-DAO	GMI-GISS	GMI-MACCM3
ΔNO_x Peak July zonal average [pptv]	60-150	20	40	45
ΔNO_x Tropospheric total, July [Tg N]		0.0021	0.0033	0.0027
ΔO_3 Peak annual, zonal average [ppbv]	7-12	2.2	1.6	2.0
ΔO_3 Tropospheric total, annual average [Tg O_3]	4-8 [a]			
	9-18	4.1	3.3	3.7
ΔCH_4 lifetime [percent]	-1.2 to –1.4[a]	-0.95	-0.76	-1.0
	-1.6 to –2.6			

*IPCC results are shown for the 2015 simulations, as in Figure 1 and 2, corresponding to a 1.27 TgN/year aircraft source of NO_x. For comparison, we also include IPCC results (denoted by [a]) corresponding to 1992 simulations with 0.5 TgN/year. The results of the 1992 IPCC simulations are more comparable to ours, since the aircraft NO_x sources are similar. However, the spatial distribution of the perturbations were not reported in IPCC for 1992.

3.3 *Conclusions*

We have presented simulations of the "chemical" impact of subsonic aircraft NO_x on the chemical composition of the troposphere, with particular emphasis on the increases in ozone concentrations and decreases in methane lifetimes. Our model simulations differ only in the adopted meteorological fields. Other model components are kept constant. The results are consistent (although slightly on the low side) of the results presented in the IPCC assessment (Penner et al., 1999), but the range of results is much smaller than that obtained from the different models participating in IPCC.

The differences in model results in assessment of aircraft perturbations have justly been ascribed to the difference in model inputs and approaches. Although not explicitly proven or stated, differences in the calculated or adopted meteorological fields are sometimes suspected to be one of the main causes of these variabilities. The results presented here indicate that this is not necessarily the case, particularly for the extremely buffered chemical processes responsible for producing ozone in the upper troposphere. In a manner similar to the above exercise, GMI can be used as a testbed for different model components to discern which model inputs/components induce the largest uncertainty in the results, thus focusing efforts in narrowing assessment uncertainties.

REFERENCES

Baughcum, S. L., et al., 1996: *Scheduled Civil Aircraft Emission Inventories for 1992: Database Development and Analysis*, NASA Contractor Report 4700, Washington, DC.

Baughcum, S. L., et al., 1998: *Scheduled Civil Aircraft mission Inventories Projected for 2015: Database Development and A nalysis*, NASA/CR-1998- 207638

Bey, I. et al., 2001: Global modeling of tropospheric chemistry with assimilated meteorology: Model description and evaluation, *J. Geophys. Res., 106*, 23,073-23,096.

Logan, J. A., 1999: An analysis of ozonesonde data for the troposphere: Recommendations for testing models, *J. Geophys. Res., 104*, 16151-16170.

McLinden, C. A., et al. 2000: Stratospheric ozone in 3-D models: A simple chemistry and the cross-tropopause flux, *J. Geophys. Res., 105*, 14653-14665.

Mortlock, A. M., and R. Van Alstyne, 1998: *Military, Charter, Unreported Domestic Traffic and General Aviation: 1976, 1984, 1992, and 2015 Emission Scenarios*, NASA CR- 1998-207639.

Penner, J. E., et al. (ed) 1999: *Aviation and the Global Atmosphere: A Special Report of IPCC Working Groups I and II*. Cambridge University Press, 1999.

Price, C., and D. Rind, 1992: A simple lightning parameterization for calculating global lightning distribution, *J. Geophys. Res., 97*, 9919-9933.

Rotman, D. A., et al, 2001: Global Modeling Initiative Assessment model: Model description, integration, and testing of the transport shell. *J. Geophys. Res., 106*, 1669-1691.

Sutkus, D. J., S. L. Baughcum, and D. P. DuBois, 2001: Scheduled Civil Aircraft Emission Inventories for 1999: Database Development and Analysis, NASA/CR-2001-211216.

Parametric Study of Potential Effects of Aircraft Emissions on Stratospheric Ozone

D.J. Wuebbles*, M. Dutta, K.O. Patten
Department of Atmospheric Sciences, University of Illinois at Urbana Champaign, Urbana, Illinois, USA

S.L. Baughcum
The Boeing Company, Seattle, Washington, USA

Keywords: stratospheric ozone, aircraft emissions, nitrogen oxides, atmospheric processes

ABSTRACT: There has been much consideration over the last decade of the potential impacts on the environment of projected fleets of passenger jets with cruise altitudes in the lower stratosphere. Existing ozone-impact studies have not fully analyzed the potential extent of possible flight and emissions criteria for such aircraft. In addition, recent improvements to our understanding of atmospheric chemical and physical processes would also affect earlier conclusions. In this study, a series of parametric studies are done with our recently updated state-of-the-art numerical zonally-averaged model of atmospheric chemistry and physics to examine potential effects of emissions from hypothetical fleets of stratospheric-flying aircraft on stratospheric ozone. The new studies examine how the modeling of aircraft effects has changed since the 1999 IPCC assessment (Aviation and the Global Atmosphere).

1 INTRODUCTION

The IPCC has assessed the potential effects that aviation, both subsonic and supersonic, have had in the past and may have in the future on stratospheric ozone depletion and climate change (Penner, et al.,1999). For NASA, Kawa, et al. (1999) assessed the stratospheric impacts of high flying aircraft. In addition to the fleets of the supersonic High Speed Civil Transport (HSCT) aircraft studied in the 1990s, lately other aircraft have been under consideration that might fly faster and higher than current commercial aircraft. So, evaluation of the potential effects of such aircraft on the global environment remains valuable. In particular, it should be noted that existing ozone-impact studies have not fully analyzed the potential extent of possible flight and emissions criteria for such aircraft. In this study, we calculate the ozone impact of a range of parametric scenarios in which cruise altitudes and nitrogen oxides (NO_x) emission levels are varied systematically. This study has focussed on aircraft that would cruise at altitudes primarily in the upper troposphere/lower stratosphere region; this includes the faster commercial aircraft that would primarily be used for intercontinental flights longer than 2500 nautical miles and a small fleet of Supersonic Business Jets (SSBJs).

2 METHODOLOGY

2.1 *Model Description*

The UIUC two-dimensional (2D) chemical-radiative-transport model is a zonally-averaged model of the chemistry and physics of the global atmosphere. The model is often used to study human related and natural forcings on the troposphere and stratosphere, but, because it is zonally-averaged, the analysis of tropospheric processes is limited. The model determines the atmospheric distributions of 78 chemically active atmospheric trace constituents. In addition to 56 photolytic reactions, the model incorporates 161 thermal reactions in the chemical mechanism, including heterogeneous

* *Corresponding author:* Donald J. Wuebbles, Department of Atmospheric Sciences, University of Illinois at Urbana Champaign, 105 S. Gregory St., Urbana IL-61801, USA. Email: wuebbles@atmos.uiuc.edu

reactions (e.g., see Wuebbles et al., 2001, or Wei et al., 2001). Reaction rates and photolysis cross-sections in the model are based on recommendations from NASA's Chemical Kinetics Review Panel (e.g., DeMore et al., 1997; Sander et al., 2000).

In the last year, there have been substantial improvements made to the model. Enhancements to treatments of atmospheric chemical processes include updating the nitrogen pentoxide (N_2O_5) and chlorine nitrate ($ClONO_2$) hydrolysis and several hypochlorous acid (HOCl) and hydrochloric acid (HCl) reactions that affect the NO_x chemistry. The temperature distribution in the model, the atmospheric radiative transfer code and PSC treatment are improved as well. The treatment of tropospheric and stratospheric dynamical processes have been updated with better data-based boundary topography and boundary winds. All of these changes in the model have resulted in significant changes in lower stratospheric ozone response to NO_x and water vapor (H_2O) emissions.

2.2 *Comparison of Model results with IPCC (1999)*

The current version of the UIUC-2D model generally shows much higher sensitivity to NO_x emissions from HSCT aircraft than the IPCC (1999) assessment models. Table 1 documents the percentage change in northern hemisphere total column ozone as calculated by the 1999 version and the most recent version of the UIUC-2D model. The scenarios are those evaluated in Chapter 4 of IPCC (1999). The overall difference with the 1999 analyses is largely due to several changes in the recommended chemistry for nitrogen oxides in the lower stratosphere, resulting in an increased sensitivity of NO_x emissions on stratospheric ozone.

Table 1. Percentage Change in Northern Hemisphere Total Column Ozone for IPCC(1999) HSCT scenarios

Scenario	Fleet Size	EI (NO_x) (g / kg of fuel)	IPCC models	UIUC-2D 1999	UIUC-2D 2003
S1b	500	0	-0.3 to -0.6	-0.37	-0.29
S1c	500	5	-0.2 to –0.4	-0.34	-0.49
S1d	500	10	-0.3 to -0.6	-0.49	-0.70
S1e	500	15	-0.4 to –0.9	-0.76	-1.39
S1i	1000	5	-0.4 to –0.9	-0.66	-0.95
S1k	500	5, SA5	-0.2 to –0.8	-0.48	-0.51
S9h	1000	5, SA6	-0.6 to –1.1	-0.72	-0.80

2.3 *Description of Scenarios of the Parametric Studies*

The set of emission scenarios used for this study were developed by Baughcum (2002b) for NASA's Ultra-Efficient Engine Technology (UEET) Program. For these parametric scenarios, the scheduled data were filtered to only consider flights with great circle distances greater than 2500 nautical miles. These scenarios span a range of flight altitudes and emission characteristics for possible future aircraft which would fly faster than today's commercial aircraft. The particular variables chosen for the parametric studies to evaluate the atmospheric effects of this type of aircraft are fuel burn (73 Mlbs / day and 146 Mlbs / day), cruise altitude (13–21 km) and E.I.(NOx) (5–20 g / kg of fuel). From fuel burn, one can readily determine the emissions of water vapor (and carbon dioxide and several other types of emissions).

In the model, the background atmosphere was set to a 2020 atmosphere with the source gas concentrations of the long-lived species changed according to the A2 scenario recommended in IPCC (Houghton et al., 2001). All results are obtained from steady state model simulations and then analyzed relative to the corresponding 2020 base that included projected subsonic emissions developed by Baughcum (2002b).

3 RESULTS AND DISCUSSION

A total of 32 scenarios have been evaluated for the conventional routing greater than 2500 nautical miles fleet scenarios from Baughcum (2002b). All the results are obtained from steady state model simulations where the model is run for 10 years with the same species input, heating rates input and

climatological input files and differing aircraft emission input files according to the scenarios studied. Figure 1 shows the relationship between the percentage change of total column ozone in the northern hemisphere relative to E.I.(NO_x) for the four different altitude bands and a total fuel burn of 73 Mlbs / day (dashed line) and 146 Mlbs / day (solid line) respectively. From this plot it is evident that the percentage change in total column ozone holds a linear relationship with E.I.(NO_x) for all the four altitude bands studied. The 13-15 km altitude band series has a slight positive slope owing to the net formation of ozone in that region of the atmosphere.

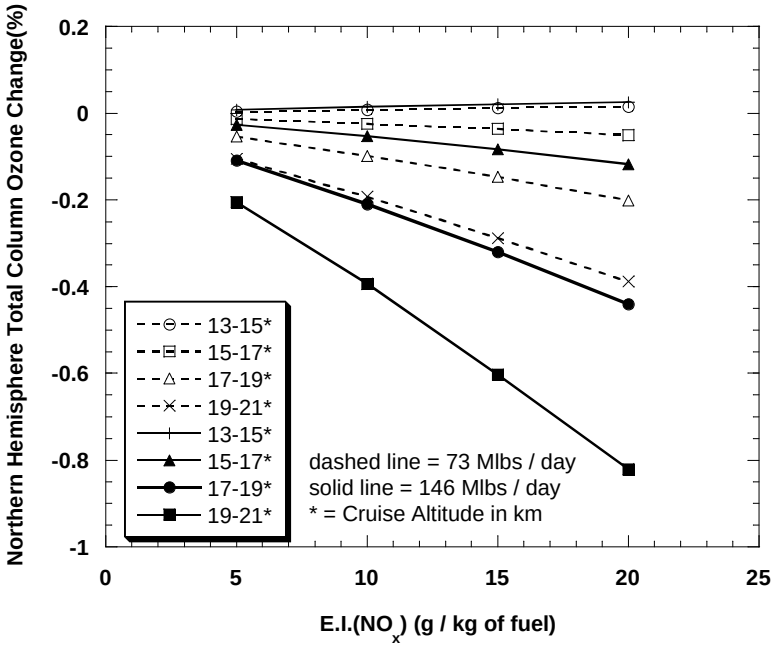

Figure 1. Percentage change in Northern Hemisphere total column zone as a function of E.I.(NOx) at different altitude bands for a total fuel burn of 73 and 146 Mlbs / day.

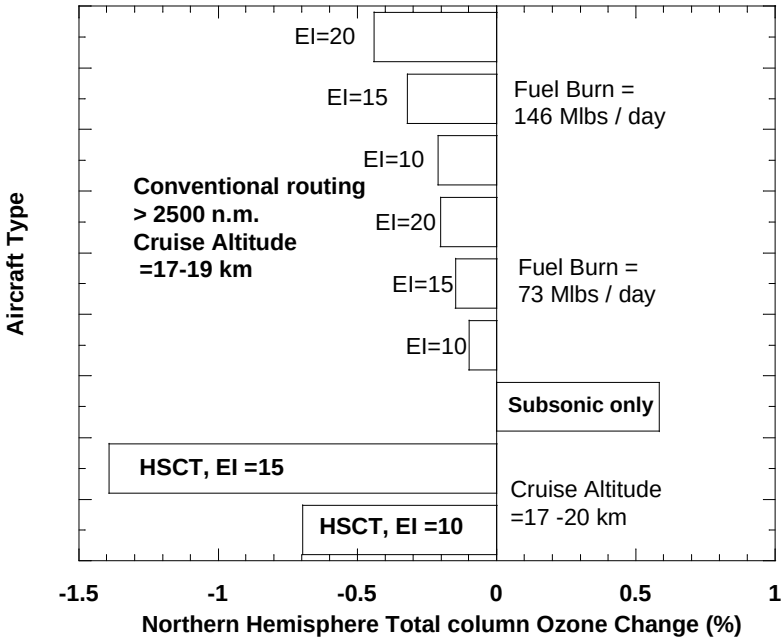

Figure 2. Comparison of effects on Northern Hemisphere change in total column ozone from UIUC-2D model studies of IPCC (1999) HSCT scenarios, the conventional routing greater than 2500 nautical miles scenarios evaluated here, and a 2020 subsonic aircraft fleet emissions case.

3.1 *Scenarios in Perspective with IPCC(1999) scenario:*

Figure 2 shows the effect on column ozone for the 17-19 km cruise altitude parametric case. For comparison, results using the HSCT scenarios (Baughcum and Henderson, 1998) are also shown. All the results in Figure 2 are calculated using the current version of the UIUC-2D model. The parametric case has a smaller fuel use at cruise altitudes, a different geographical distribution since no constraints are assumed for flights overland (unlike the HSCT scenarios), and a different cruise altitude band. The parametric scenarios are developed under the premise that any economically viable faster aircraft would have to be more fuel efficient than the HSCT concept. The calculated column ozone impact of the subsonic fleet is positive but such tropospheric perturbations are better posed for 3-dimensional CTM calculations.

3.2 *Supersonic Business Jets*

A number of aerospace companies have shown some interest in the concept of a supersonic business jet, commonly termed as SSBJ, over the last decade (Baughcum, 2002a). These aircraft would be designed to accommodate up to roughly 12 passengers and might fly at a speed of Mach 1.6 to 2. A set of parametric scenarios, which might be representative of future SSBJ fleets has been developed by Baughcum (2002a). A total of 24 SSBJ scenarios have been evaluated for determining their potential impact on stratospheric ozone. For this class of aircraft also it is found that ozone concentrations show a strong linear correlation with fuel burn and E.I.(NO_x).

Figure 3 below presents the calculated column ozone impact for the Northern Hemisphere as a function of cruise altitude for the two E.I.(NO_x) of 10 and 20 g / kg of fuel and the two fuel burn cases of 12 and 18 Mlbs/day. In this figure the altitude sensitivity of the studies show the point in the lower atmosphere where the effect on ozone transitions from a positive effect on ozone to a negative impact. The inflection point is near 14.5 km. When these SSBJ scenarios are compared with the effect on Northern Hemisphere total column ozone due to the fleets of HSCT (IPCC, 1999), they show much smaller effects. The effect of the SSBJ aircraft is seen to be at least a factor of 10 less than the HSCTs studied in IPCC (1999).

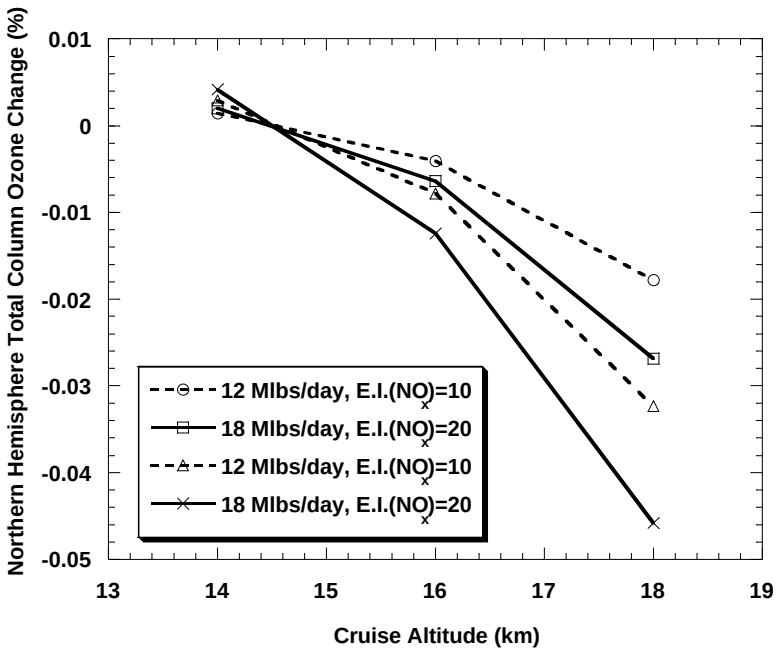

Figure 3. Calculated total column ozone impact for the Northern hemisphere as a function of cruise altitude for E.I.(NOx) = 10 and 20 g/kg of fuel for two fuel burns of 12 and 18 Mlbs/day respectively.

4 CONCLUSIONS

Some of the key conclusions from this study start with the effects of the new NASA chemistry recommendations, where emissions of NO_x from stratospheric aircraft emissions are now more effective at destroying ozone than in IPCC (1999) whereas water emissions are less effective at ozone depletion. The series of parametric analyses show that ozone concentrations have strong sensitivity to cruise fuel use, cruise altitude and E.I.(NO_x). The ozone change is linear with cruise fuel use and EI(NOx) for the cases studied.

Emissions near the tropopause at midlatitudes result in slight ozone increases (13-15 km scenarios; 43,000-49,500 kft) due to chemistry related to the smog cycle.

Effects on total ozone get more and more negative for higher cruise altitudes, higher E.I.(NO_x) and higher fuel use. The altitude in the atmosphere above which net ozone depletion begins due to these projected flights is around 14.5 km. As in past studies, the largest local ozone effects have been determined at northern hemisphere high latitudes.

REFERENCES

Baughcum, S. L., and S. C. Henderson, 1998: *Aircraft Emission Scenarios Projected in Year 2015 for the NASA Technology Concept Aircraft (TCA) High Speed Civil Transport*, NASA/CR-1998-207635.

Baughcum, S. L., 2002a: First Order Ozone Impact of a Fleet of Supersonic Business Jets (SSBJS). Report prepared for NASA Glenn Research Center, , NASA/CR-2002-211898, pp 35.

Baughcum, S. L., 2002b: Informal Report Describing the Development of Parametric Emission Scenarios, NAS3-01140 Revolutionary Aero-Space Engine Research Task Order #5 prepared for NASA Glenn Research Center, Cleveland, pp 13.

DeMore, W. B., S. P. Sander, D. M. Golden, R. F. Hampson, M. J. Kurylo, C. J. Howard, A. R. Ravishankara, C. E. Kolb, and M. J. Molina, 1997: *Chemical Kinetics and Photochemical Data for Use in Stratospheric Modeling*, Evaluation Number 12, Jet Propulsion Laboratory (JPL) Publication 97-4, Pasadena, California.

IPCC, 2001: *Climate Change 2001 The Scientific Basis. Contribution of Working Group I to the Third Assessment Report of the Intergovernmental Panel of Climate Change* [Houghton, J. T., Y. Ding, D. J. Griggs, M. Noguer, P. J. van der Linden, X. Dai, K. Maskell, and C. A. Johnson (eds)], Appendix II, Cambridge University Press, Cambridge, UK, pp 807-816.

Isaksen, I., C. Jackman, S.L. Baughcum, F. Dentener, W. Grose, P. Kashibatla, D. Kinnison, M. Ko, J. McConnell, G Pitari, and D. Wuebbles., 1999: Modeling the Chemical Composition of the Future Atmosphere, Chapter 4 in the Intergovernmental Panel of Climate Change (IPCC) Special Report on *Aviation and the Global Atmosphere*,[J.E. Penner, D.H. Lister, D.J. Griggs, D.J. Dokken, and M. McFarland (eds.)], Cambridge University Press, Cambridge, UK, pp121-163.

Kawa, S. R., J. G. Anderson, S. L. Baughcum, C.A. Brock, W.H. Brune, R.C. Cohen, D.E. Kinnison, P.A. Newman, J.M. Rodriquez, R.S. Stolarski, D. Waugh, and S.C. Wofsy, 1999: *Assessment of the Effects of High-Speed Aircraft in the Stratosphere: 1998*, NASA/TM-209237, chap 4, Greenbelt, Maryland, pp 71-101.

Sander, S. P., R. R. Friedl, W. B. DeMore, D. M. Golden, M. J. Kurylo, R. F. Hampson, R. E. Huie, G. K. Moortgat, A. R. Ravishankara, C. E. Kolb, and M. J. Molina, 2000: *Chemical Kinetics and Photochemical Data for Use in Stratospheric Modeling*, Supplement to Evaluation 12: Update of Key Reactions, Jet Propulsion Laboratory (JPL) Publication 00-3, Pasadena, California.

Wei, C. -F., S. M. Larson, K. O. Patten and D. J. Wuebbles, 2001: Modeling of ozone reactions on aircraft-related soot in the upper troposphere and lower stratosphere, *Atmospheric Environment*, 35, 6167-6180.

Wuebbles, D. J., K. Patten, M. T. Johnson and R. Kotamarthi, 2001: New Methodology for Ozone Depletion Potentials of short-lived compounds:n-Propyl bromide as an example, *J. Geophys. Res.*, 106, 14,551-14,571.

Stratospheric Ozone Sensitivity to Aircraft Cruise Altitudes and NOx Emissions

S. L. Baughcum*
The Boeing Company, Seattle, Washington, USA

I. C. Plumb, P. F. Vohralik
Commonwealth Scientific and Industrial Research Organization (CSIRO), Telecommunications and Industrial Physics, Lindfield, New South Wales, Australia

Keywords: ozone, NOx, aircraft emissions

ABSTRACT: The stratospheric ozone impact of higher flying aircraft is sensitive to the cruise altitude, NOx emission levels, and fleet fuel use at cruise altitude. In this paper, we explore the sensitivity of stratospheric ozone impact for a fleet of supersonic aircraft to the choice of the recommended rate constant compilations (e.g., JPL97, JPL00 or JPL02) using the CSIRO 2-D chemical transport model (CTM). We also present the results obtained for a range of parametric aircraft emission scenarios using the JPL00 recommendations. The parametric scenarios were based on aircraft emissions for long range (greater than 2500 nautical mile) missions projected to the year 2020. Cruise altitudes were varied in 2 km increments over the 13 to 21 km altitude range and NOx emission indices [EI(NOx)] of 5, 10, 15, and 20 grams(NO_2)/kilogram fuel use are considered. The column ozone impact was found to depend strongly on cruise altitudes for flights above 15 km. Very little impact on annual average column ozone was calculated for emissions at 13-15 km, but this would be an altitude band better suited for studies with a coupled stratosphere/troposphere 3-D CTM. Ozone response was found to depend linearly on NOx emissions.

1 INTRODUCTION

The impact on stratospheric ozone by emissions from fleets of supersonic aircraft has been of interest for a number of years. Most recently, the impact of possible fleets of Mach 2.4 supersonic aircraft (referred to as high speed civil transport, HSCT) cruising at altitudes of 18-20 km was evaluated by the IPCC (Isaksen et al., 1999, hereafter referred to as IPCC99) and by NASA (Kawa et al., 1999). These studies concluded that both NOx and water vapor emissions could contribute to ozone loss in the stratosphere. In addition, production of sulfate aerosols in the exhaust plume was shown to have an effect if conversion of SO_2 to SO_3 in the engine was high (i.e., tens of percent). More recent studies (Curtius et al., 2002) have shown that the conversion of SO_2 to sulfate in the plume is 2-3%, which is smaller than the values used in the IPCC report. The ozone perturbation is sensitive to the competition between NOx, HOx, and ClOx chemistry in the lower stratosphere. As a consequence, recent changes in recommended reaction rate constants from those used in the IPCC99 studies may change the calculated perturbations.

In this study, we use the CSIRO two-dimensional chemical transport model to evaluate the stratospheric ozone impact of a parametric scenario for aircraft emissions as a function of cruise altitude and NOx emission index (EI), focusing on cruise altitudes higher than the current subsonic fleet of commercial aircraft. Results are evaluated using the same rate constant set (DeMore et al., 1997, hereafter referred to as JPL97) used in the IPCC report and more recent recommendations (Sander et al., 2000, referred to as JPL00; Sander et al., 2003, referred to as JPL02).

* *Corresponding author:* Steven L. Baughcum, Boeing Company, P. O. Box 3707, MC 02-XL, Seattle, WA 98124, USA. Email: Steven.L.Baughcum@boeing.com

2 SENSITIVITY OF HSCT OZONE IMPACT TO MODEL CHANGES

The CSIRO 2-dimensional chemical transport model (Randeniya et al, 2002 and references cited therein) has been upgraded since its use in the IPCC report. Major changes include the following: 1) The addition of low temperature aerosol chemistry; 2) Radiative heating rates are now calculated using the NCAR CCM column radiation model using NCEP temperatures, the MMII ozone climatology (Park et al., 1999), and mean ISCCP cloud parameters (Rossow and Schiffer, 1991); 3) Zonal temperature variations based on the NCEP reanalysis (Kalnay et al., 1996) are used for both gas phase and heterogeneous chemistry calculations; 4) A complete implementation of the JPL00 chemical and photolysis recommendations is used as the baseline although other reaction rate sets can be used; 5) The vertical resolution of the model has been upgraded to 1 km, while the latitudinal resolution remains 5 degrees.

To evaluate the sensitivity of the calculated ozone impact to changes in the model and sensitivities to the choice of reaction rate constants, the HSCT emission scenarios (Baughcum and Henderson, 1998) used in IPCC99 were run for the case of a fleet of 500 HSCTs with NOx emission indices of 5, 10, and 15 grams of NO_2 per kilogram of fuel. The SA0 case (no additional sulfate aerosol) from the IPCC99 study was chosen with a 2015 background atmosphere.

Figure 1 shows the results comparing four cases: the IPCC99 results using the 1997 version of the CSIRO model, the current version of the model using the JPL97 rate recommendations, the current version of the model using the JPL00 rate recommendations, and the current version of the model using a partial update to the JPL02 recommendations in which the bimolecular and termolecular reactions have been updated but not the photolysis rates.

As seen in Figure 1, the current version of the model using JPL97 chemistry (curve labelled JPL97) predicts a larger ozone impact than the IPCC99 version. The new version has greater accumulation of exhaust emissions and lofts more NOx to the higher altitudes where NOx chemistry dominates the ozone removal process. As a consequence, the current version of the model predicts a stronger dependence on EI(NOx). Updating the reaction rate constants and photolysis cross sections to the JPL00 recommendations increases the calculated ozone perturbation. The partial update to the JPL02 recommendations results in a further increase in the impact, but not as large as that from JPL97 to JPL00 chemistry. More discussion of the latter awaits a complete implementation of the JPL02 recommendations.

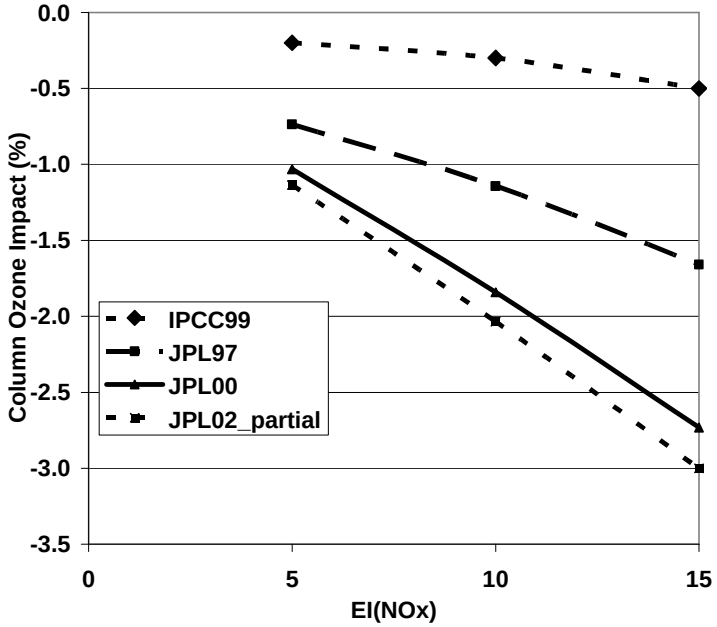

Figure 1. Annual average column ozone change (%) in the Northern Hemisphere as a function of EI(NOx) for different model versions and choice of reaction rate recommendations for an assumed fleet of 500 HSCTs flying at 18-20 km cruise altitudes.

3 PARAMETRIC SENSITIVITY

As aircraft speed increases, the cruise altitude increases. Emission scenarios for possible future aircraft types need to consider the accessible market, airplane/engine performance, emissions characteristics, and possible route structure. These will vary depending on the size, range, detailed design, year of entry into service, and cost of the aircraft with different markets for different airplane concepts. Rather than trying to forecast different scenarios for different airplane types, in this study we consider a parametric approach in which the geographical distribution of the emissions is fixed and the emissions are moved up/down systematically in altitude. The fleet fuel use at cruise altitudes depends on the number of aircraft, the single airplane fuel use rate, and the number of hours spent at cruise altitude. For the results presented here, we treat fleet fuel use as a constant and systematically vary cruise altitude and EI(NOx).

The parametric aircraft scenarios are based on a projection of scheduled air traffic for 2020 (Sutkus et al., 2003). For this study, we focus on aircraft which are faster than today's commercial aircraft and which would presumably be used primarily on long range routes where speed is important. We therefore include only flights longer than 2500 nautical miles. The 2020 scenario was rerun using only such flights. The geographical distribution of the projected fuel use of this 2020 long range scenario on a 1 degree latitude x 1 degree longitude grid in the 9-13 km altitude band was used as the geographical distribution for the parametric scenarios. Such flights account for approximately 50% of the total projected cruise fuel use in 2020 which was projected to be 242 Tg/year.

The geographical distribution of the fuel consumption in the parametric scenarios is shown in Figure 2. For the parametric studies, we assume that a viable new airplane type could account for approximately 20% of the cruise fuel use of the flights longer than 2500 nautical miles (24 Tg/year). The cruise emissions are then assumed to be uniformly distributed vertically over a 2 km band. These parametric emissions are then added to the base case 2020 scenario. Model runs are done using these combined parametric scenarios and then the perturbations are calculated relative to a model run with the base case emissions only. For comparison, the earlier HSCT studies assumed a cruise fuel use of 47 Tg/year but the HSCT was a very fuel-inefficient concept compared to modern subsonic aircraft.

For the parametric calculations of altitude and NOx level, a 2020 background atmosphere based on the IPCC SRES A2 scenario (IPCC, 2001) is used. The stratospheric aerosol background was assumed to be that of the SA0 case from IPCC99. These model runs were done using the JPL00 recommendations for rate constants and photolysis cross sections. Four altitude bands were considered: 13-15 km, 15-17 km, 17-19 km, and 19-21 km. These altitudes are higher than those of current subsonic aircraft and correspond to higher speeds than today's commercial aircraft. As a sensitivity study, EI(NOx) values of 5, 10, 15, and 20 grams (NO_2)/kg(fuel) were considered to cover a range of possible emission technology levels from the very aggressive (EI=5) to a value four times higher. The model calculations consider both NOx and water vapor emissions but do not consider the effects of sulfate aerosol emissions.

The change in absolute ozone profile as a function of height for the four different aircraft cruise altitudes is shown in Figure 3. For each parametric scenario considered, the major impact on ozone column occurs at altitudes above the cruise altitudes with the ozone impact increasing with higher cruise altitudes.

Since most of the emissions are predicted to occur in the Northern Hemisphere, the largest ozone impact occurs there with increasing impact at higher latitudes (not shown). As shown in Figure 4, the model predicts a strong dependence of ozone impact on cruise altitude, increasing with higher cruise altitudes and with higher NOx levels. The ozone impact for aircraft flying in the 13-15 km altitude band is calculated to be very small. However, a 3-dimensional model calculation is required to support this conclusion because of the limitations of using a 2-D CTM near the tropopause. The sensitivity to NOx increases with flight altitudes, as shown by the slopes of the lines in Figure 4.

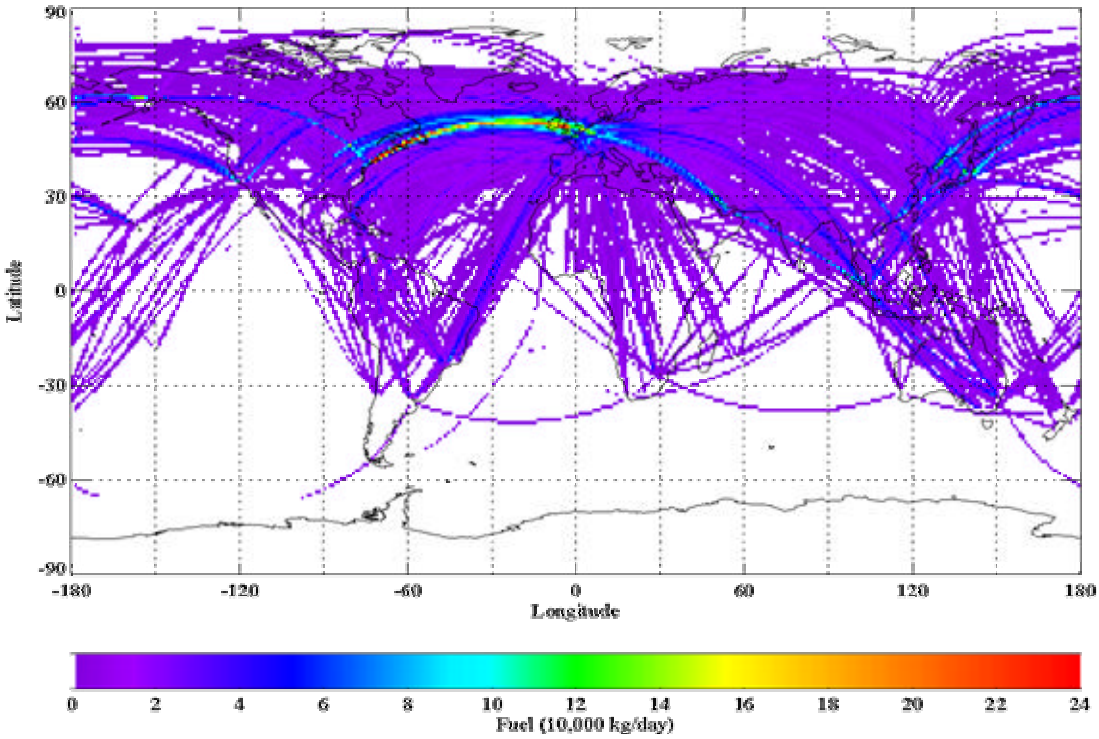

Figure 2. Geographical distribution of cruise fuel use in parametric scenarios.

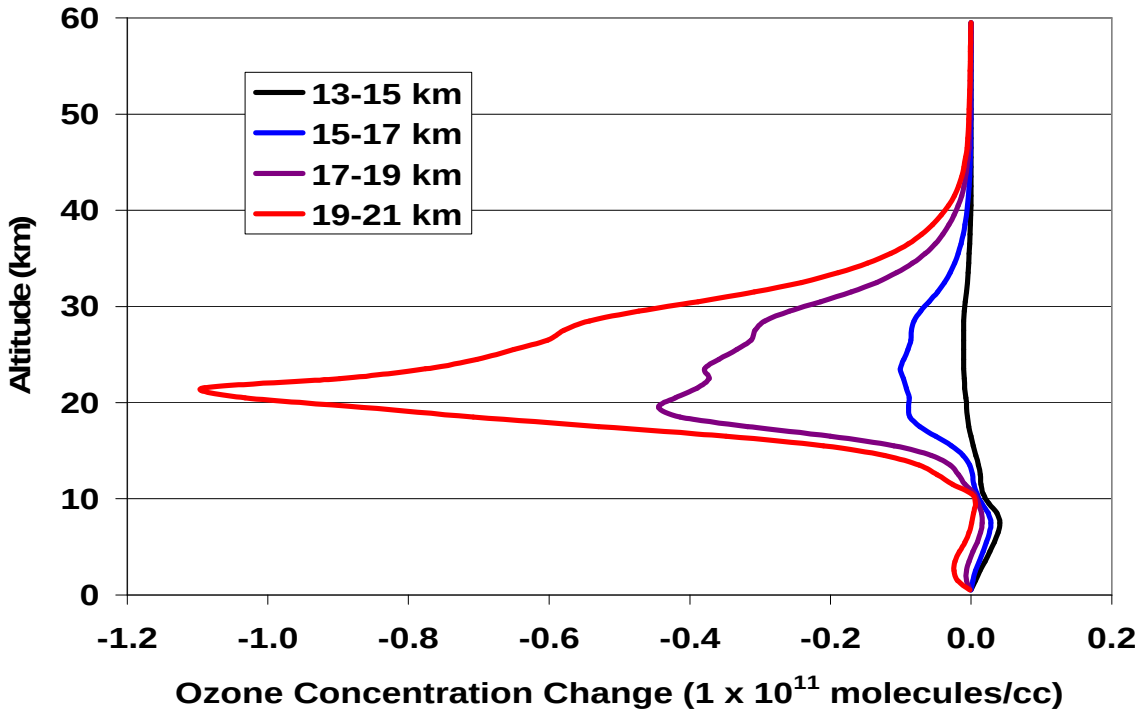

Figure 3. Absolute ozone concentration change as a function of altitude for four different cruise altitudes. The results shown are for the EI(NOx)=10 case at 40-45 degree North latitude in July.

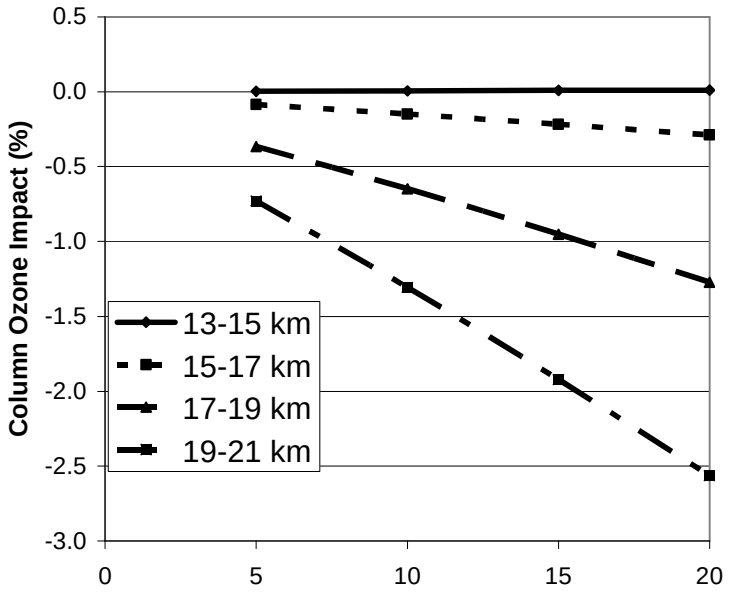

Figure 4. Annual average northern hemisphere column ozone change for the parametric emission scenarios as a function of EI(NOx) for four different cruise altitude bands.

4 CONCLUSIONS

The updated version of the CSIRO 2-D model calculates larger ozone perturbations for aircraft flying at 18-20 km than were obtained using the older version of the model in the IPCC99 assessment. These differences are due to both changes in the model transport and to the use of the updated JPL reaction rate coefficients (e.g., the reduced rate of the $OH + NO_2 + M \rightarrow HNO_3 + M$ reaction) and photolysis cross sections. This results in a greater sensitivity of ozone depletion to NOx emission levels than in the previous assessments. We expect that other models (both 2-D and 3-D) will calculate larger ozone impacts when using the latest JPL recommendations.

The parametric results showed the calculated ozone impact was small for cruise altitudes in the 13-15 km altitude band. The ozone depletion increased sharply as the flight altitudes exceeded 15 km. The sensitivity of ozone to NOx emissions was found to increase with higher cruise altitudes. This suggests that low NOx combustors will be important if large fleets of supersonic aircraft ever become viable.

Uncertainties in the transport and accumulation of aircraft emissions remain significant, particularly for cruise altitudes near the tropopause. This will require continued development of models (e.g., 3-D models) to better quantify the aircraft impact.

REFERENCES

Baughcum, S. L., and S. C. Henderson, 1998: *Aircraft Emission Scenarios Projected in Year 2015 for the NASA Technology Concept Aircraft (TCA) High Speed Civil Transport*, NASA/CR-1998-207635.

Curtius, J., F. Arnold, and P. Schulte, 2002: Sulfuric acid measurements in the exhaust plume of a jet aircraft in flight: Implications for the sulfuric acid formation efficiency, *Geophys. Res. Lett*., 29, No. 7, 10.1029/2001GL013813.

DeMore, W. B., S. P. Sander, D. M. Golden, R. F. Hampson, M. J. Kurylo, C. J. Howard, A. R. Ravishankara, C. E. Kolb, and M. J. Molina, 1997: *Chemical Kinetics and Photochemical Data for Use in Stratospheric Modeling, Evaluation Number 12*, JPL Publication 97-4. (http://jpldataeval.jpl.nasa.gov/)

IPCC, 2001: *Climate Change 2001: The Scientific Basis. Contributions of Working Group I to the Third Assessment Report of the Intergovernmental Panel on Climate Change* [Houghton, J. T., Y. Ding, D. J. Griggs, M. Noguer, P. J. van der Linden, X. Dai, K. Maskell, and C. A. Johnson (eds.)]. Cambridge University Press, Cambridge, United Kingdom, 881 pp.

Isaksen, I., C. Jackman, S. L. Baughcum, F. Dentener, W. Grose, P. Kasibhatla, D. Kinnison, M. Ko, J. McConnell, G. Pitari, and D. Wuebbles, 1999: "Modeling the Chemical Composition of the Future Atmosphere,", Chapter 4 in the *Intergovernmental Panel on Climate Change (IPCC) Special Report on Aviation and the Global Atmosphere*, [J. E. Penner, D. H. Lister, D. J. Griggs, D. J. Dokken, and M. McFarland (eds.)] Cambridge University Press.

Kalnay, E., et al., 1996: The NCEP/NCAR 40-year reanalysis project, *Bull. Am. Meterolog. Soc.*, 77, 437-471.

Kawa, S. R., J. G. Anderson, S. L. Baughcum, C. A. Brock, W. H. Brune, R. C. Cohen, D. E. Kinnison, P. A. Newman, J. M. Rodriguez, R. S. Stolarski, D. Waugh, and S. C. Wofsy, 1999: *Assessment of the Effects of High-Speed Aircraft in the Stratosphere: 1998*, NASA Technical Report TP-1999-20923.

Park, J. H., M. K.W. Ko, C. H. Jackman, R. A. Plumb, J. A. Kaye, and K. H. Sage, 1999: *Models and Measurements Intercomparison II*, NASA/TM-1999-209554.

Randeniya, L. K., P. F. Vohralik, and I. C. Plumb, 2002: Stratospheric ozone depletion at northern mid latitudes in the 21st century: The importance of future concentrations of greenhouse gases nitrous oxide and methane, *Geophys. Res. Lett.*, 29, No. 4, 10.1029/2001GL014295.

Rossow, W.B. and R.A. Schiffer, 1991: ISCCP cloud data products, *Bull. Am. Meteorol. Soc.*, *72*, 2-20.

Sander, S. P., R. R. Friedl, W. B. DeMore, A. R. Ravishankara, D. M. Golden, C. E. Kolb, M. J. Kurylo, R. F. Hampson, R. E. Huie, M. J. Molina, G. K. Moortgat, 2000: *Chemical Kinetics and Photochemical Data for Use in Stratospheric Modeling, Supplement to Evaluation 12: Update of Key Reactions, Evaluation Number 13*, JPL Publication 00-3. (http://jpldataeval.jpl.nasa.gov/)

Sander, S. P., R. R. Friedl, D. M. Golden, M. J. Kurylo, R. E. Huie, V. L. Orkin, G. K. Moortgat, A. R. Ravishankara, C. E. Kolb, M. J. Molina, and B. J. Finlayson-Pitts, 2003: *Chemical Kinetics and Photochemical Data for Use in Atmospheric Studies, Evaluation Number 14*, JPL Publication 02-25. (http://jpldataeval.jpl.nasa.gov/)

Sutkus, D. J., S. L. Baughcum, and D. P. DuBois, 2003: *Commercial Aircraft Emission Scenario for 2020: Database Development and Analysis*, NASA contractor report NASA/CR-2003-212331. (http://gltrs.grc.nasa.gov/reports/2003/CR-2003-212331.pdf)

Investigating the Global Atmosphere by Using Commercial Aircraft: CARIBIC

Andreas Zahn*
Forschungszentrum Karlsruhe, Institute of Meteorology and Climate Research, Karlsruhe, Germany

Carl Brenninkmeijer
Max-Planck-Institute for Chemistry, Atmospheric Chemistry Division, Mainz, Germany

Keywords: passenger aircraft, stratosphere-troposphere exchange, chemical composition troposphere and stratosphere

ABSTRACT: CARIBIC (Civil Aircraft for the Regular Investigation of the atmosphere Based on an Instrument Container, www.caribic-atmospheric.com) is based on the deployment of an automated laboratory inside an airfreight container that is loaded once or twice per month for conducting measurements during intercontinental flights. The advantages of this approach are obvious: for moderate effort and costs it allows detailed (>60 trace gases and aerosol parameters) and long-term (>10 years) monitoring of the upper troposphere / lower stratosphere (UTLS) along certain flight routes. The data are especially suitable for comparisons with model results and satellite observations and allows for instance the determination of seasonal variations of the species measured (which is hardly possible using data from dedicated short-term aircraft campaigns). Here, we give an overview about results gained in CARIBIC phase I (1997-2002) using a Boeing 767 by LTU Airlines and about the technical design planned for a new container deployed onboard a new Airbus A340-600 by Lufthansa AG as of 2004 (CARIBIC phase II).

1 THE USE OF PASSENGER AIRCRAFT FOR ATMOSPHERIC RESEARCH

There are some intrinsic originalities of the deployment of passenger aircraft for atmospheric research, in the following listed for CARIBIC phase II: (a) the endurance of the Airbus A340-600 is 14.800 km which enables an almost global data coverage, (b) Lufthansa promised the use of the CARIBIC container for at least 10 years which leads to a total measurement duration of more than 15 years, (c) 16 instruments are integrated which enables the measurement of more than 60 trace gases and 20 aerosol parameters, and (d) the flight costs (only airfreight costs) are (for doing research) quite moderate (~300 Euro per hour). For Lufthansa on the other hand it is financially attractive to transport the container which will guarantee the long-term deployment.

2 OBJECTIVES OF CARIBIC

The major objectives of CARIBIC are: (a) to systematically monitor the chemical composition of the UTLS (in support of the Montreal and Kyoto protocol) over a long period of time, (b) to collect representative data for the validation of results from detailed atmospheric models and satellite observations, (c) to better quantify the budgets of various trace gases and aerosol particles in UTLS, in particular to distinguish between natural and anthropogenic processes, but also to better assess the impact of aircraft emissions, (d) to better specify the emissions of the continents (possible by comparing the data measured upwind and downwind of the continents), (e) to better quantify tracer transport from the Earth surface to the UTLS and in the UTLS (convection, long-range transport, stratospheric-tropospheric exchange), and (f) to study various specific atmospheric processes such as aerosol particle formation and life cycle, the oxidation capacity of the atmosphere, cirrus clouds formation in the UT/LS etc.

* *Corresponding author:* Andreas Zahn, Forschungszentrum Karlsruhe, Institute of Meteorology and Climate Research, P.O. Box 3640, D-76021 Karlsruhe, andreas.zahn@imk.fzk.de

3 STATUS OF CARIBIC

In 1993 LTU Airlines agreed to help to realize CARIBIC and to carry a measurement container (type: LD 4) for atmospheric research. After a planning and construction phase, the first measurement phase (80 flights along three flight routes) took place between November 1997 and April 2002 using a Boeing 767-ER. The CARIBIC consortium steadily increased from 3 German institutes to nowadays 11 European institutions (www.caribic-atmospheric.com).

As of spring 2004 a new, larger container (LD 11) having a gross weight of ~1.4 tons will be flown onboard an Airbus A340-600 of Lufthansa AG. The new inlet system installed just in front of the belly fairing is shown in Figure 1.

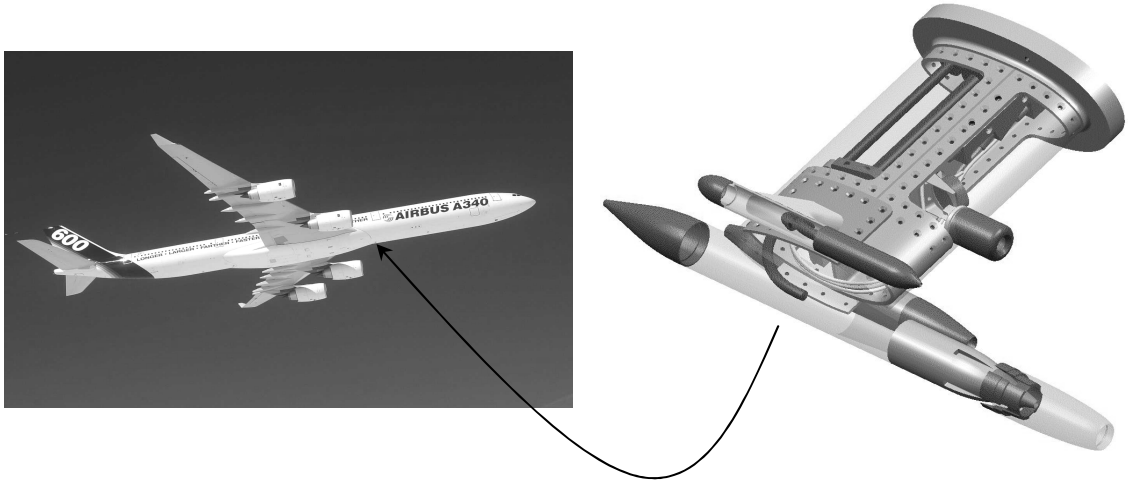

Figure 1: The new CARIBIC Airbus A340-600 with the air inlet system. It has 4 inlet tubes, a camera, and 3 telescopes for a DOAS spectrometer. Various heating foils prevent icing on the surface and minimize the absorption of sticky species such as H_2O or HNO_3 within the lines to the container.

4 MEASUREMENTS (1997-2002)

4.1 *Tropospheric distributions of ozone and carbon monoxide*

Figure 2 displays the seasonal variations of O_3 and CO in tropospheric air along the flight route Germany – Indian Ocean.

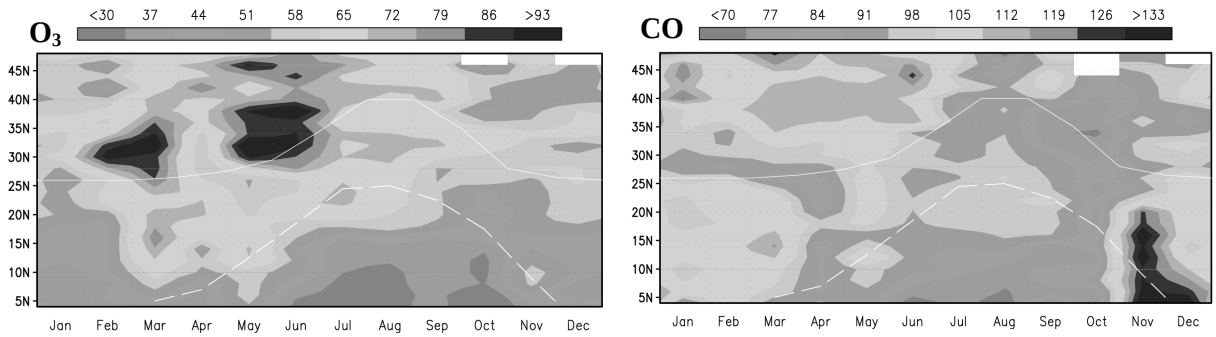

Figure 2: Seasonal variation of the mean mixing ratio (in ppbv) of O_3 (left) and CO (right) along the flight track Germany - Indian Ocean at 9-11 km altitude. The dashed line marks the mean location of the ITCZ and the straight line indicates the mean location of the subtropical jet stream.

In the extra-tropics, O_3 minimizes early winter, in spite of its just then maximum chemical lifetime. This demonstrates that the sum of the two O_3 sources, import from the stratosphere and photochemical generation in the troposphere, minimizes during early winter north of ~20°N. In the tropics, O_3 minimizes (at ~30 ppbv) from July to October which is caused by the northern location of the ITCZ that leads to supply of O_3-poor southern hemispheric air. The maximum in ozone is found from March to June, just north of the subtropical jet stream; this alludes to some stratospheric influence. The springtime O_3 maximum extends even into the tropics (from March to May) suggesting that injection of stratospheric O_3 near the sub-tropical jet significantly impacts the O_3 budget of the tropical troposphere, in agreement with findings by *Zachariasse et al.* [2000].

CO undergoes significant, but compared to the ground weak seasonal and latitudinal variations, on which occasional high CO events are superimposed. North of 30°N, CO maximizes from February until as late as June and minimizes in September-October. Along the sub-tropical jet stream low CO mixing ratios are found. This is due to the fact that this region is primarily affected by clean, chemically aged air subsiding in the downward branch of the Hadley cell. Around 20°N no clear seasonality in CO appears. This is mainly because of the unusually high concentrations from July to September, just when the actual short chemical CO lifetime (~8 weeks) suggests the lowest CO levels. This CO excess of ~30 ppbv over an estimated background of ~65 ppbv is due to outflow of the ITCZ that is located just below the CO plume (Figure 2). The ITCZ outflow area covers an extensive region at 9-11 km altitude from 10° to 30°N and 40° to 75° E, that are at least 7 10^6 km^2. Our CO data (supported by other CARIBIC data) thus provide strong evidence that large amounts of pollutants emitted in southern Asia (Indian, Bangladesh, China, Indonesia) are lofted into the upper troposphere during the Indian summer monsoon.

South of 20°N, CO minimizes from June to October (with ~75 ppbv) when the ITCZ is situated far north (reaching ~25°N in August), and hence, mainly cleaner southern hemispheric air was probed. The pronounced tropical CO plume in November/December is due to forest fires in Indonesia, a region ~4000 km south-east of the CARIBIC flight corridor, confirming that these fires can also constitute a considerable source of pollutants to the tropical free troposphere.

4.2 *Correlation between O_3 and CO in tropospheric air*

At the ground the enhancement ratio $\Delta O_3/\Delta CO$ (with ΔO_3 and ΔCO denoting the excess in the examined air mass over background air) is frequently used as a measure of the net O_3 formation that has occurred. In the upper troposphere where the excess values ΔO_3 and ΔCO are mostly small and where the air masses are mostly chemically aged, the slope of the O_3-CO correlation dO_3/dCO will give the more meaningful information on the origin of ozone [*Zahn et al.*, 2002a]. In Figure 3 the seasonal variation of the mean slope dO_3/dCO observed in tropospheric air is shown.

In the tropics, clearly positive O_3-CO slopes are measured at all seasons, i.e. 0.20-0.25 in autumn/winter and ~0.50 in spring/summer. Furthermore, the O_3-CO slopes are almost identical. Both findings demonstrate that the O_3 budget of the tropical 10 km altitude range is controlled by in situ photochemical O_3 formation year-around and that the fraction of stratospheric O_3 is small. Model calculations likewise estimate that in the tropics only 10-15 % [*Roelofs and Lelieveld*, 1997] and 5-10 % [*Lamarque et al.*, 1999], respectively, of the O_3 abundance at 10 km altitude originates from the stratosphere.

The annual mean O_3-CO slope observed in the tropics allows us to roughly estimate the net ozone production in the NH tropical troposphere arising from surface emission of O_3 precursors. Using the formula given by *Parrish et al.* [1993] and *Mauzerall et al.* [1998, 2000], this net ozone production is calculated as product of the "tropical ground-based CO emission plus atmospheric CO generation by the oxidation of hydrocarbons below 11 km" and the annual mean O_3-CO slope measured during CARIBIC in the tropics of 0.37. An annual net ozone production of 564 Tg O_3 or 17.6 x 10^{10} O_3 molecules cm^{-2} s^{-1} is inferred [*Zahn et al.*, 2002a]. This is somewhat higher than the O_3 export from East Asia in the mid-1980s estimated by *Mauzerall et al.* [2000] to 13.2 x 10^{10} O_3 molecules cm^{-2} s^{-1} and a factor of 2.5-5.9 larger than the annual mean flux of stratospheric O_3 into the troposphere estimated to be 3-7 x 10^{10} O_3 molecules cm^{-2} s^{-1} [*Lelieveld and Dentener*, 2000; *McLinden et al.*, 2000; and references therein].

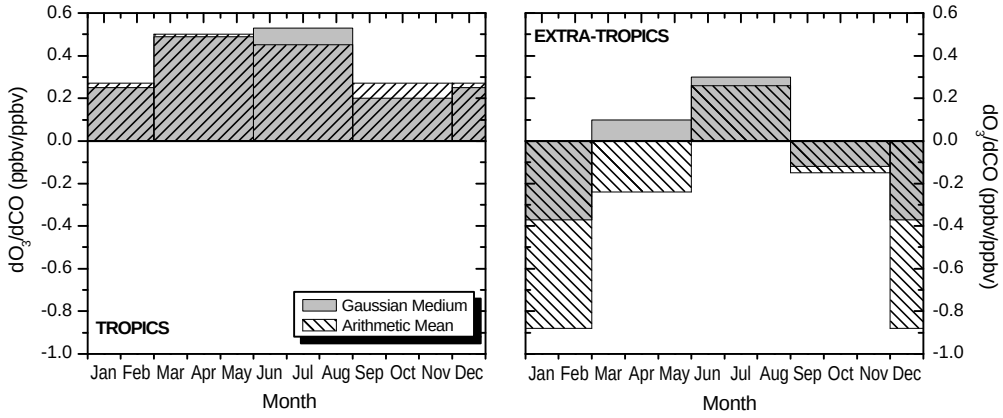

Figure 3: Seasonal variation of mean O3/CO slopes averaged along flight distances of 200-500 km. Grey bars: Mean values of the line centers of the Gaussian curves fitted to the distribution of O3-CO slopes. Shaded bars: Arithmetic mean O3/CO slopes. Left: 4-28° N (tropics), right: 28-51°N (extra-tropics).

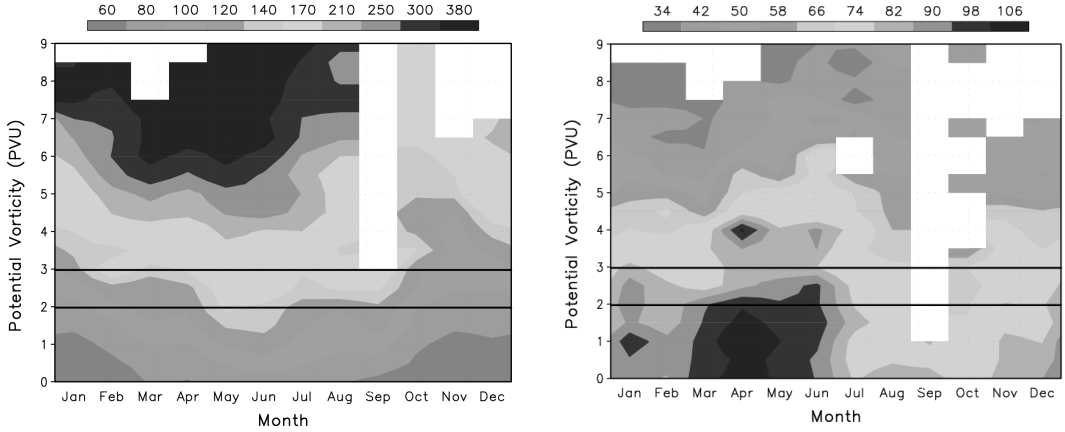

Figure 4: Mean seasonal variation of ozone (left, in ppbv) and carbon monoxide (right, in ppbv) observed during CARIBIC in the UTLS from 1997 to 2002, as function of the potential vorticity taken from ECMWF analysis.

In the extra-tropics, per contra, the two O_3-CO slopes agree well only in summer and autumn. whereas both O_3-CO slopes are negative in autumn and winter. This indicates that in winter/spring and maybe even in autumn the stratosphere is a major O_3 source for the extra-tropical 10 km altitude range, but of minor importance in summer. In summer, photochemical O_3 production clearly dominates. A more detailed analysis of the partitioning of stratospheric influx and photochemical formation is given in [*Zahn et al.*, 2002a].

4.3 *Bi-directional tracer exchange across the extra-tropical tropopause*

In Figure 4a mean CARIBIC ozone data are plotted relative to PV iso-surfaces of up to 9 PVU, which cover the upper troposphere and the lowest ~2.5 km of the lowermost stratosphere. It illustrates the downward propagation of stratospheric ozone into the troposphere. In the LS, ozone clearly maximizes in late winter/spring and strongly decreases towards the tropopause, as seen in other studies, e.g. [*Logan*, 1999].

The time lag of the O_3 maximum between the 7-9 PVU PV iso-surface (~2 km above the tropopause), and the dynamical tropopause (2-3 PVU) is ~4 weeks. Figure 4 does not take into account the 3-dimensional nature of downward transport, so that the inferred transport time of 4 weeks has to be interpreted with care. Moreover, as ozone is quite long-lived in the lowermost stratosphere, the strong O_3 decrease towards the tropopause has largely to due with dilution of in-flow of (O_3-poor) tropospheric air. This in-flow of tropospheric air into the LS is traced by the CO data (see Figure 4b). CO decreases from 70-100 ppbv at the tropopause to 35-40 ppbv at PV = 8-9

PVU, strongly exceeding the chemical equilibrium level in the LS of 10-20 ppbv. Moreover, CO undergoes a clear seasonal variation in the LS, with a gradual phase shift with altitude above the tropopause. CO maximizes in April in the UT and at the tropopause, but in mid-summer at PV = 8-9 PVU, i.e. ~2 km above the tropopause. This phase shift must also be associated with the seasonal variation of the in-flow of tropospheric air. Chemistry would result in an opposite seasonal variation in the LS, because the lifetime of CO reaches its minimum of ~2 months in summer. The gradual phase shift with altitudes can only be explained by the increasing impact of in-flowing CO-rich tropospheric air at higher potential temperatures (lower latitudes), which is expected to maximize in summer.

5 CONCLUSIONS

The first measurement phase of CARIBIC from fall 1997 to spring 2002 (with ~80 measurement flights) demonstrated the strength of using a measurement container onboard passenger aircraft. This approach guarantees a long-term and multi-tracer monitoring of the UTLS on an almost global scale. One major strength is the collection of distributions of trace gases and aerosol in the UTLS which allows to identify seasonal and (for certain species) inter-annual variations (such as CO) and trends (such as SF_6). Substantial seasonal and latitudinal variations of the distributions of O_3 and CO and of the partitioning between influx of stratospheric O_3 and photochemical O_3 production are found. The distinction of the two major O_3 sources is accomplished by applying CO as a tracer of O_3 precursors. Positive O_3-CO co-variations are assigned to O_3 formed photochemically and negative ones to O_3 imported from the stratosphere. In the tropics, photochemical O_3 production clearly dominates year around, which is demonstrated by the ever positive O_3-CO slopes of 0.20-0.27 in autumn/winter and of 0.45-0.53 in spring/summer. In the extra-tropics, the well-documented O_3 maximum was confirmed. Stratospheric O influx and photochemical O_3 production contribute equally to this maximum. In winter, the O_3-CO slopes are with –(0.4-0.8) strongly negative, indicating dominance of import of stratospheric O_3. In summer, on the contrary, the O_3-CO slopes are with 0.3 positive and photochemical O_3 formation clearly dominates. In autumn, both O_3 sources are weak. Strong seasonal variations of O_3 and CO are observed above the extra-tropical tropopause. These seasonal variations can only be explained by active bi-directional tracer exchange across the extra-tropical tropopause. Further details can be found in *Zahn et al.* [2002a, 2002b] and *Zahn and Brenninkmeijer* [2003].

REFERENCES

Lelieveld, J., and F.J. Dentener, What controls tropospheric ozone?, *J. Geophys. Res., 105*, 3531-3551, 2000.

Logan, J.A., An analysis of ozonesonde data for the troposphere: Recommendations for testing 3-D models and development of a gridded climatology for tropospheric ozone, *J. Geophys. Res., 104*, 16,115-16,149, 1999.

Mauzerall, D.L., et al., Photochemistry in biomass burning plumes and implications for tropospheric ozone over the tropical south Atlantic, *J. Geophys. Res., 103*, 8401-8423, 1998.

Mauzerall, D.L., D. Narita, H. Akimoto, L. Horowitz, S. Walters, D.A. Hauglustaine, and G. Brasseur, Seasonal characteristics of tropospheric ozone production and mixing ratios over East Asia: A global three-dimensional chemical transport and model analysis, *J. Geophys. Res., 105*, 17,895-17,910, 2000.

McLinden, C.A., S.C. Olsen, B. Hannegan, O. Wild, M.J. Prather, and J. Sundet, Stratospheric ozone in 3-D models: A simple chemistry and the cross-tropopause flux, *J. Geophys. Res., 105*, 14,653-14,665, 2000.

Zahn, A., C.A.M. Brenninkmeijer, P.J. Crutzen, G. Heinrich, H. Fischer, J.W.M. Cuijpers, and P.F.J. van Velthoven, Distributions and relationships of O_3 and CO in the upper troposphere: The CARIBIC aircraft results 1997-2001, *J. Geophys. Res., 105(D17)*, 4337, doi: 10.1029/2001JD001529, 2002a.

Zahn, A., et al., The origin of tropospheric ``ozone clouds", *J. Geophys. Res., 105(D22)*, 4638, doi: 10.1029/2001JD002345, 2002b.

Zahn, A., C.A.M. Brenninkmeijer, New Directions: A chemical tropopause defined, *Atmos. Environment*, 37(3), 439-440, 2003.

The Importance of Aviation for Tourism – Status and Trends

S. Gössling*
Dept. of Service Management, Lund University, Sweden

Keywords: Air travel, disease, energy use, risk perception, tax, tourism, terror, war

ABSTRACT: In industrialized countries, leisure-related travel has continuously increased and accounts now for about 50% of all distances traveled. On average, leisure-related mobility in industrialized countries is in the order of 20 pkm per capita per day, with air travel accounting for 15-20% of the distances covered (3.5 pkm per capita per day). In the future, air travel is likely to increase substantially, both as a result of changing leisure conceptions in industrialized countries, the emergence of low fare airlines, and the increasing participation of people from developing countries in air travel. There is, however, some uncertainty about i) the role of energy taxes, soon to be introduced in industrialized countries, and ii) the changing risk perception of tourists and its consequences for travel behavior; this is, the importance of terror attacks, war, and globally spreading diseases such as SARS. The paper seeks to discuss the development of leisure-related air travel with respect to these aspects and makes suggestions for mitigation strategies.

1 INTRODUCTION

Purposes of travel can be divided into leisure, work, service/shopping, and other (Carlsson-Kanyama and Lindén, 1999). Evidence from travel surveys suggests that leisure-related travel accounts for about 50% of all travel in the industrialized countries. This proportion has, for example, been found in travel surveys in Norway (for travel distance, Høyer, 2001), Sweden (for travel time, travel distance, and travel frequency; Carlsson-Kanyama and Lindén, 1999), Germany (for travel distance, excluding travel abroad; Heinze, 2000) and Austria (for travel distance; Knoflacher, 2000). In more detail, the average per capita mobility in Norway was about 33 pkm per day in 1992, half of this (17 pkm) for leisure-related purposes (Høyer, 2001). In Australia, average mobility was about 44 pkm per day (Lenzen, 1999), and in Sweden, daily travel was 45 pkm in 2000 (car: 33 pkm, other: 12 pkm), about 45% of this for leisure (SCB/SIKA, 2001). In Germany, per capita mobility was 33 pkm in 1995 (car: 24 pkm, air travel: 4 pkm, train: 2 pkm, other: 3 pkm), about half of this for leisure-related purposes (BMV, 1996, excluding distances traveled abroad). An analysis by Schafer (2000) indicates daily per capita travel distances of 29 pkm in Great Britain (1995/97, leisure-related: 41%), 41 pkm in The Netherlands (1995, leisure-related: 36%), 33 pkm in Switzerland (1994, leisure-related: 50%), and 62 pkm in the United States (1995, leisure-related: 31%).

Available data seem to indicate that daily mobility in industrialized countries is in the order of 40 pkm per day, about half of this for leisure-related purposes. Out of the roughly 20 pkm traveled for leisure, car travel may account for 70-75%, air travel for 15-20%, and other means of transport for 5-10%. The distribution of the means of transport is different in reforming and developing countries (cf. Schafer and Victor, 1999; Schafer, 2000), with a lower share of leisure-related travel and a greater proportion of public transport. Table 1 shows the distribution of leisure distances traveled in industrialized, reforming and developing countries.

According to this estimate, world travel was 23,970 billion pkm in 2001, which compares to 23,231 billion pkm calculated by Schafer and Victor (1999) for the mid 1990s. Leisure-related travel may, according to this estimate, only constitute one third of the total global (roughly 8 billion pkm), which is mainly a result of the low proportion of leisure-related travel in reforming and developing countries. Overall, leisure-related transport is unequally distributed: the industrialized countries, which constitute only 15% of the world's population, account for 82% of the global leisure-related transport. This figure is even more skewed with respect to air travel. The

* *Corresponding author:* Stefan Gössling, Department of Service Management, Lund University, Box 882, SE-251 08 Helsingborg, Sweden. Email: stefan.gossling@msm.hbg.lu.se

industrialized countries account for 97.5% of the distances covered globally by air for leisure-related purposes (Table 2).

Table 1. Leisure mobility in industrialized, reforming and developing countries[2], 2001

	Industrialized countries		Reforming countries		Developing countries	
	% distances	pkm/day	% distances	pkm/day	% distances	pkm/day
Car	70-75	14.5	40	1.5	20	0.1
Air travel	15-20	3.5	5	0.2	0	< 0.1
Other	5-10	2.0	55	3.8	80	0.5

Source: Gössling 2002a

Table 2. Distances Travelled Globally by Air in 2001, Leisure-related Purposes

	billion pkm	% total
Industrialized countries	1,150	97.5
Reforming countries	29	2.5
Developing countries	<0.1	<0.1
Total	1,179	100

Source: Gössling 2002a

Furthermore, the calculation suggests that global air travel for leisure-related purposes may have accounted for roughly 50% (1,179 billion pkm) of the total passenger kilometers flown (2,410 billion pkm in 1996; Schumann, 1997). However, this is a comparison of data for 1996 and 2001, and the actual figure may thus be somewhat lower than 50%, even though it also needs to be considered that some national statistics exclude distances traveled by air abroad (cf. Heinze, 2000 for Germany). The leisure-related proportion of air travel in the industrialized countries may thus be underestimated: for example, in the UK, international leisure trips represented 79% of all air trips (in 1996; Graham 2000), and in Germany, leisure trips accounted for 69% of the total distances flown (in 1993; Knisch and Reichmuth, 1996).

In order to calculate the energy use associated with leisure-related air travel, the passenger kilometers flown were multiplied by factor of 2.0 MJ per pkm. Leisure related air travel may thus have contributed with 2,360 PJ to global energy use, which represents about 18% of the leisure mobility-related energy use of 13,200 PJ, or 0.6% of the global energy use in 2001. It should be noted, though, that these figures are conservative because they do not consider the energy used during the life-cycle of an aircraft for production, maintenance, etc. Lenzen (1999), for example, assumes that such energy requirements are the order of 25% to 65% of the direct energy use for passenger transport.

2 CONTINUED GROWTH?

In 2001, about 715 million international tourist arrivals were counted, the large majority of these originating from the industrialized countries (WTO, 2003a). The World Tourism Organization (WTO) predicts growth rates of 4.1% per annum to 2020 (WTO, 2001). Air travel seems to gain importance: while the observed growth rate in international tourist arrivals was on average 5.2% per year in the period 1991-1996, arrivals by air increased by 7.8% per year during the same period. In the following, the driving and limiting factors of air-travel related tourism development will be discussed.

[2] 1) Industrialized countries: Australia, Canada, *Europe*, New Zealand, Japan, USA; Reforming countries: Bulgaria, Chile, Croatia, Czech Republic, Estonia, Hungary, South Korea, Lithuania, Latvia, Macedonia, Malaysia, Poland, Romania, Russia, Slovak Republic, Ukraine; Developing countries: all other

2.1 *Factors that may lead to further growth*

Travel surveys indicate a strong correlation between income, education and distances travelled. For example, in Sweden, men with postgraduate education and men in the highest income group, travelled 70% and 54% more (travel distances) than men on average (SCB/SIKA, 2001). With globally rising incomes and better education, it can thus be assumed that leisure-related travel will see further growth, particularly if the so far largely underrepresented reforming and developing countries will start to travel more frequently. Furthermore, within the industrialized countries, growth in air travel has been accelerated through the emergence of low fare carriers. For example, Ryanair announced to have carried more than 2 million passengers in July 2003. In order to "celebrate" this, the airline offers 2 million seats from £15 one way on routes within Europe, including all taxes, fees and charges (Ryanair, 2003). Prices for air travel in many European countries are now far lower than those for trains and busses. With respect to international journeys, there is a strong trend towards last-minute tourism, reflecting the fact that destinations become increasingly replaceable. The price for a vacation and the time it takes to get there are now dominating many travel decisions. This, in turn, has led to more competition within the travel markets, often with the result of further decreasing prices.

From a psychological point of view, the growth in leisure-related travel can be explained with changes in the perception and understanding of the environment, a process of cosmopolitization (Gössling 2002b). Social identities emerge out of particular social structures that incorporate the elements space, time, and memory. These elements are continuously negotiated, a process in which travel plays an important role. While limited or virtual travelling (e.g. by watching TV) might enforce local embedment in juxtaposition to an imagined or perceived other (such as a neighbouring country), massive mobility might instead transform social identities towards a cosmopolitan configuration of the self as localities and their characteristics lose importance (Urry, 1995). In other words: the world may "shrink" in the eyes of frequent travellers, and travel, both for work and tourism, may disrupt the very sense of what is a person's home. Without this sense, citizens do not perceive themselves as part of places any longer, and develop cosmopolitan identities. Tourism could thus be seen as an agent of modernization, which decontextualizes and dissolves the relationships individuals have with certain places. In the context of global environmental change, this is problematic because cosmopolitan people may increasingly lose their understanding of the ecological limits of places, for which local knowledge is required, and, ultimately, they may also lose the very responsibility to care for places. As a result of this process, the environment becomes "global" and global mechanisms need to be found for safeguarding it. This is problematic, because it is individual behavior that sums up to global problems, and thus individual behavior that can reduce environmental problems - however, cosmopolitan people tend to travel more frequently, and thus cause more environmental problems. In this context, another aspect deserves to be mentioned. One of the major factors leading to the global increase in tourism is an environmental consciousness, which results in an interest to experience unknown places or other environments (Urry, 1995). Environmental consciousness comes basically into existence through education, film, or written media and the comparison of the character of the physical and built environment of different places. It has thus been argued that tourism will lead to a growing environmental consciousness and interest. However, as tourism is also a result of this very environmental consciousness, the entire process could be seen as self-reinforcing, leading to more travel.

2.2 *Factors that may inhibit growth*

Given a stable economic situation, two major aspects could counter the current trend of growing tourist numbers. First, as mentioned above, the price of a vacation has a strong influence on travel decisions. There are some signs that a tax on aviation fuels will be introduced in the industrialized countries (WTO, 2003b), which could inhibit growth in air travel, even though Brons et al. (2002) have shown that price elasticities in air travel are indeed very complex. Second, the tourists' risk perception plays an important role, as it guides travel behaviour. Three important events have influenced tourism in the last years: terror attacks, war, and the global spread of diseases such as SARS. The single most important event in 2001 was the 11th September. Immediately after the event, 40–50 per cent of tourist reservations were canceled, and after three months international tourism had dropped by about 30 per cent on average (di Castri, 2002b). However, seen over the

entire year, international tourist arrivals declined by only 0.6%. In 2002, a range of attacks on tourists occurred. 19 tourists were killed in Djerba, 202 in Bali and 16 in Kenya. Despite of these events, which were also reported on the global news, international tourist arrivals grew by 3.1%. Finally, in 2003, the Severe Acute Respiratory Syndrome (SARS) spread worldwide. On June 2003, 8,459 cases had been reported in more than 30 countries, leading to 60% less long-distance arrivals in the region of origin of the disease, Hongkong. Furthermore, the United States and Great Britain waged a war in Iraq, which received broad media-coverage. Nevertheless, the WTO (2003a) reports that tourist arrivals are on the increase and it seems likely that international visitor numbers will outpace those of 2002. In conclusion, tourism seems surprisingly resilient to terror, war, and epidemics, which is reflected in constantly growing tourist numbers. However, countries with travel warnings or countries that are immediately affected by such events may see plummeting tourist numbers, as tourists tend to travel to regions perceived as safe instead.

3 SUSTAINABILITY

The tourism industry argues that air travel accounts only for a minor share of the global energy use, and – given its economic importance – that it thus be neglected when planning for sustainability. This view ignores the fact that a minor proportion of the world's population is responsible for this energy use. With respect to leisure, one estimate is that 5% of the world's population is responsible for about 40% of the global leisure-related energy use, in particular including air-based transport (cf. Gössling, 2002a). Per capita calculations of energy use, CO_2-equivalent emissions, or ecological footprints associated with air travel all suggest that air travel is not sustainable (cf. Carlsson-Kanyama and Lindén, 1999; Gössling, 2000; Gössling et al., 2002; Høyer, 2001). The environmental impacts of air travel should thus be calculated on a per capita level, which can be illustrated with an example: extrapolating the current level of air travel in industrialized countries to reforming and developing countries would result in a six-fold increase of passenger kilometres flown (to 7,730 billion pkm), with a corresponding energy use of 15,460 PJ.

In view of aviations' current impact on the environment, mitigation strategies have been suggested. These are so far primarily technological in character (see, for instance, Ponater et al.; Noland et al. this volume), and the potential of socio-economic mitigation strategies should thus also be analyzed. Some suggestions will be made here, even though it is beyond the scope of this paper to provide an in-depth analysis of this topic. First of all, the knowledge that flying is harmful to the environment seems not as widespread as one might think. There has certainly been some media-coverage in the late 1990s, but judging from current developments in air travel, the broader public seems not concerned. A first step towards mitigation might thus be to launch information campaigns about the environmental consequences of aviation in order to ensure that everybody is aware of these. However, this might not necessarily lead to changing travel behavior. For example, the Germans with the highest environmental consciousness were also identified as those traveling most for leisure-related purposes (Preisendörfer, 1998). Environmental knowledge needs thus to go along with the right attitude to result in altered travel behavior. Information should thus be provided in combination with attempts to change basic attitudes (Nilsson and Küller, 2000), while prices for air travel should be substantially increased (cf. Crouch, 1994; Brons et al., 2001). In this context it is worth mentioning that future aircraft powered by hydrogen and/or fuel cells might have a substantial effect on travel behavior – less because of the additional costs involved (30-50 billion of dollars for the development of this aircraft seem likely, and operating costs will also be higher), but rather because such aircraft would be 20-40% slower in cruise flight (Paul Peeters, 2003; personal communication).

Another aspect to be considered is that a minor proportion of tourists accounts for the majority of the distances covered – this has been termed the 20 : 80 rule of thumb (Paul Peeters, 2003; personal communication), which implies that 20% of the journeys cause 80% of the environmental impact. In Germany, for example, the 14% of the longer vacation journeys to destinations outside Europe were responsible for almost 55% of the energy use (in 1993; Knisch and Reichmuth, 1996). An identification of these most harmful journeys and their substitution for other forms of vacations could thus be of great help in reducing the overall impact of air travel. Obviously, the tourist

industry and their advertisement campaigns play an important role in this process, particularly in the supply-driven tourist markets.

Finally it should be acknowledged that the tourist industry itself has now recognized that leisure tourism is a problem for the environment (WTO, 2003b). However, there is still a tendency to play down the importance of aviation, and claims for action seem purely rhetoric. Furthermore, there is a trend to present the benefits of tourism to the public in order to create a positive discourse. For example, the new buzzword of the World Tourism Organization is "sustainable tourism - poverty alleviation", and the TUI, Germany's largest tour operator, claims that the world needs more tourism in order to shut down environmentally harmful industries.

4 CONCLUSIONS

Some basic conclusions can be drawn from this analysis. First, the spatial globalization of travel seems to have reached its limits: virtually any place in the world is accessible within 24 hours, provided the financial means. However, not all regions of the world are equally connected to each other, and it can thus be expected that the network of airports will become denser, particularly in reforming and developing countries. In line with these developments, the societal globalization of travel, this is the participation of all human beings in air travel on an equal footing, will lead to further growth in international tourist arrivals.

The article has also shown that leisure tourism is responsible for half of the distances travelled by air, and its share is continuously increasing. Given the current trends in low fare air travel, the wish to experience other places, and tourism's resilience to terror, war, and globally spreading diseases, growth in leisure-related mobility seems likely even from this perspective.

Finally, mitigation strategies should consider socio-economic aspects and not purely focus on technical solutions in order to make aviation more sustainable.

REFERENCES

Brons, M., E. Pels, P. Nijkamp, P. Rietveld, 2002: Price elasticities of demand for passenger air travel: a meta-analysis, *Journal of Air Transport Management* 8 (3): 165-175

Bundesverkehrsministerium (BMV), 1996: Verkehr in Zahlen. Deutsches Institut für Wirtschaftsforschung, Berlin.

Carlsson-Kanyama, A. and A.-L. Lindén, 1999: Travel patterns and environmental effects now and in the future: implications of differences in energy consumption among socio-economic groups. *Ecological Economics* 30, 405-417.

Crouch, G. I., 1994: Demand Elasticities for Short-Haul versus Long-Haul Tourism. *Journal of Travel Research*, Fall 1994: 2-7.

di Castri, F., 2002b: ‘Tourism revisited after 11 September 2001’, in F. di Castri and V. Balaji (eds), Tourism, Biodiversity and Information, Leiden, The Netherlands: Backhuys Publishers, pp. 483–8.

Gössling, S., 2000: Sustainable tourism development in developing countries: some aspects of energy-use. *Journal of Sustainable Tourism* 8(5), 410-425.

Gössling, S., C. Borgström-Hansson, O. Hörstmeier and S. Saggel, 2002: Ecological Footprint Analysis as a Tool to Assess Tourism Sustainability. *Ecological Economics* 43(2-3): 199-211.

Gössling, S., 2002a: Global environmental consequences of tourism. *Global Environmental Change* 12(4): 283-302.

Gössling, S., 2002b: Human-environmental relations with tourism. *Annals of Tourism Research* 29(4): 539-556.

Graham, A., 2000: United Kingdom. In European Conference of Ministers of Transport (ECMT) (ed.) Transport and Leisure. Report of the hundred and eleventh round table on transport economics. Paris, 15-16th October 1998. ECMT, Paris: 147-173.

Heinze, G.W., 2000: Germany. In European Conference of Ministers of Transport (ECMT) (ed.) Transport and Leisure. Report of the hundred and eleventh round table on transport economics. Paris, 15-16th October 1998. ECMT, Paris: 5-51.

Høyer, K.G., 2001: Sustainable Tourism or Sustainable Mobility? The Norwegian Case. *Journal of Sustainable Tourism* 8(2), 147-160.

Knisch, H. and M. Reichmuth, 1996: Verkehrsleistung und Luftschadstoffemissionen des Personenflugverkehrs in Deutschland von 1980 bis 2010. Texte des Umweltbundesamtes, 16/96. Umweltbundesamt, Berlin.

Knoflacher, H., 2000: Austria. In European Conference of Ministers of Transport (ECMT) (ed.), Transport and Leisure. Report of the hundred and eleventh round table on transport economics. Paris, 15-16th October 1998. ECMT, Paris: 53-88.

Lenzen, M., 1999: Total requirements of energy and greenhouse gases for Australian transport. *Transportation Research Part D* 4, 265-290.

Nilsson, M. and R. Küller, 2000: Travel behaviour and environmental concern. *Transportation Research Part D* 5: 211-234.

Preisendörfer, P., 1998: Umwelteinstellungen und Freizeitmobilität. *Tourismus Journal* 2(4): 441-456.

Ryanair, 2003: Available at: www.ryanair.com. Accessed 6 August 2003.

Schafer, A., 2000: Regularities in Travel Demand: An International Perspective. *Journal of Transportation and Statistics*, December 2000: 1-31.

Schafer, A. and D.G. Victor, 1999: Global passenger travel: implications for carbon dioxide emissions. *Energy* 24, 657-679.

Schumann, U., 1997: The impact of aviation on the atmosphere - An overview on atmospheric research within the programme 'Pollutants from Air Traffic'. In Schumann, U., A. Chlond, A. Ebel, B. Kärcher, H. Pak, H. Schlager, A. Schmitt and P. Wendling, (eds.), Pollutants from Air Traffic - Results of Atmospheric Research 1992-1997. Deutsches Zentrum für Luft- und Raumfahrt, Mitteilung 97-04 (pp. 1-21), Oberpfaffenhofen.

Statistiska centralbyrån/Statens institut för kommunikationsanalys (SCB/SIKA) 2001: RES 2000. Den nationella reseundersökningen. Birger Gustafsson AB, Stockholm.

Urry, J., 1995: Consuming Places. Routledge, London.

World Tourism Organization (WTO), 2003a: News Release. World Tourism in 2002: Better than expected. Available at: http://www.world-tourism.org/newsroom/Releases/2003/jan/numbers 2002.htm. Accessed 6 August 2003

World Tourism Organization (WTO), 2003b: Climate Change and Tourism. Available at: http://www.world-tourism.org/sustainable/climate/final-report.pdf. Accessed 6 August 2003.

World Tourism Organization (WTO), 2001: Tourism 2020 Vision. World Tourism Organization, Madrid.

The SCENIC Project: Impact of Supersonic Aircraft on the Atmosphere

O. Dessens, H.L. Rogers, J.A. Pyle.
Centre for Atmospheric Science, University of Cambridge, Lensfield Road, Cambridge, CB2 1EW, United Kingdom

ABSTRACT: New model calculations suggest that the potential impact on the atmosphere of a future fleet of supersonic aircraft, for the year 2015, is highly dependent upon the amount of nitrogen oxides (NO_x) emitted from the fleet. This result contrasts with the most recent assessment which suggested that the impact of supersonic aircraft on the atmosphere was primarily through the role of water vapour emissions both on atmospheric ozone and climate change.

1 INTRODUCTION

In the 1970s, plans to build a large fleet of high-flying supersonic aircraft led to concerns that their exhaust emissions (principally NO_x, but also H_2O, SO_2, hydrocarbons, etc.) could cause a reduction in stratospheric ozone (*Johnston 1971, Crutzen 1972*). In the event, only a small number of supersonic passenger aircraft were built, and attention switched to other possible causes of ozone depletion. However, in recent years, the growth in the number of long-haul subsonic passenger aircraft, and the projection for further expansion in the future, has reawakened a general concern for the effects of aircraft on the atmosphere. The *IPCC Special Report* went some way to quantifying the impact of aircraft on the atmosphere. However, our recent modelling calculations have produced conclusions significantly different from those reached in that report. This difference has resulted from an update of atmospheric reaction rates which now act to reduce modelled column ozone in the presence of supersonic aircraft emissions.

2 MODEL CALCULATIONS

In this study, an established 3D chemical transport model, SLIMCAT (*Chipperfield 1999, Rogers et al. 2000*) has been used to assess the impact of aircraft emissions. The model has been used with a resolution of 7.5º in latitude and longitude and with 12 vertical levels from 12 to 60 km. The model is driven by daily meteorological data. Each simulation begins with a 6-year spin-up of repeated annual meteorological data, and is followed by a one year integration.

All the calculations for the reference atmosphere and the perturbations due to the supersonic fleet emissions are as describe in chapter 4 of the *IPCC Special Report* and are listed in table 1.

Table 1 SLIMCAT Model Simulations Performed

Scenario	EI(NOx)-supersonic*
D	2015 Reference
S1b	0
S1c	5
S1d	10
S1e	15

*$EI(NO_x)$ (in $g(NO_2)/kg(fuel)$) is the nitrogen oxides emission index for the supersonic fleet.

The 2015 reference atmosphere, scenario D, includes only subsonic aircraft emissions, whilst scenarios S1 include additional supersonic aircraft emissions under various $EI(NO_x)$ conditions. Both subsonic and supersonic aircraft emissions of NO_x and H_2O are prescribed using the NASA-2015 database (*Baughcum et al. 1998*).

Crucially for this study the SLIMCAT model has been updated to include new kinetic data. The main reactions affected include the formation of HNO_3 from NO_2 and OH, the reduction of NO_2 to NO and the oxidation of HNO_3 by OH:

$$NO_2 + OH + M? \ HNO_3 + M \quad (1)$$

$$OH + HNO_3 \ ? \ H_2O + NO_3 \quad (2)$$

$$O(^3P) + NO_2 \ ? \ O_2 + NO \quad (3)$$

With the new data the first reaction rate affected (R1) shows a strong decrease in the conversion rate of NO_2 to HNO_3 in the lower stratosphere (*Brown et al. 1999a*). The rate coefficient of the second reaction (R2) has been modified to increase its temperature and pressure dependence (*Brown et al. 1999b*) resulting in a doubling of the rate in the lower stratosphere. Reaction R3 leads to ozone destruction, and its rate is increased by 20 to 30% in the lower stratosphere (*Gierzack et al. 1999*). The combination of these reaction rates lead to higher concentrations of NO_x in the lower stratosphere and therefore to lower ozone concentrations.

3 DISCUSSION

Fig. 1 shows the percentage change in ozone column over the northern hemisphere, due to various supersonic aircraft NO_x emission indices (S1b to S1e), each referenced to scenario D. Comparing these results with those given in the *IPCC Special Report* highlights the effect of the new kinetic data in the SLIMCAT model. Formerly an increase in the EI(NO_x) had only a small effect on the ozone column, with H_2O emissions having the most significant impact. For all models shown in the report, there are only modest changes in ozone with EI(NO_x). In contrast, with the inclusion of the updated rates, an increase in the EI(NO_x) has a significant effect on the ozone column, with a reduction in the Northern Hemisphere ozone column of -3.2% for EI(NO_x)=15.

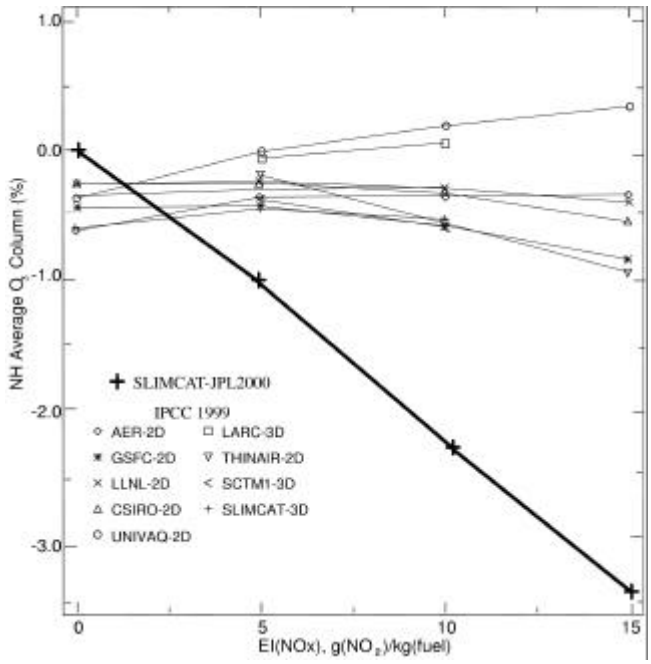

Figure 1: Northern Hemisphere total ozone column change as a function of EI(NOx) in 2015 for a supersonic fleet with SA0 sulfate distribution. The black line with symbol '+' represents the SLIMCAT model calculation with updated reaction rates. The grey lines are taken from the *IPCC Special Report.*

The reason for the large dependence of column ozone on EI(NO_x) can be seen by considering the zonal mean ozone perturbation due to supersonic aircraft emissions. Fig. 2 shows the modelled effect of supersonic aircraft emissions with EI(NO_x)=5 (scenario S1c) on the zonal mean ozone distribution for June 2015. The top panel presents the SLIMCAT calculation previously included in the *IPCC Special Report.* The bottom panel uses the SLIMCAT calculation performed with the new kinetic data. In the *IPCC Special Report* a cross-over point in the ozone chemical production and destruction terms, due to NO_x chemistry, could be seen at an altitude of ~20 km. With the new kinetic data the cross-over point is at a much lower altitude in the model calculations. With the injection of supersonic aircraft emissions at ~18 km almost all NO_x and H_2O emissions now take place in the region of ozone chemical destruction. This has resulted in an ozone decrease throughout the stratosphere and therefore in the ozone column.

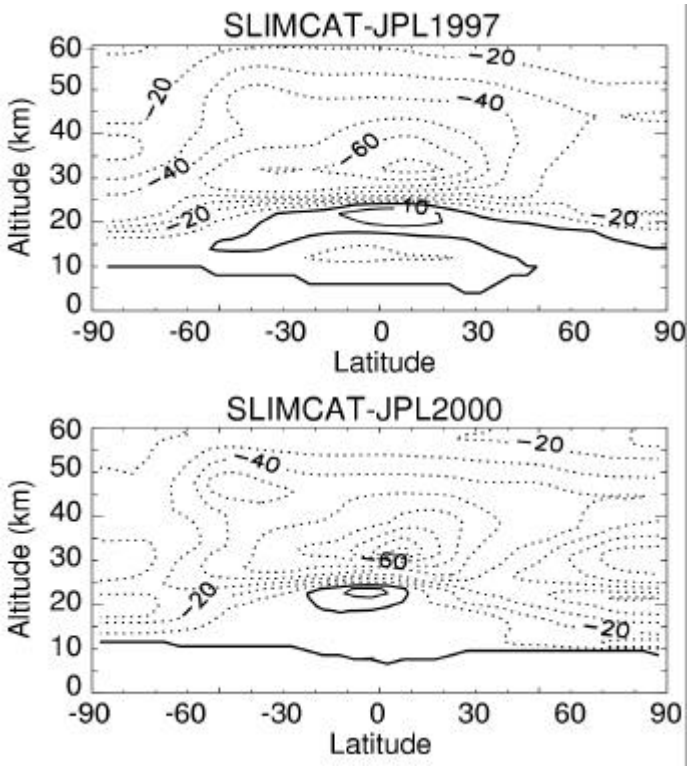

Figure 2**:** Ozone profile change (in ppbv) for S1c [EI(NOx)=5, SA0] relative to D [reference, SA0] in June 2015 (top : SLIMCAT-IPCC1999, bottom: SLIMCAT-updated).

4 CONCLUSION

The results of this study, highlight the impact of supersonic aircraft emissions with varying EI(NO_x). This is in contrast to the results from previous assessments such as the *IPCC Special Report*. This significant difference results from the inclusion of new kinetic data in our atmospheric chemical-transport model. This conclusion underlines the potential impact of a fleet of supersonic aircraft on the atmosphere and emphasises the necessity to continue to develop low NO_x combustion engines for the future as well as the importance of maintaining state of the art kinetic data.

REFERENCES

Baughcum, S.L., Sutku Jr., D.J. & Henderson, S.C. Year 2015 aircraft emissions scenario for scheduled air traffic (*Contractor Rep. No. 207638,* NASA Langley Research Center, 1998).

Brown, S., Talukdar, R. & Ravishankara, A., Rate constants for the reaction OH + NO_2 + M ? HNO_3 + M under atmospheric conditions, *Chem. Phys. Lett.*, **299**, 277-284 (1999a).

Brown, S., Talukdar, R. & Ravishankara, A., Reconsideration of the rate constants for the reaction of hydroxyl radical with nitric acid, *J. Phys. Chem. A*, ***103***, 3031-3037 (1999b).

Chipperfield, M.P. Multiannual simulations with a three-dimensional chemical transport model. J. Geophys. Res. ***104****, 17811805 (1999).*

Crutzen, P.J. SSTs: a threat to the earth's ozone shield. *Ambio* ***1***, 41-51 (1972).

IPCC Special Report : Aviation and the Global Atmosphere. Intergovernmental Panel on Climate Change (Rep. No. 8, World Meteorological Organisation and United Nations Environment Programme, Cambridge University Press, UK, 1999).

Johnston, H.S. Reduction of stratospheric ozone by nitrogen dioxide catalysts from supersonic transport exhaust. *Science* **173**, 517–522 (1971).

Rogers, H.L., Chipperfield, M.P., Bekki, S. & Pyle, J.A. The effects of future supersonic aircraft on stratospheric chemistry modeled with varying meteorology, *J. Geophys. Res.* **105**, 29359-29367 (2000).

Gierczak, T., Burkholder, J.B. & Ravishankara, A., Temperature dépendent rate coefficient for the reaction $O(^3P)$ + NO_2 ? NO + O_2, *J. Phys. Chem. A*, **103**, 877-883 (1999)

The SCENIC project webpage: http://www-scenic.ch.cam.ac.uk/

A 3D Model Intercomparison of the Effects of Future Supersonic Aircraft on the Chemical Composition of the Stratosphere

Giovanni Pitari*, Eva Mancini
Dipartimento di Fisica - Università L'Aquila -Italy

Helen Rogers, Olivier Dessens
Department of Chemistry - University of Cambridge – UK

Ivar Isaksen, Bjorg Rognerud
Department of Geophysics – University of Oslo- Norway

Keywords: Supersonic Aircraft, Stratospheric Chemistry, Aerosol, Ozone, Global Models

ABSTRACT: Gas and aerosol emissions from future supersonic aircraft may affect the chemical composition of the stratosphere in a significant way. The large scale accumulation of H_2O and NO_y is one key point to be assessed with models. The relative importance of the different catalytic cycles for ozone depletion is another key point, and for this it is important to determine the ability of models to predict the actual background abundance of radical species affecting the ozone photochemistry (i.e. OH, HO_2, NO_2, ClO, BrO). Here we focus on pure photochemical effects and compare the results of three completely independent three-dimensional chemical-transport models (CTM) (University of L'Aquila, University of Cambridge, University of Oslo), as part of the EC-funded TRADEOFF project. It should be noted that the 1999 IPCC assessment was largely based on the results of zonally averaged two-dimensional models. The University of L'Aquila CTM is run in interactive mode with a microphysics code for aerosol formation and growth, in order to calculate the aircraft forced changes of surface area density (SAD) of sulphuric acid aerosols. This SAD perturbation is then provided off-line to the other two models, in order to assess the sensitivity of the three CTMs to both NO_x and SO_x emissions. We first validate the aerosol results in the stratosphere (surface area density) and then discuss similarities and differences between the three CTMs in terms of the effect of aircraft forced changes of ozone and radical species on atmospheric chemistry.

1 INTRODUCTION

In the last decade several modelling studies have been made on the issue of supersonic aircraft impact on the chemical composition of the stratosphere (NASA, 1992; IPCC, 1999). The net effect on the global ozone distribution is not easy to assess with photochemical models, due to the complex interactions of different catalytic cycles for ozone destruction in the stratosphere, with partially opposing effects at different altitudes (Weisenstein et al., 1991). A realistic transport parameterization is essential to obtain a proper spatial and seasonal behaviour of the radical species involved in the ozone photochemistry (i.e. OH, HO_2, NO_2, ClO, BrO) and also to simulate in a realistic way the large-scale accumulation of gases emitted by the aircraft (H_2O, NO_y, SO_2, particles). To a first approximation, these emissions can be considered as localized tracers (Rogers et al., 2002). In addition, ozone and water vapour absorb planetary radiation in the middle atmosphere, so that changes in their distribution may feedback on stratospheric dynamics (Pitari and Mancini, 2001).

Here we focus on the pure photochemical effects and compare the results of three independent 3D global chemical-transport models (CTM) of the stratosphere for the purpose of assessing, in a

* *Corresponding author:* G.Pitari, Dipartimento di Fisica, Università dell'Aquila, Via Vetoio, 67100, L'Aquila, Italy. Email: gianni.pitari@aquila.infn.it

more accurate way, the tracer distribution in the lower stratosphere compard with the previously considered zonally averaged 2D models. Another important update with respect to the IPCC (1999) assessment is that here the models include the new rate constants for the NO_x reactions (Brown et al., 1999a; Brown et al., 1999b; Gierczak et al., 1999) that significantly increase the relative importance of the NO_x catalytic cycle with respect to the previous numerical simulations including the rates listed in JPL (1997).

2 DESIGN OF MODEL EXPERIMENTS

The overall strategy of this study was to run three independent CTMs under similar conditions: the same chemistry boundary conditions appropriate for the year 2015 (IPCC, 2001; WMO, 2002); the same chemistry kinetics and photochemical data (JPL, 1997); NASA emission scenarios (IPCC, 1999) for future supersonic aircraft (HSCT); and meteorology appropriate for present time conditions (i.e. year 2000). An important exception to the chemical rates reported in JPL (1997) are the three reactions relevant for stratospheric NO_x (i.e. $NO_2 + O(^3P)$; $NO_2 + OH + m$; $HNO_3 + OH$): for these we use the values listed in Brown et al. (1999a, 1999b) and in Gierczak et al. (1999).

The participating models are: the SLIMCAT model from the University of Cambridge (UCAM), SCTM-1 model from the University of OSLO (UiO) and the CTM model from the University of L'Aquila (ULAQ). All three models have chemical schemes containing the main stratospheric families for ozone depletion and include heterogeneous reactions on PSCs and sulphuric acid aerosols. The UCAM model is an off-line CTM for the stratosphere formulated on isentropic surfaces, with forcing winds from the UKMO analyses. The UiO and ULAQ models use pre-calculated transport fields from the output of climate-chemistry models, GISS and ULAQ respectively. The ULAQ model is a low-resolution global CTM coupled to a microphysics code for aerosol formation and growth. For more details see Pitari et al. (2001).

Ten numerical experiments have been made by each model, with 10-yeas spin-up to allow a meaningful steady-state: one without aircraft emissions, another one with subsonic aircraft only, and the remaining eight including also supersonic aircraft emissions with $0 \leq \text{EI-NO}_x \leq 15$, with and without the perturbation of the aerosol surface area density calculated off-line in the ULAQ model. The latter assumption allows the same distribution of aerosols in all three models. The major assumptions made for sulphur emissions by supersonic aircraft are: $\text{EI-SO}_2 = 0.4$ g/kg-fuel, with 10% fraction of sulphuric acid plume particles and a radius of aircraft emitted aerosols of 5 nm.

We will first discuss the calculated impact of sulphur emissions by HSCT on the stratospheric surface area density of sulphuric acid aerosols (SSA-SAD), and then the combined effects of sulphur and NO_x emissions on stratospheric tracers, ozone and radical species affecting the ozone photochemistry.

3 RESULTS

3.1 *Aerosol surface area density*

Fig. 1 shows how the ULAQ model calculation of aerosol surface area density compared with observations in the stratosphere (SAGE-II data for 1996-2000), and the magnitude of the predicted change forced by sulphur emissions from HSCTs. The aircraft perturbation of SAD has a maximum in the source region (close to 45N at 20 km altitude) and our calculation predicts a change as large as 0.27 $\mu m^2/cm^3$, that is close to 40% of the background value, with a much smaller penetration in the Southern Hemisphere. Ultrafine plume particles are the major cause of this SAD increase. A significant enhancement of N_2O_5 and $BrONO_2$ hydrolysis is to be expected as a consequence of this large increase of the sulphuric acid aerosol surface area (IPCC, 1999; Weisenstein et al.,1998).

3.2 *HSCT perturbation on chemical species*

Water vapour and NO_y are the chemical species directly affected by HSCT emissions in the lower stratosphere. Transport rates in the CTMs affect the accumulation of these tracers, so that we may expect a significant spread in the magnitude of the perturbation close to the source region and also

in the model ability to export tracers on the planetary scale outside the flight corridors (see Rogers et al. (2002) for a comprehensive study of the evolution of localized tracers in numerical models). Fig. 2 summarizes the model results for the accumulated H_2O and NO_y. Typical features are: ULAQ has a tendency to keep the tracers more efficiently confined into the emission region (this is consistent with the results of the Rogers et al. (2002) paper); ? H_2O from UiO is about half that calculated by the other two models (0.15-0.3 ppmv compared with 0.3-0.5 ppmv in the 20-30 km altitude layer); ? NO_y in the UCAM model penetrates more efficiently above the source region, compared with UiO and ULAQ (0.8 ppbv compared with 0.4 ppbv at 30 km, with EI-NO_x=10 g/kg).

An enhancement of water vapour produces more OH and thus increases the mid-stratospheric ozone loss; it also affects lower stratospheric ozone via the HO_x catalytic cycle and indirectly by converting more NO_2 into nitric acid. Emissions of NO_x make the odd nitrogen catalytic cycle more efficient and thus increase the ozone loss above 20 km, where the NO_x cycle dominates. The net effect on ozone above the tropopause up to about 20 km depends on the balance between the nearly compensating effects of the increasing efficiency of the NO_x cycle, with the decreasing efficiencies of Cl, Br and HO_x cycles. Fig. 3 summarizes the vertical profile changes of those radical species wich strongly affects mid-latitude lower stratospheric ozone (OH, NO_2, ClO). As expected from Fig. 2, the mid-stratospheric OH increase in the UiO model is smaller than in the other two models. The NO_2 percent increase in the UiO model is 30 to 50% larger than in UCAM and ULAQ even though the absolute perturbation of NO_y is similar or smaller (Fig. 2). The reason is that the Oslo model predicts a rather low amount of $NO+NO_2$ below 25 km altitude (see above). UCAM and ULAQ models are generally very consistent in the prediction of these relative changes of the radicals, although the ClO response to the NO_2 increase is larger in the ULAQ model: this may have a significant impact on ozone below 20 km altitude.

Fig. 4 shows the ozone profile changes for a set of EI-NO_x and EI-S cases. EI-NO_x=0 corresponds to a pure water vapour emission by the aircraft: here OH increases and NO_2 decreases, more efficiently when the aerosol SAD is enhanced by HSCT emissions. The fact that in this last case ozone increases in the UCAM model (opposite to ULAQ and UiO) is a clear indication that the ozone response in the lower stratosphere is dominated by the NO_x cycle in the Cambridge model. This becomes even more clear when direct injection of NO_x is considered (EI-NOx > 0): ULAQ and UiO show a clear cross-over point in the ozone profile change at about 20 km altitude (O_3 increase below and decrease above) while in UCAM the ozone depletion is extended to all heights. In addition the enhancement of aerosol SAD produces an increase of ozone loss in ULAQ and UiO models contrary to UCAM. These are clear indications that any perturbation of the NO_x in the lower stratosphere is more effectively compensated in ULAQ and UiO models by changes of OH, ClO and BrO than in UCAM (see Fig. 3).

The behaviour of the model calculated ozone profile changes discussed above is again visible in Fig. 5, where we present the globally integrated ozone changes with respect to the pure subsonic case for different EI-NO_x and EI-S values. An interesting comparison can be made with the values reported in the IPCC (1999) volume with fixed SSA-SAD: in that case the ULAQ-2D model ranges between –0.35% (with EI-NO_x = 0) and 0.35% (with EI-NO_x = 15 g/kg), while here ULAQ-3D ranges between –0.35% and –0.25%. The corresponding ? O_3 spread for SLIMCAT was about –0.6% (with EI-NO_x = 0) to –0.5% (with EI-NO_x = 10 g/kg) in IPCC (1999), versus –0.03% (with EI-NO_x = 0) to –2.85% (with EI-NO_x = 15 g/kg) in the present study. The update of the NO_x cycle reaction rates to the Brown et al. (1999a, 1999b) and in Gierczak et al. (1999) values seems to affect the UCAM results much more than those from the ULAQ model, at least with high EI-NO_x values.

A validation of background model results (i.e. pure subsonic case) for mid-latitude conditions is presented in Fig. 6. The models are rather consistent with satellite observations. Notable exceptions are however water vapour, where UCAM underestimates the observations, and NO_x and NO_y where in the mid-stratosphere UiO underestimates the observations and in the mid-stratosphere ULAQ and UCAM overestimate the observations. Some caution has to be used for the NO_x data in the lowermost stratosphere, due to the residual abundance of Pinatubo aerosols in March 1993, which make heterogeneous conversion of NO_x into NO_y faster than during volcanically clean conditions. It should to be noted that UCAM has tested the O_3 sensitivity to HSCT emissions with a doubled lower stratospheric H_2O content, and the results discussed above are only marginally affected.

Figure 1. (Left) ULAQ-CTM calculations (solid lines) and SAGE-II measurements (symbols) of springtime mid-latitude SSA-SAD; units are $10^{-8}cm^{-1}$. (Right) Annually averaged SAD changes due to HSCTs at 20 km.

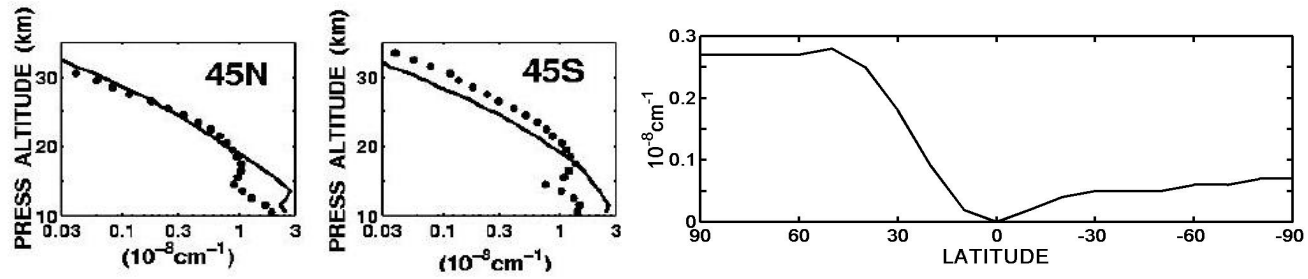

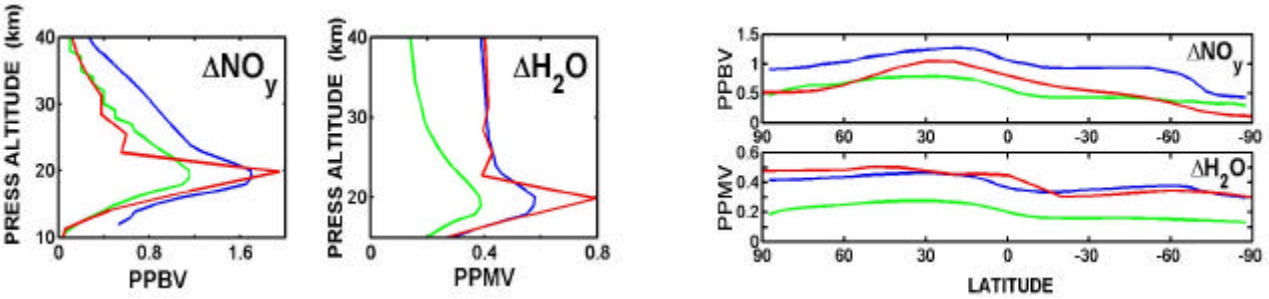

Figure 2. (Left) Vertical profiles of annually averaged changes of NO_y (ppbv) and H_2O (ppmv) at 45N, due to HSCT emissions (EI-NO_x=10 g/kg). (Right) Calculated NO_y and H_2O changes in the 20 - 30 km layer. Blue, green and red lines are for UCAM, UiO and ULAQ models, respectively.

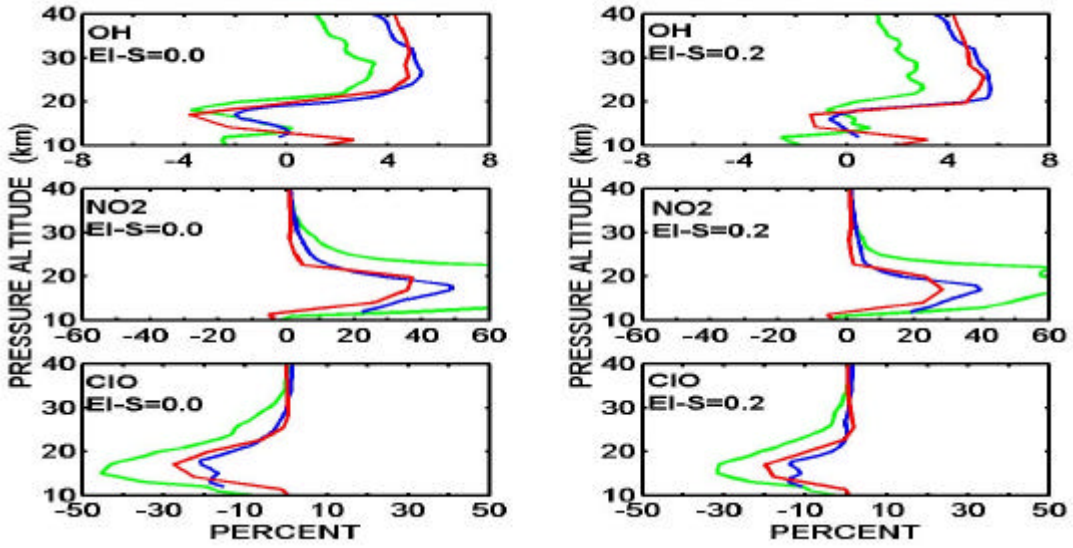

Figure 3. As in Fig. 2, but for percent changes of OH, NO2 and ClO in the 30N-60N band for the EI-NOx=10 g/kg experiment. Left panels are with unchanged SSA-SAD; right panels include the SAD change of Fig. 1.

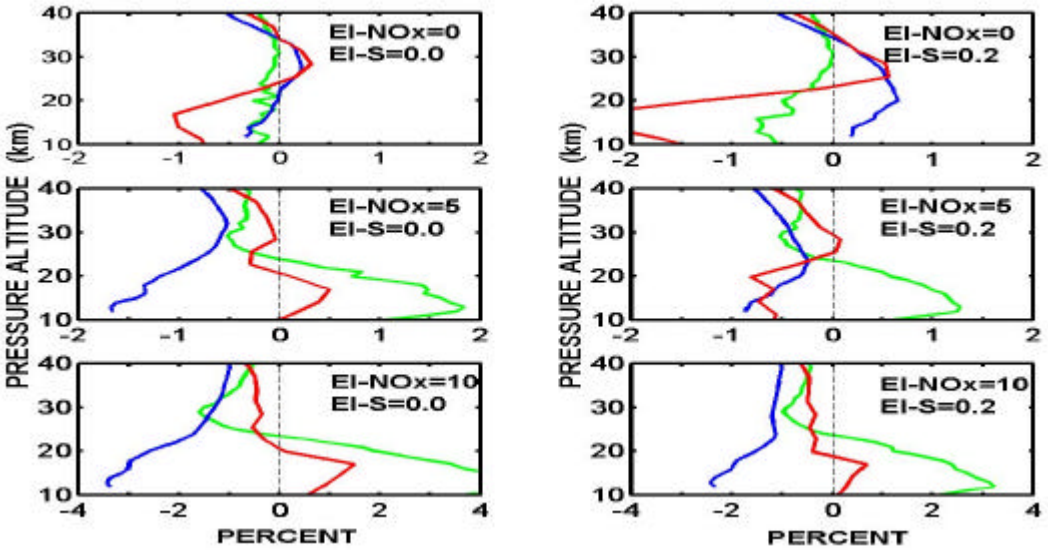

Figure 4. As in Fig. 3, but for ozone percent changes with EI-NO_x=0, 5, 10 g/kg.

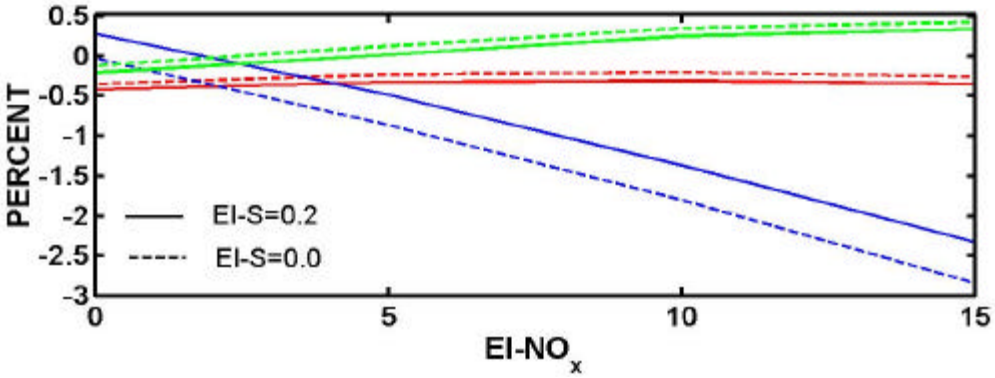

Figure 5. Global ozone percent changes as a function of EI-NO_x and EI-S. Colours are as in Fig. 2.

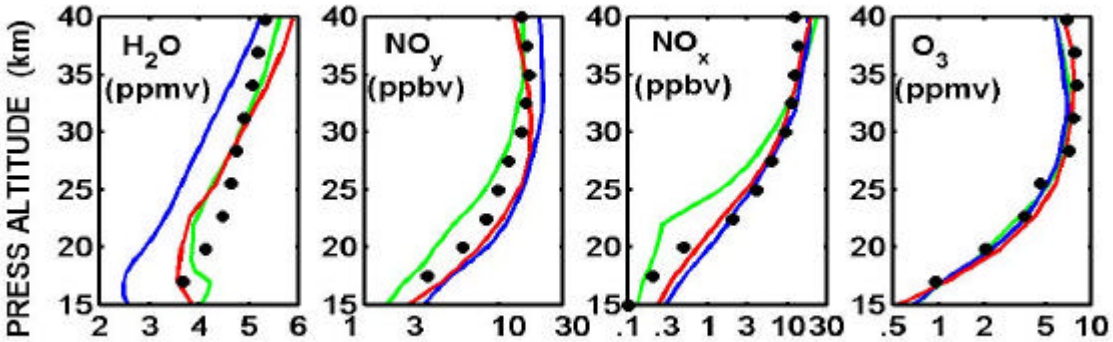

Figure 6. Calculated annually averaged vertical profiles in the 30N-60N latitude band. Colours are as in Fig. 2; symbols are for observations: H_2O (HALOE, April 1992); NO_x (HALOE, March 1993); NO_y (HALOE NO_x + CLAES HNO_3, March 1993); O_3 (climatology) (NASA, 1999).

4 CONCLUSIONS

The main conclusion of this study is that, while relative profile changes of the most important radical species affecting the ozone photochemistry (i.e. NO_x, HO_x, ClO, BrO), are similar between the three models (with respect to the pure subsonic case), the perturbation to ozone is increasingly variable with increasing EI-NO_x. In particular, the UCAM model no longer predicts a crossover point between ozone production and destruction in the lower stratosphere with updated kinetic rates. For EI-NO_x > 5 g/kg: here the mid-stratospheric ozone depletion penetrates below 20 km, having an impact on the ozone column much larger and negative compared with the ULAQ and UiO models. Analysis of the results shows that a possible cause for this difference is that any perturbation of the NO_x amount in the lower stratosphere is more effectively compensated for in the ULAQ and UiO models by changes of OH, ClO and BrO than in UCAM.
Even assuming a rather low sulphur emission index (EI-S =0.2 g/kg) and a lower limit estimate for plume particle formation (4% of total emitted sulphur), a future fleet of 500 HSCTs may produce a substantial perturbation of SSA-SAD (up to 40% at 20 km). In the ULAQ and UiO models, for a given NO_x injection, SO_x emissions increase the O_3 loss by removing part of NO_x and increasing reactive Cl/Br. In UCAM the prevailing effect of the additional SSA-SAD is to decrease reactive nitrogen (i.e. prevailing NO_x effect), so that the ozone loss decreases. A more systematic comparison of the models performance in the lower stratosphere, as well as a comparison of the calculated O_3 loss rates for the different catalytic cycles, will be made in the current EC-project SCENIC.

5 ACKNOWLEDGEMENTS

This work is supported by the EC, contract ENK2-CT-1999-00030.

REFERENCES

Brown, S., R. Talukdar and A. Ravishankara, 1999a: Rate constants for reaction OH + NO_2 + M ? HNO_3 + M under atmospheric conditions, *Chem. Phys. Lett., 299*, 277-284.

Brown, S., R. Talukdar and A. Ravishankara, 1999b: Reconsideration of the rate constants for reaction of hydroxyl radical with nitric acid, *J. Phys. Chem.,103*, 3031-3037.

Gierczak, T., J.B. Burkholder and A. Ravishankara, 1999: Temperature dependent rate coefficient for the reaction $O(^3P)$ + NO_2 ? NO + O_2 An ozone climatology based on ozonesonde and satellite measurements, *J. Phys. Chem.,103*, 877-883.

IPCC, 1999: *Special report on aviation and the global atmosphere*, J. E. Penner et al. Eds. Cambridge University Press, Cambridge, 373 pp.

IPCC, 2001: *Climate change 2001- The Scientific Basis*, J.T. Houghton et al. Eds. Cambridge University Press, Cambridge, 881 pp.

JPL, 1997: *Chemical kinetics and photochemical data for use in stratospheric modeling*, JPL publ. 97-4, Pasadena, California.

NASA, 1992: *The atmospheric effects of stratospheric aircraft*: *A first program report*, M.J. Prater et al. Eds., *NASA Ref. Publ. 1272*.

NASA, 1999: *Model and Measurements Intercommparison II*, J.H. Park et al. Eds., NASA/TM-1999-209554.

Pitari, G., and E. Mancini, 2001: Climatic impact of future supersonic aircraft: role of water vapour and ozone feedback on circulation, *Phys. Chem. of Earth C, 26/8*, 571-576.

Pitari, G., E. Mancini, A. Bregman, H.L. Rogers, J.K. Sundet, V. Grewe, and O. Dessens, 2001: Sulphate particles from subsonic aviation: Impact on upper tropospheric and lower stratospheric ozone, *Phys. Chem. of Earth C, 26/8*, 563-569.

Rogers, H.L., H. Teyssedre, G. Pitari, V. Grewe, P. van Velthoven, and J. Sundet, 2002: Model intercomparison of the transport of aircraft-like emissions from sub- and supersonic aircraft, *Meteorol. Z., 11*, 151-159.

Weisenstein, D.K., M.K.W. Ko, J.M. Rodriguez, and N.-D. Sze, 1991: Impact of heterogeneous chemistry on model-calculated ozone change due to high speed civil transport aircraft, *Geophys. Res. Lett., 18*, 1991-1994.

Weisenstein, D.K., M.K.W. Ko, I. Dyominov, G. Pitari, L. Ricciardulli, G. Visconti and S. Bekki, 1998: A model intercomparison of the effects of sulfur emissions from HSCT aircraft, *J. Geophys. Res., 103*,1527-1547.

WMO, 2002: *Scientific Assessment of Ozone Depletion: 2002*, WMO/UNEP rep. # 47, Geneva, Switzerland.

Modelling the Impact of Subsonic Aircraft Emissions on Ozone: Future Changes and the Impact of Cruise Altitude Perturbations

M.O. Köhler*, H.L. Rogers, J.A. Pyle
Centre for Atmospheric Science, Chemistry Department, University of Cambridge, Cambridge, U.K.

Keywords: Atmospheric Chemistry and Composition, Aircraft NO_X Emissions, UTLS Ozone, Cruise Altitude Perturbations

ABSTRACT: The impact of aircraft NO_X emissions on ozone in the UTLS region has been studied within the framework of the TRADEOFF project. Model integrations have been performed using TOMCAT, a 3-dimensional tropospheric chemistry transport model. Perturbations to aircraft emissions have been incorporated by changing the cruise altitude and flight routing of the present day subsonic fleet. The effects of tropospheric gas-phase chemistry on ozone mixing ratios and tropospheric ozone column have been investigated. A selection of results from the TRADEOFF project will be presented here.

1 MODEL DESCRIPTION

TOMCAT is a global 3D Eulerian chemistry transport model, and integrates a tropospheric methane-oxidation scheme with included ethane/propane degradation (Carver et al., 1998) on 31 hybrid pressure levels. The model uses an advection scheme that conserves 2nd order moments (Prather, 1986). A more detailed description of the TOMCAT model can be found in Law et al. (2000). The model has undergone recently a complete overhaul with numerous improvements, which include the treatments of photolysis, deposition, mid-level convection and cumulus downdraft, and makes use of updated emission data sets. Standard emissions appropriate for the year 2000 are chosen according to recommendations from IPCC (2001). Surface emissions appropriate for the year 2050 are chosen according to the IPCC SRES Scenario A2 (IPCC, 2000). Emissions for NO_X, CO, CH_4 and NMHCs are implemented with a seasonal cycle, aircraft emissions appropriate for the year 2050 are chosen according to Scenario Fa1 from IPCC (1999).

2 SCENARIO OVERVIEW

All TOMCAT model integrations have been performed using identical boundary conditions in order to achieve optimal comparability. All integrations have been forced by meteorological analyses from the European Centre for Medium-Range Weather Forecast (ECMWF) of the year 1995. Both the initialisation of the chemical model fields as well as a 7-month "spin-up" integration have been performed identically for each of the experiments listed in Table 1. Scenarios 3a, 3b, 5a, and 5b have been performed using equal surface emissions for the year 2000 and specifically developed aircraft emissions, appropriate for the year 2000, reflecting the corresponding cruise altitude perturbations for each of the four scenarios have been used. The treatment of chemistry and dynamics in the model remains consistent between model integrations. The TOMCAT model output is provided every 6 hours, at a horizontal resolution of $5.6° \times 5.6°$ for a 13-month period from 1 January, 1995, to 31 January, 1996.

* *Corresponding author:* Marcus Köhler, Centre for Atmospheric Science, Department of Chemistry, Lensfield Road, Cambridge, CB2 1EW, United Kingdom. Email: marcus.koehler@atm.ch.cam.ac.uk

Table 1. Scenario Overview

Scenario	Surface Emissions	Aircraft Emissions
NAE	2000 IPCC TAR	no aircraft
2000	2000 IPCC TAR	2000 TRADEOFF
2050[A]	2000 IPCC TAR	2050 IPCC Fa1
2050	2050 IPCC SRES A2	2050 IPCC Fa1

Scenario	Perturbation to Cruise Altitudes	
3a	cruise altitude 6000 feet lower	(normalized to 2000)
3b	cruise altitude 6000 feet lower	(non-normalized)
5a	cruise altitude 2000 feet higher	(normalized to 2000)
5b	cruise altitude 2000 feet higher	(non-normalized)

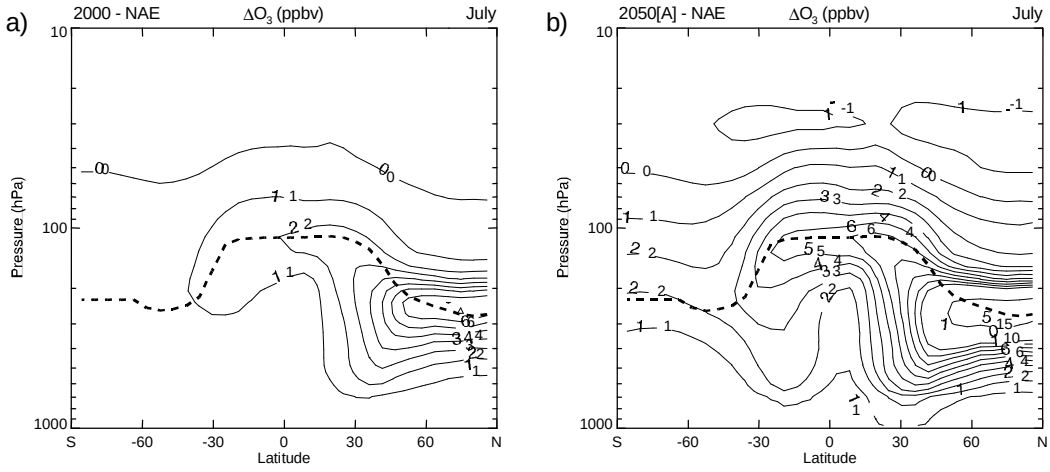

Figure 1. Zonally averaged ozone perturbation produced by aircraft emissions in 2000 (left figure) and 2050 (right figure).

3 AIRCRAFT IMPACT IN 2000 AND 2050

Present-day aircraft emissions lead to the production of ozone in the UTLS region and in the northern upper and middle troposphere. Aircraft NO_X emissions released inside the stratosphere have the capability to catalytically destroy ozone and lead to small reductions in ozone mixing ratios in the stratosphere. The maximum ozone increase due to present-day aircraft in the troposphere ranges between 4–9 ppbv, depending on season, which corresponds to approximately 4–6%. The largest perturbations occur around the northern hemispheric tropopause where the bulk of the aircraft emissions is released (Fig. 1a).

Increasing aircraft and surface emissions, projected for the year 2050, lead to increases in the tropospheric ozone column. These increases are strongest in the northern hemisphere, where the emissions are predominantly higher. In the northern hemisphere the tropospheric ozone column is increased by 30%. The increase in aircraft emissions projected for the year 2050 leads to enhanced ozone formation in the UTLS region and throughout the troposphere and moreover to a stronger reduction in stratospheric ozone. The strongest ozone increases are between 9–18 ppbv in the UTLS region, also depending on season (Fig. 1b).

Increasing methane surface emissions in the year 2050 lead to a larger abundance of hydroxyl radicals in the tropical lower stratosphere and subsequently to enhanced formation of nitric acid, which represents a sink for stratospheric nitrogen oxides. The correlation between NO_X and O_3 burdens in the northern hemisphere exhibits near-linearity for small perturbations to present-day aircraft emissions (NAE, 2000 and 2050[A] scenarios). Larger perturbations to surface emissions (2050 scenario) however lead to a non-linear increase in the ozone burden (Fig. 2).

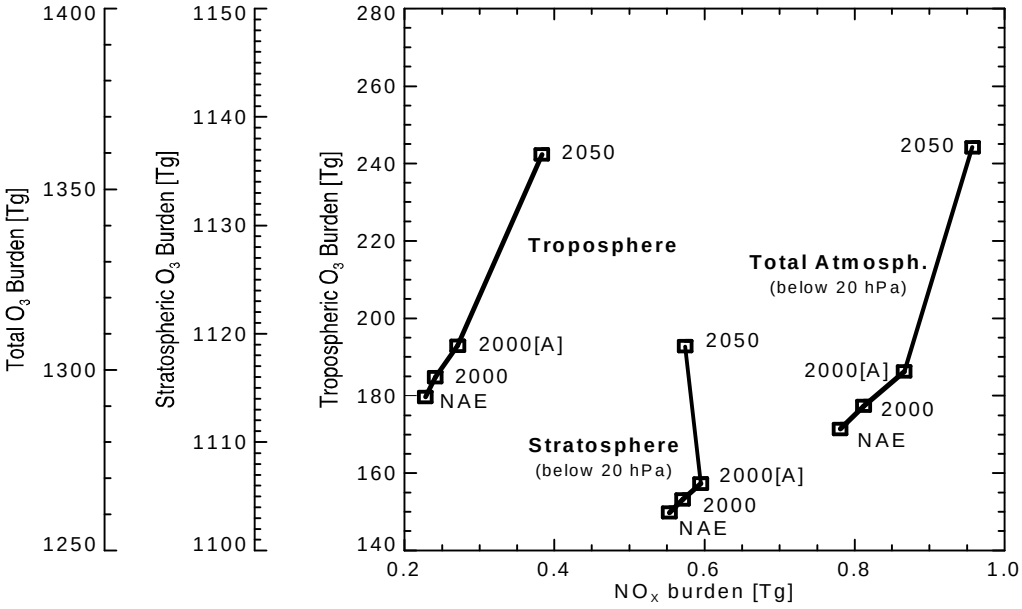

Figure 2. NOx and O3 burden correlations in the tropopshere, stratosphere and total atmosphere (stratosphere and total atmosphere below 20 hPa only).

4 CRUISE ALTITUDE PERTURBATIONS

A change in cruise altitude will lead to perturbations in the geographical distribution of aircraft emissions. Due to the large variability in atmospheric dynamics and chemistry the shift in the location of aircraft emissions has potentially large implications for atmospheric chemistry. Experiments with both higher and lower cruise altitudes have been performed with respect to a "present-day" scenario. For each perturbation a normalized scenario, where the location of cruise altitude has been changed without globally altering the total amount of emissions, and a non-normalized experiment, which additionally accounts for a change in the EI(NO_X) due to the changes in operational procedure, have been performed.

The experiments have shown that changes in cruise altitudes can lead to significant differences in ozone mixing ratios. The transport of aircraft emissions by atmospheric motion is highly dependent upon the geographical location and the altitude at which the emissions are released. The amount of emissions released, in combination with the NO_X mixing ratio of the ambient air, determine the amount of ozone produced from aircraft emissions.

In order to evaluate the total impact of the ozone changes in the northern hemisphere, both the tropospheric ozone column (from the surface to the tropopause) and the stratospheric ozone column (between the tropopause and 20 hPa, approximately 27 km altitude) have been calculated. The altitude range of the stratospheric ozone column was chosen as a suitable domain to represent the region of perturbation due to subsonic aircraft. Figure 3 displays the average value for the northern hemispheric ozone column under "present-day" conditions (s1) and for both higher (s5a, s5b) and lower (s3a, s3b) cruise altitudes.

In the stratosphere the ozone column below 20 hPa exhibits an almost linear relationship with the change of cruise altitude (Fig. 3a). The magnitude of ozone column change due to a 2000 ft rise in cruise altitudes is approximately a third of that resulting from a 6000 ft fall in cruise altitudes. The difference in ozone column change between the normalized scenarios (s3a, s5a) and the non-normalized scenarios (s3b, s5b) is negligible and as such indicates that the ozone column change in the stratosphere is independent of the total amount of aircraft emissions.

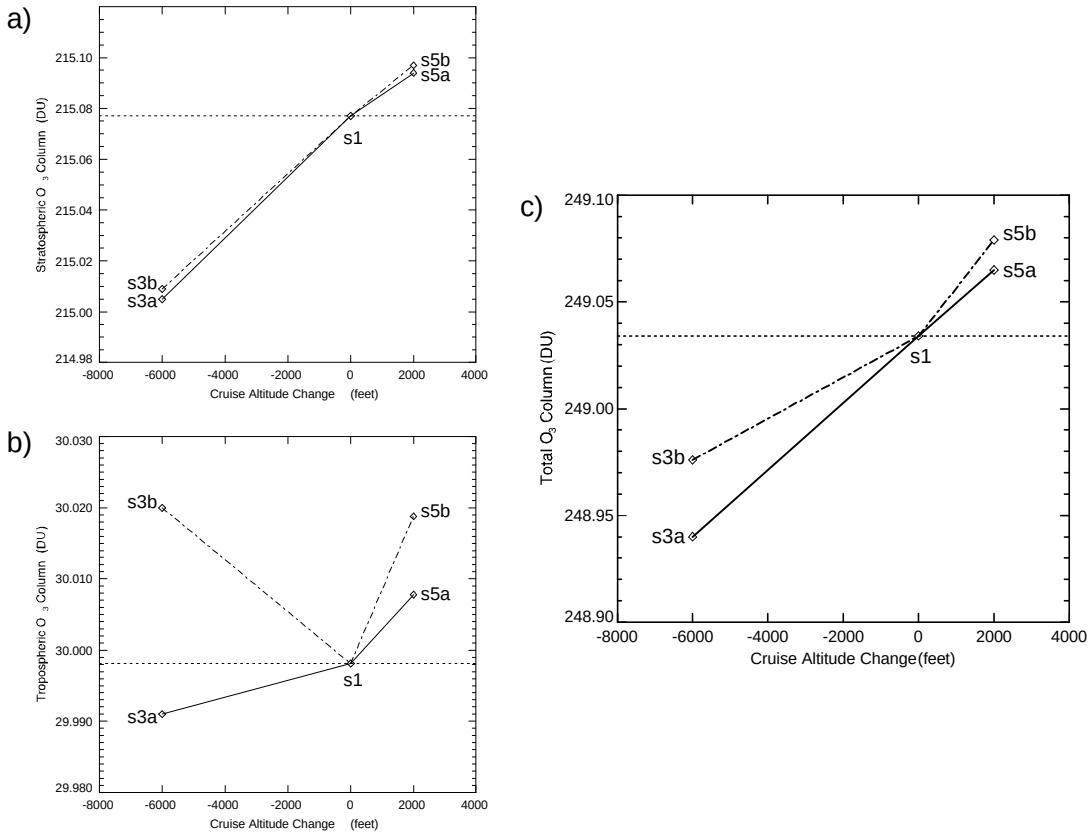

Figure 3. Average northern hemispheric ozone column and perturbations due to changes in cruise altitudes (stratosphere and total atmosphere below 20 hPa only).

The tropospheric ozone column shows a substantial difference between the normalized and non-normalized scenarios (Fig. 3b). In the experiments with normalized aircraft emissions the magnitude of the ozone column change for a reduction in cruise altitude by 6000 ft is ~30% smaller than the change in ozone column due to an increase in cruise altitude by 2000 ft. The relationship between the perturbed ozone column and the change in cruise altitude is therefore non-linear. In the non-normalized experiments, where the total emitted NO_X varies, both cruise altitude perturbations lead to an increase in tropospheric ozone column. This shows that the tropospheric ozone column is sensitive to the total amount of aircraft emissions. This difference between normalized and non-normalized scenarios in the troposphere and stratosphere could be explained by the low background NO_X mixing ratios in the troposphere in comparison with the lower stratosphere. An increase in NO_X due to aircraft emissions in the troposphere (where background values are low) could result in a higher chemical ozone production rate compared to the stratosphere.
The total ozone column up to 20 hPa shows that an increase in cruise altitudes leads to an increase of ozone column and lower cruise altitude lead to a reduction in total ozone for both scenarios (Fig. 3c). In each case the main effect occurs around the tropopause region where increased NO_X will increase ozone in the model. For scenarios with normalized emissions the relationship between ozone column and cruise altitude appears again to be almost linear. For non-normalized emissions the reduction of ozone column due to lower cruise altitudes is decreased by approximately 30% relative to the normalized emission scenario. Similarly, the increase in ozone column at higher cruise altitudes is further enhanced by nearly 30% relative to normalized emissions.

5 CONCLUSIONS

On a global scale NO_X emissions from the 2000 aircraft fleet have only a small effect on atmospheric ozone (4–9 ppbv), which can be observed predominantly in the northern UTLS region

and mid-troposphere. The 2050 aircraft fleet however has a more substantial effect (9–18 ppbv), exhibiting a similar zonal distribution in the perturbations. In the case of the 2000 atmosphere it has been shown that for small perturbations (e.g. the addition of the global aircraft fleet) the ozone perturbation is linearly dependent upon the NO_X enhancement.

Results have also shown that changes in cruise altitude affect the total ozone column (below 20 hPa) in the northern hemisphere. Lower cruise altitudes lead generally to a decrease in the total ozone column, such that for scenarios with normalized emissions the relationship between ozone column and cruise altitude appears to be almost linear. For non-normalized emissions the reduction of ozone column due to lower cruise altitude is decreased by approximately 30% relative to the normalized scenario. Similarly, the increase in ozone column at higher cruise altitude with non-normalized emissions is further enhanced by nearly 30% relative to higher cruise altitudes with normalized emissions.

REFERENCES

Carver, G.D., P.D. Brown, and O. Wild, 1998: The ASAD atmospheric chemistry integration package and chemical reaction database. *Comput. Phys. Commun*., *105*, 197–215.

IPCC, 1999: *Aviation and the Global Atmosphere. A Special Report of Working Groups I and III of the Intergovernmental Panel on Climate Change*. Edited by J.E. Penner et al., Cambridge Univ. Press, Cambridge, UK and New York, NY, USA, 373 pp.

IPCC, 2000: *Emissions Scenarios. A Special Report of Working Group III of the Intergovernmental Panel on Climate Change*. Edited by N. Nakicenovic and R. Swart. Cambridge Univ. Press, Cambridge, UK, 570 pp.

IPCC, 2001: *Climate Change 2001: The Scientific Basis. Contribution of Working Group I to the Third Assessment Report of the Intergovernmental Panel on Climate Change*. Cambridge Univ. Press, Cambridge, UK, and New York, NY, USA, 881 pp.

Law, K.S., P.-H. Plantevin, V. Thouret, A. Marenco, W.A.H. Asman, M. Lawrence, P.J. Crutzen, J.-F. Muller, D.A. Hauglustaine, and M. Kanakidou, 2000: Comparison between global chemistry transport model results and Measurement of Ozone and Water Vapor by Airbus In-Service Aircraft (MOZAIC) data. *J. Geophys. Res*., *105* (D1), 1503–1525.

Prather, M.J., 1986: Numerical advection by conservation of second order moments. *J. Geophys, Res*., *91* (D6), 6671–6681.

Nitric Acid Partitioning in Cirrus Clouds and the Role of Interstitial Aerosol

M. Krämer*, J. Beuermann, C. Schiller
FZ Jülich, Institut für Chemie der Geospäre I: Stratosphäre, Germany

F. Grimm, F. Arnold
MPI für Kernphysik, Heidelberg, Atmospärenphysik, Germany

T. Peter
ETH Zürich, Institut für Atmosphärenphysik, Switzerland

S. Meilinger
MPI für Chemie Mainz, Abt. für Het. Chemie und Mikrophysik, Germany

A. Meier
Universität Köln, Inst. für Geophysik & Meteorologie, Germany

J. Hendricks, A. Petzold, H. Schlager
DLR Oberpfaffenhofen, Inst. für Physik der Atmosphäre, Germany

Keywords: cirrus clouds, HNO_3 partitioning, interstitial particles

ABSTRACT: The parameters controlling the partitioning of HNO_3 in cirrus clouds between ice particles, interstitial aerosol and the gas phase are identified from field, laboratory and model studies in the temperature range 190 K – 240 K. Temperature, ice surface area and chemical composition of the interstitial particles are found to govern the HNO_3 partitioning. Moreover, the partitioning is very sensitive on the in-cloud relative humidity with respect to ice (RH_{ice}), which recently is found to range from 1.0 – 1.6.

1 INTRODUCTION

Cirrus clouds have attracted increasing attention in recent years, in particular because of their role in the forcing of climate, both through direct radiative and through indirect aerosol forcing. Further, cirrus clouds are important for the chemistry of upper tropospheric ozone. One possible mechanism relevant for atmospheric chemistry and trace gas distribution is the denitrification of the tropopause region by sedimenting cirrus ice particles (Lawrence and Crutzen, 1998).

However, up to now the question on the partitioning of nitric acid (HNO_3) under cirrus cloud conditions is not satisfactorily answered. It is unclear which parameters determine the HNO_3 partitioning between the gas phase, ice particles and interstitial aerosol particles. The interstitial aerosol particles grow to liquid solutions inside a cirrus cloud in dependence on the in-cloud relative humidity, thereby taking up HNO_3 according to their chemical composition. In spite of the potential importance of interstitial aerosol particles, however, their impact on HNO_3 partitioning is largely unexplored.

Here, we present a preliminary overview of the HNO_3 partitioning in cirrus clouds derived from field, laboratory and model studies for the temperature range 200 K < T < 230 K. To investigate the impact of interstitial aerosol in HNO_3 partitioning, we performed sensitivity model studies on the uptake of HNO_3 in interstitial particles at different in-cloud relative humidities, different initial amounts of HNO_3, and assuming two different particle compositions, namely ternary HNO_3-H_2SO_4-H_2O) or ammoniated, quarternary (HNO_3-H_2SO_4-H_2O-NH_3) solutions.

* *Corresponding author:* Martina Krämer, Forschungszentrum Jülich GmbH, D-52425 Jülich, ICG-I, Germany. Email: m.kraemer@fz-juelich.de

2 METHODS

The partitioning of HNO_3 is determined – assuming ternary and quarterny solution interstitial particles – with the help of the interactive gas-particle equilibrium model AIM (Aerosol Inorganics Model, http://www.hpc1.uea.ac.uk/~e770/aim.html) for the field experiments POLSTAR 1997 (199 K), POLSTAR 1998 (202 K), SUCCESS 1996 (209 K), a model study (225 K) and a laboratory study on ice particles (230 K) (Meilinger et al., 1999; Krämer et al., 2003; Weinheimer et al., 1998; Meier and Hendricks, 2002 and Arora et al., 1999). For a detailed description of the procedure see Krämer et al. (2003).

The equilibrium model is also used to perform sensitivity studies for different particle compositions, initial amounts of HNO_3 and in-cloud RH_{ice}. It is not yet known to which degree the gaseous HNO_3 equilibrates with the interstitial and ice particles inside a cirrus at RH_{ice} larger than the saturation value. Since the aim of this study is to identify the parameters controlling the partitioning of HNO_3 in cirrus, the sensitivity studies are performed at equilibrium conditions.

3 RESULTS

3.1 *Nitric acid partitioning: results from field, model and laboratory studies*

The HNO_3 partitioning in cirrus clouds is shown in Table 1. The upper three rows show the relative partitioning of HNO_3 between the interstitial particles, the gas phase and the ice particles. The straight numbers show the partitioning in case the interstitial particles are ternary solutions, the slanted numbers represent the partitioning in the presence of quaternary solution interstitial particles. The middle rows show the basic measured (black) and calculated (grey) parameters and the lower three rows the temperature, H_2O and the ice surface.

Interstitial particle HNO_3 (HNO_3^{ptcl}): in the presence of ternary solution interstitial aerosol, a substantial amount of HNO_3 was found in the interstitial particles. This amount decreases with increasing ambient temperature (see also Figure 1, upper left panel). If the interstitial particles are quaternary solutions, this temperature dependence is also seen, but more HNO_3 resides in the interstitial particles, because the additional large amount of ammonia causes, by neutralizing the sulphuric acid, a stronger uptake of HNO_3 (see also Figure 1, lower left panel).

Gas phase HNO_3 (HNO_3^{gas}): in the presence of ternary solution interstitial particles, a large amount of the initial HNO_3 remains in the gas phase. A smaller amount is found in the presence of quaternary solutions, but the gas phase is still not completely depleted.

Ice particle HNO_3 (HNO_3^{ice}): For both particles types, only very little HNO_3 was taken up by the ice particles under cold cirrus conditions (see also Meilinger et al., 1999), while in warm cirrus the main fraction of HNO_3 is scavenged by ice particles. This increase is related to the ice surface area ($A = f(H_2O)$), which in turn increases with the temperature.

In summary we find that both HNO_3^{ptcl} and HNO_3^{ice} are controlled by the temperature of the cirrus: $HNO_3^{ptcl} = f(1/T)$ and $HNO_3^{ice} = f(A\ (H_2O\ (T)\ )\ )$ for both types of interstitial particles, ternary and quaternary solutions. In cold cirrus clouds with low water content and a small ice surface area, the partitioning is in favour of the interstitial particles, while in warmer cirrus clouds with a greater water content and a large ice surface area the uptake on ice preponderates. Denitrification via sedi-menting ice particles may happen merely in the – most frequently appearing – warm cirrus clouds with large ice surface areas.

3.2 *Nitric acid partitioning: sensitivity studies*

The calculations and measurements of HNO_3^{ptcl} and HNO_3^{ice} shown in section 3.1 are made at different initial HNO_3 concentrations ($HNO_3^{init} = HNO_3^{total}$ in Table 1), which has an influence on the uptake in particles and on ice. For a higher/lower initial HNO_3 vapour pressure HNO_3^{ptcl} and HNO_3^{ice} would be larger/smaller.

A further aspect influencing HNO_3^{ptcl} is the in-cloud amount of water. HNO_3^{ptcl} could be larger, if the H_2O vapour pressure inside cirrus exceeds its saturation value $RH_{ice} = 1.0$. In this case the interstitial particles can take up more water and subsequently more HNO_3^{ptcl} . Ovarlez et al. (2002)

re-cently reported from field measuremenst that RH_{ice} inside a cirrus can reach values up to 1.6, the threshold for homogeneous ice nucleation.

In this section we present some simple equilibrium sensitivity studies to get an insight in the dependence of HNO_3^{ptcl} on HNO_3^{init} and RH_{ice} and to identify the main parameters controlling the partitioning of HNO_3 in cirrus clouds. The sensitivity studies are performed on the basis of the data of POLSTAR 1998, event II.

Table 1: HNO_3 partitioning between gas phase, interstitial aerosol and ice particles in cirrus clouds from field, labora-tory and model studies. a: ternary solutions: HNO_3-H_2SO_4-H_2O, b: quaternary solutions HNO_3-H_2SO_4-H_2O–NH_3; the gas-particle equilibrium calculations are performed using the interactive aerosol models AIM (http://www.hpc1.uea.ac.uk/~e770/aim.html); ★: based on data of Meilinger et al. (1999) with ★[1]: data taken from Schiller et al. (1999); §: based on data of Weinheimer et al. (1998) with §[1]: data taken from Baumgardner et al. (1998) and §[2]: data taken from Jensen et al. (1998); ‡: based on data of Meier and Hendricks (2002); = †: data taken from Schlager (2002); note that in-cloud RH_{ice} = 1.0 is assumed here; for more details see text.

Nitric acid partitioning in cirrus clouds:

	Field experiments								Model study		Lab. experiment
	POLSTAR 1997★		POLSTAR 1998 I		POLSTAR 1998 II		SUCCESS 1996 *Weinh. (1998)*§		*M & H (2002)*‡		*Arora et al. (1999)*
HNO_3 partitioning											
Interst. particles: ternary[a] *quaternary*[b] solutions											
Interst. particles (%)	33.2	*88.6*	33.2	*69.3*	21.2	*68.1*	3.8	*72.2*	0.0	*7.8*	–
Gas phase (%)	66.5	*11.3*	66.2	*30.4*	71.6	*29.1*	0.0 ?	*0.0 ?*	34.0	*31.4*	65 – 0.0
Ice particles (%)	0.3 (0.1 – 0.9)	*0.1*	0.6 (0.2 – 2.0)	*0.3*	7.2 (2.2 – 25.2)	*2.8*	96.2	*27.8*	66.0	*60.8*	35 – 100
Basic measured and calculated parameters											
$H_2SO_4^{total}$ (ppb)	0.600	*0.60*	0.55	*0.55*	0.70	*0.70*	0.50	*0.50*	0.60	*0.60*	–
NH_3^{total} (ppb)	–	*0.70*	–	*0.70*	–	*0.70*	–	*0.70*	–	*0.70*	–
HNO_3^{total} (ppb)	0.075	*0.44*	0.75	*1.64*	0.26	*0.653*	0.052	*0.18*	0.47	*0.51*	≈ 6.7
HNO_3^{ptcl} (ppb)	0.025	*0.39*	0.25	*1.14*	0.06	*0.445*	0.002	*0.13*	0.0	*0.04*	0.0
HNO_3^{gas} (ppb)	0.05		0.5		0.19		0.0 ?		0.16		≈ 4.4 – 0.0
HNO_3^{ice} (ppt)	0.2		4.6†		18†		50		310		≈ 2300 – 6700
Altitude (km)	11.8		12.5		11.0		–		–		–
Ozone (ppb)	60★[1]		200		50		–		–		–
Pot. Temp. (K)	313		325		311		–		–		–
Pressure (hPa)	200		178		219		193§[1]		270		–
Temp. (K)	196		199		202		209§[2]		225		230
H_2O (ppm)	20		21		41		–		215		–
Ice surface ($\frac{\mu m^2}{cm^3}$)	≈ 120		≈ 125†		≈ 330†		≈ 2000		≈ 5.100		$(59 – 1300) \cdot 10^3$

3.2.1 *Dependence of HNO_3^{ptcl} on HNO_3^{init}*

The HNO_3 uptake in interstitial particles is calculated for low, middle and high initial HNO_3 (0.05 ppbv, 0.26 ppbv and 1.7 ppbv; the values are taken from Table 1) in the temperature range 190 K – 230 K for ternary and quaternary solution interstitial aerosol and at RH_{ice} = 1.0.

The results of the sensitivity studies are shown in Figure 1, upper and lower left panels. At first, the results of the field and model studies shown in section 3.1 are confirmed: if the interstitial

particles are quaternary solutions (Figure 1, lower left panel), more HNO_3 resides in the particles over the whole temperature range than in the case of ternary solution particles (Figure 1, upper left panel). Secondly, it becomes obvious that the temperature dependence of HNO_3 uptake in interstitial aerosol dominates the influence on the initial HNO_3 amount for both types of interstitial particles.

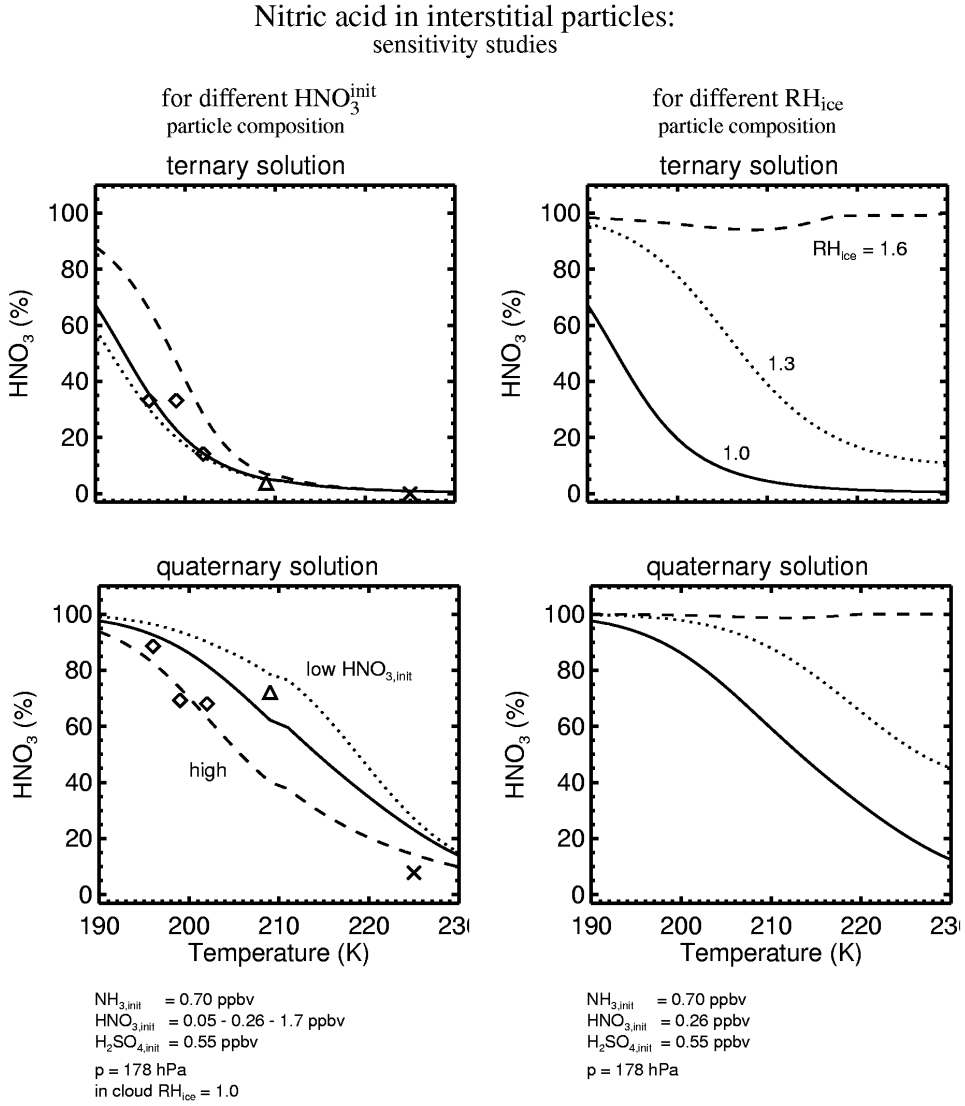

Figure 1: Nitric acid in interstitial particles versus temperature for two types of particles. Ternary solutions: H_2O-H_2SO_4–HNO_3; quaternary solutions: H_2O-H_2SO_4–HNO_3–NH_3; sensitivity studies are presented as solid, dotted and dashed lines; in addition, the field measurements POLSTAR (◊) and SUCCESS (Δ), and the model study (X) from Table 1 are plotted. For more details see text.

3.2.2 *Dependence of HNO_3^{ptcl} on in-cloud RH_{ice}*

The HNO_3 uptake in interstitial particles is determined for RH_{ice} = 1.0, 1.3 and 1.6 (see Figure 1, upper and lower right panels). For both ternary and quaternary solution interstitial aerosol, a strong dependence of the HNO_3 uptake on RH_{ice} is found: the more water is available, the more HNO_3 is taken up by the interstitial particles, even at higher temperatures. At RH_{ice} = 1.6, almost all HNO_3 would be taken up in the interstitial aerosol independently on the temperature. In this case, competition between the uptake of HNO_3 in interstitial and ice particles could take place (see section 3.2.3) and therefore denitrification via sedimenting cirrus ice particles may not occur.

3.2.3 *Implications for cirrus clouds*

Considering the findings of the sensitivity studies, the history of cirrus formation and development may be regarded under new aspects:

During the cooling process of the air, RH_{ice} increases to values up to 1.6. Depending on the supersaturation and the particle chemistry, HNO_3 is scavenged by those particles grown by water uptake due to rising RH_{ice}. When ice particles are forming, a part of the HNO_3 freezes together with the water. The amount of HNO_3 in ice originating from this freezing path depends on the fraction of frozen on the total particle number. If only few particles are frozen, as in most cases, then only a small part of the HNO_3 in ice will originate from this process. But in a case where a large part of the particles would be frozen, a major part of the HNO_3^{ice} could be captured via this path by the ice particles. Friedl (2003) observed very high HNO_3 coverages in contrail ice particles, coupled with a high number of small ice crystals. The above described pathway could explain these observations.

After this first freezing step, RH_{ice} reduces to a certain value between 1.0 and 1.6. The interstitial particles equilibrate to that lower value by evaporating H_2O and HNO_3 (the evaporation of HNO_3 from the interstitial particles for $RH_{ice} = 1.0$ is demonstrated for POLSTAR 1997 by Meilinger et al., 1999 in a detailed model study). The amount of HNO_3 available for adsorption on the ice surface is now determined by the current RH_{ice}, temperature and particle composition. At low RH_{ice}, the interstitial particles will evaporate HNO_3 to the favour of the ice particles, similar to the Bergeron-Findeisen process known for water. At high RH_{ice}, the inverse effect will take place: HNO_3 resides in the interstitial particles to the disadvantage of the ice particles.

The in-cloud RH_{ice} can rise again after the first freezing cycle (Haag et al., 2003). Then, the repeated growth of interstitial particles by water vapour and uptake of HNO_3 can transform them to ice nuclei that induce a second freezing step. After that, equilibrium of H_2O and HNO_3 between ice and interstitial particles has to be established again. For a complete understanding of these complex interactions in cirrus clouds, more and detailed kinetic studies considering the total system of H_2O, HNO_3 and coexisting ice and interstitial particles are needed.

4 SUMMARY AND CONCLUSIONS

From field, laboratory and model studies it is found that the parameters controlling the HNO_3 partitioning in cirrus clouds between ice particles, interstitial aerosol and the gas phase are temperature, ice surface area and chemical composition of the interstitial particles. Moreover, from a sensitivity model study there is a hint that HNO_3 is very sensitive to the in-cloud RH_{ice}.

A part of nitric acid always remains in the gas phase as long as the in-cloud RH_{ice} remains smaller than the maximum value of 1.6. In this case, the amount of HNO_3 residing in the interstitial particles is dependent on temperature: in cold cirrus clouds ($T < 205$ K) with small ice surface areas the partitioning is in favour of the interstitial particles, while in warmer cirrus clouds with large ice surface areas the uptake on ice preponderates. This dependence is observed for both, ternary and quaternary solution interstitial particles, whereby the quaternary solutions contain a larger amount of HNO_3. When RH_{ice} comes close to 1.6, almost all nitric acid resides in the interstitial particles independent on temperature and particle composition. Here, denitrification via sedimenting cirrus ice particles may not occur even at higher temperatures. Consequently, extensive uptake of nitric acid on ice with subsequent denitrification likely occurs in the most frequently appearing warm cirrus clouds at low RH_{ice}.

An additional hypothesis concerning the HNO_3 distribution in cirrus clouds arises from the sensitivity studies: adsorption on the ice surface seems not to be the only pathway for HNO_3 to ice particles. When the ice particles form at high RH_{ice} from grown interstitial particles, HNO_3 was already incorporated in those particles and freezes together with the water. In a case where a large part of the particles would be frozen, a major part of the HNO_3 could be captured via this pathway by the ice particles. For a better understanding of the complex interactions in cirrus clouds, we encourage more and detailed kinetic model studies considering the total system of H_2O, HNO_3 and coexisting ice and interstitial particles.

REFERENCES

Arora, O., D. Cziczo, A. Morgan, J. Abbatt, and R. Niedziela, 1999: Uptake of nitric acid by sub-micron-sized ice particles. *Geophys. Res. Lett*., 26, 3621-3621.

Baumgardner, D. and B. E. Gandrud, 1998: A comparison of the microphysical and optical properties of particles in an aircraft contrail and mountain wave cloud. *Geophys. Res. Lett*., 25, 1129-1132.

Friedl, R., WB-57 CRYSTAL-FACE science team, 2003: Overview of contrail and cirrus cloud measurements from the WB-57 aircraft in the CRYSTAL-FACE mission. Conference on Aviation, Atmosphere and Climate (AAC), Friedrichshafen, Germany.

Haag, W., B. Kärcher, J. Ström, A. Minikin, U. Lohmann, J. Ovarlez, and A. Stohl, 2003: Freezing thresholds and cirrus cloud formation mechanisms inferred from in situ measurements of relative humidity. *Atmos. Chem. Phys. Discuss*., 3, 3267-3299.

Jensen, E. J., O. B. Toon, A. Tabazadeh, G. W. Sachse, B. E. Anderson, K. R. Chan, C. W . Twohy, B. Gandrud, S. M. Aulenbach, A. Heymsfield, J. Hallett and B. Gary, 1998: Ice nucleation processes in upper tropospheric wave-clouds observed during SUCCESS. *Geophys. Res. Lett*., 25, 1363-1366.

Krämer, M., J. Beuermann, C. Schiller, F. Grimm, F. Arnold, Th. Peter, S. Meilinger, A. Meier, J. Hendricks, A. Petzold and H. Schlager, 2003: Nitric acid partitioning in cirrus clouds: a synopsis based on field, laboratory and model studies. *Atmos. Chem. Phys. Discuss*., 3, 413-443.

Lawrence, M., and P. Crutzen, 1998: The impact of cloud particle gravitational settling on soluble trace gas distributions. *Tellus*, 50B, 263-289.

Meier, A., and J. Hendricks, 2002: Model studies on the sensitivity of upper tropospheric chemistry to heterogeneous uptake of HNO_3 on cirrus ice particles. *J. Geophys. Res*., 107, 4696, doi:10.1029/2001JD000735.

Meilinger, S., A. Tsias, V. Dreiling, M. Kuhn, C. Feigl, H. Ziereis, H. Schlager, J. Curtis, B. Sierau, F. Arnold, M. Zöger, C. Schiller and T. Peter, 1999: HNO_3 partitioning in cirrus clouds. *Geophys. Res. Lett*., 26, 2207-2210.

Ovarlez, J., J.-F. Gayet, K. Gierens, J. Ström, H. Ovarlez, F. Auriol, R. Busen, and U. Schumann, 2002: Water vapour measurements inside cirrus clouds in Northern and Southern hemispheres during INCA. *Geophys. Res. Lett*., 29, 1813, doi:10.1029/2001GL014440.

Schiller, C., A. Afchine, N. Eicke, C. Feigl, H. Fischer, A. Giez, P. Konopka, H. Schlager, F. Tuitjer, F.G. Wienhold and M. Zöger, 1999: Ice particle formation and sedimentation in the tropopause re-gion: A case study based on in situ measuremenst of total water during Polstar 1997. *Geophys. Res. Lett*., 26, 2219-2222.

Schlager, H., A. Petzold, H. Ziereis, A. Dörnbrack, F. Grimm, F. Arnold and C. Schiller, 2000: In situ observations of particulate NOy in cirrus clouds for different atmospheric conditions. Proceedings of the workshop 'Aviation, aerosols, contrails and cirrus clouds (A2C3)', Seeheim (Frankfurt), Germany, 68-73.

Weinheimer, A. J., T. L. Campos, J. G. Walega, F. E. Grahek, B. A. Rodley, B. D. C. H. Twohy, and B. Gandrud, 1998: Uptake of NOy on wave-cloud ice particles. *Geophys. Res. Lett*., 25, 1725-1728.

Radiative Forcing on Climate from Stratospheric Aircraft Emissions

D.J. Wuebbles*, M. Dutta, A.K. Jain
Department of Atmospheric Sciences, University of Illinois at Urbana Champaign, Urbana, Illinois, USA

S.L. Baughcum
The Boeing Company, Seattle, Washington, USA

Keywords: radiative forcing, aircraft emissions, stratospheric ozone, water vapor

ABSTRACT: The 1999 Intergovernmental Panel on Climate Change report on Aviation and The Global Atmosphere estimated that emissions from a fleet of one thousand High Speed Civil Transport aircraft (flying at Mach 2.4) could produce a non-negligible impact on the radiative forcing driving changes in climate. The radiative forcing for this fleet was +0.1 Wm^{-2}, with +0.10 Wm^{-2} coming from the increase in stratospheric water vapor, along with smaller contribution from increased CO_2 (+0.01 Wm^{-2}) and from effects on stratospheric ozone (-0.01 Wm^{-2}). In this study, we reexamine the radiative forcing from fleets of aircraft flying at stratospheric altitudes. We use our narrowband radiative transfer model in these studies, along with model calculations of calculated changes in ozone and water vapor from our zonally-averaged model of atmospheric chemical and physical processes. The radiative transfer model used here has higher resolution in the tropopause and lower stratosphere region than the models used in the IPCC assessment. Preliminary results suggest that the radiative forcing for the water vapor emissions from aircraft was overestimated in the IPCC assessment. Along with reconsideration of the radiative forcing for the HSCT scenarios used in IPCC, we also consider the radiative forcing from a set of parametric scenarios for which the cruise altitudes are systematically varied.

1 INTRODUCTION

Aircraft emissions can affect climate both directly and indirectly. Direct effects on climate from aircraft emissions can occur due to resulting changes in the atmospheric distributions of radiatively important gases, especially carbon dioxide (CO_2) and water vapor (H_2O). Changes in ozone, resulting from emissions of nitrogen oxides and water vapor, can produce an indirect effect on climate from aircraft emissions. In the troposphere, under the right conditions, water vapor emissions can produce contrails that can radiatively affect climate directly, but also can affect climate indirectly through possible resulting changes in natural cloudiness (Ponater et al., 1996; Rind et al., 1996; Seinfeld, 1998; IPCC, 1999).

Even though several studies indicate aircraft emissions of water vapor in the troposphere are unlikely to be important contributors to climate change, emissions of water vapor in the lower stratosphere, where natural levels of water vapor are much smaller, could produce a potentially significant radiative effect on climate.

The IPCC (1999) assessment on Aviation and The Global Atmosphere used several radiative transfer models to examine the potential effects of fleets of High Speed Civil Transport (HSCT) aircraft. These studies concluded that a fleet of 1000 HSCTs, with assumed very low emission of nitrogen oxides (NO_x), could result in radiative forcing of +0.006 Wm^{-2} from the additional CO_2, -0.010 from ozone concentration changes, and +0.10 Wm^{-2} from increased stratospheric H_2O. At this point, these findings have not been verified in the literature, and there remain questions about the validity of the relatively large radiative forcing from the increase in stratospheric water vapor.

* *Corresponding author:* Donald J. Wuebbles, Department of Atmospheric Sciences, University of Illinois at Urbana Champaign, 105 S. Gregory St., Urbana IL-61801, USA. Email: wuebbles@atmos.uiuc.edu

An important goal in this study is to reexamine the effects on climate associated with changes in radiative forcing resulting from the perturbations to stratospheric ozone and water vapor as a result of aircraft emissions in the stratosphere. In addition to reexamining the radiative effects on climate from fleets of HSCTs, we will also consider more recent scenarios that parametrically consider the effects of cruise altitudes while holding the geographical distribution and fuel use constant.

2 MODEL DESCRIPTIONS

2.1 *Two-Dimensional Chemistry Transport Model*

The UIUC two-dimensional (2D) chemical-radiative-transport model is a zonally-averaged model of the chemistry and physics of the global atmosphere. The model is often used to study human related and natural forcings on the troposphere and stratosphere, but, because it is zonally-averaged, the analysis of tropospheric processes is limited. The model determines the atmospheric distributions of 78 chemically active atmospheric trace constituents. In addition to 56 photolytic reactions, the model incorporates 161 thermal reactions in the chemical mechanism, including heterogeneous reactions (e.g., see Wuebbles et al., 2001, Wei et al., 2001). Reaction rates and photolysis cross-sections in the model are based on recommendations from NASA's Chemical Kinetics Review Panel (e.g., DeMore et al., 1997; Sander et al., 2000).

In the last year, there have been substantial improvements made to the model, which have resulted in significant changes in lower stratospheric ozone response to NO_x and H_2O emissions.

2.2 *Radiative Transfer Model*

The narrowband radiative transfer model (RTM) is used in these studies is a component of the Integrated Science Assessment Model (ISAM) (Jain et al., 2000). In addition to water vapor and ozone changes considered in this study, the model calculates radiative forcing due to other gases such as carbon dioxide (CO_2), methane (CH_4), nitrous oxide (N_2O), chlorofluorocarbons (CFCs), and other halocarbons. This model was formulated for efficiency (allowing infrequent calculation of atmospheric absorptivity and emissivity), as well as generality (5-10cm^{-1} spectral resolution allows easy incorporation of many trace gases). The radiative transfer analyses are evaluated on a 5^o latitude grid from 82.5^oS to 82.5^oN. The thickness of vertical layers is 100 mbar in the troposphere, decreasing to 5-10 mbar near the tropopause and lower stratosphere.

The long wave component of the radiative transfer model is a Malkmus random band model. The model calculates absorptivities and emissivities in the 0-3000cm^{-1} range band with of 10 cm^{-1} for H_2O and 5 cm^{-1} for CO_2, O_3, CH_4, and N_2O. The short-wave radiative fluxes are based on the Delta-Eddington model developed by Briegleb (1992). Line parameters for H_2O, CO_2, O_3, CH_4, and N_2O, were based on the HITRAN-1992 database (Rothman et al., 1992). Absorption cross-section data for CFC-11, and CFC-12 were taken from McDaniel et al. (1991). The vertical profiles of temperature, H_2O, and O_3 are important parameters in the calculations of radiative forcing. The latitudinal and seasonal variations of temperature, H_2O, O_3, and clouds are based on in situ and satellite data. A detailed description of the data used in this study can be found in Jain et al. (2000).

The adjusted calculations are performed by allowing stratospheric temperatures to adjust such that stratospheric heating/cooling rates are identical to values calculated for the pre-perturbation stratosphere. This approach essentially assumes a fixed dynamical heating/cooling approximation. Temperature are adjusted iteratively until the net heating rate changed by less than $0.5x10^{-3}$ per day at all levels above the tropopause.

3 RESULTS AND DISCUSSION

3.1 *Radiative forcing from HSCT Scenarios*

Of the many scenarios considered for analyses of effects on stratospheric ozone from fleets of HSCT aircraft in Chapter 4 (Isaksen et al., 1999) of the IPCC assessment, only two were considered for analyses of radiative forcing in Chapter 6 (Prather et al., 1999) (see Table 1).

Table 1. Percentage change in Northern Hemisphere total column ozone for HSCT scenarios used for calculation of radiative forcing in Chapter 6 (IPCC 1999)

IPCC Scenario	Fleet Size	E.I.(NO_x) [g/kg of fuel]	Sulphate Conversion (%)	Cl_y (ppbv)	IPCC Models	AER model	UIUC -2D model
S1k	500	5	10 (SA5)	3.0	-0.2 to -0.8	-0.8	-0.51
S9h	1000	5	10 (SA6)	2.0	-0.3 to -1.1	-0.8	-0.8

Table 2. Comparison of radiative forcing, after stratospheric adjustment, due to water vapor and ozone perturbations from the two HSCT scenarios discussed in Table 1. The radiative forcing values are calculated using the UIUC RTM, for AER and UIUC-2D model results and compared with the results shown in Chapter 6 (Prather et.al., IPCC 1999).

IPCC scenario	IPCC (1999)		AER model		UIUC model	
	H_2O	O_3	H_2O	O_3	H_2O	O_3
S1k	+0.050	-0.010	+0.019	-0.013	+0.039	-0.006
S9h	+0.100	-0.010	+0.034	-0.014	+0.048	-0.007

For the changes in ozone, Chapter 6 reports radiative forcing values of -0.010 Wm^{-2} for both scenarios, with a range amongst the models of -0.040 to +0.010. The adjusted radiative forcings for the two scenarios, -0.006 for S1k and -0.007 for S9h, are shown in Table 2. For perturbations of water vapor our radiative transfer model calculates a radiative forcing of +0.039 and +0.048 as compared to +0.050 and +0.100 for the two scenarios respectively.

We also considered results used in the IPCC assessment from the AER chemical-transport model. The derived radiative forcing due to ozone are in good agreement with the IPCC(1999) values. But water vapor perturbations derived from AER model give radiative forcings of +0.019 Wm^{-2} for S1k and +0.034 Wm^{-2} for S9h scenarios (see Table 2), much lower than the IPCC assessment findings. We are currently trying to investigate this underestimation of water vapor impact on radiative forcing as calculated in our RTM compared to the IPCC(1999). The differences in the radiative transfer models, like the higher altitude and wavelength resolutions used in our model could make a significant difference. We are also analysing the role of the difference in treatments of transport of water vapor emissions in the different CTMs used in the IPCC (1999) and our UIUC 2D model.

3.2 *Radiative forcing from Parametric Scenarios*

Current considerations for new aircraft concepts are quite different than the original HSCT concept. Such aircraft would likely have different cruise speeds, and hence cruise altitudes, different sizes, different design ranges, and different markets, than the original HSCT concept. A set of parametric emissions scenarios has been developed to evaluate the sensitivity of the atmospheric perturbations to cruise altitudes by Baughcum (2002). One set of parametric scenarios in Baughcum (2002) is based on conventional routing for scheduled flights greater than 2500 nautical miles. The changes in ozone calculated with the two-dimensional model for these scenarios are presented in Table 3.

Table 3. Percentage change in Northern Hemisphere total column ozone calculated with the UIUC-2D model for eight conventional routing greater than 2500 nautical miles scenarios relative to 2020 background atmosphere for E.I.(NOx) = 10 g/kg of fuel. These results were then used in radiative forcing studies.

Fuel Burn [Mlbs/day]	E.I.(NO_x) [g/kg of fuel]	Cruise Altitudes (km)			
		13-15	15-17	17-19	19-21
73	10	0.0081	-0.0239	-0.0989	-0.1930
146	10	0.0148	-0.0525	-0.2090	-0.3930

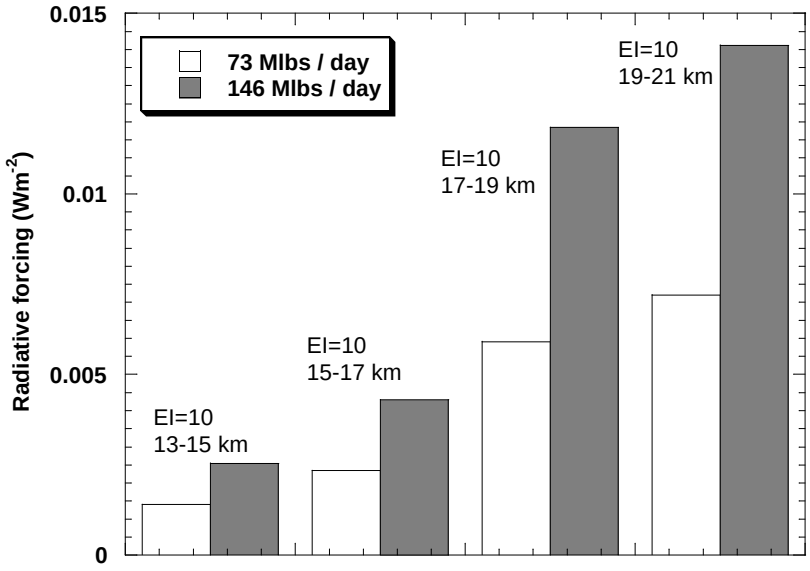

Figure 1. Annually and globally averaged radiative forcing due to water vapor perturbation, after stratospheric adjustment foreight aircraft parametric study scenarios

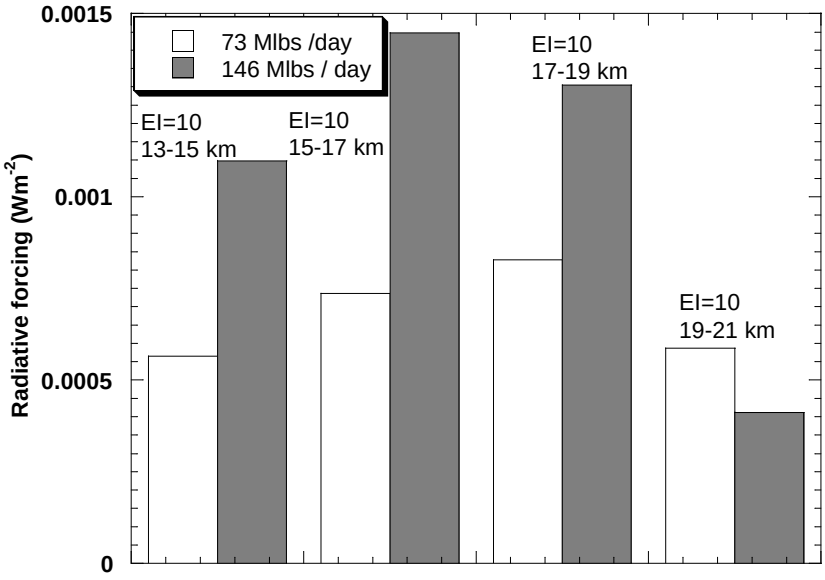

Figure 2. Annually and globally averaged radiative forcing due to ozone perturbation, after stratospheric adjustment, for eight aircraft parametric scenarios

The annually and globally averaged radiative forcing, after stratospheric adjustment, from the water vapor perturbations are shown in Figure 1, while Figure 2 shows the same for ozone perturbations from the parametric scenarios chosen. From Figure 1 we can conclude that radiative forcing of water vapor shows a linear scaling with fleet size. In Figure 2 we see that the radiative forcing increases in the lower two cruise altitude bands of 13-15 and 15-17 km, whereas it has a decreasing trend for the higher altitude bands of 17-19 and 19-21 km. In the troposphere and lower stratosphere region, ozone increases with increase in fuel burn and above the cross over point, the derived decrease in ozone gets larger with increase in fuel burn. The balance in the ozone concentration below and above the cross over point determines the net radiative forcing. Although these effects likely explain the results in the figures, we are still investigating this further. The figures also indicate that the radiative forcing impact of water vapor is much more significant than that due to ozone, which is consistent with the IPCC(1999) conclusions.

The derived radiative forcing in each of the cases is much smaller for both the ozone and the water vapor perturbations than those for the HSCT scenarios analyzed in Isaksen et al. (1999) and the first part of this study. The parametric scenarios are based on assumptions of lower fleet use than the HSCT case and most consider cruise altitudes lower than the 18-20 km altitudes projected for the HSCT. For the scenario of 13–15 km cruise altitude, E.I. (NO_x) = 10 g/kg of fuel and fuel burn of 146 Mlbs/day, the radiative forcing from water vapor perturbation is less than +0.0025 Wm^{-2} and for ozone perturbation it is less than +0.0011 Wm^{-2}.

3.3 *Sensitivity Experiment*

There have been increases in stratospheric water vapor observed in recent decades, which may have contributed significantly to both stratospheric cooling and tropospheric warming (Forster and Shine, 2002). Although our results are smaller than those from IPCC, future fleets of aircraft flying extensively in the lower stratosphere could raise radiative forcing concerns related to stratospheric water vapor increases. The recent paper by Zhong and Haigh (2003) has studied the effect of increased stratospheric water vapor on radiative forcing and compared it with five broad and multiple band radiation schemes. For testing the model sensitivity to stratospheric water vapor, we follow the experiment done by Zhong and Haigh (2003). The effective cloud cover was set to zero and the concentration of all other absorbing gases except water vapor was set to negligible amounts. Above the tropopause of the particular latitude belt, an increase of 0.7 ppmv has been imposed in the background water vapor profile. Table 4 compares the results obtained with line-by-line (LBL) reference calculations, showed in Zhong and Haigh (2003) and we see that the derived instantaneous radiative forcing from our model agrees well with their results, much better than some of the models they analysed in their study.

Table 4. Comparison of instantaneous shortwave radiative forcing (Wm-2) in our narrowband radiative transfer model due to a 0.7 ppm increase in stratospheric water vapor relative to the LBL calculation described in Zhong and Haigh (2003).

Type of Radiation Model	Solar Zenith Angle (degrees)	Radiative forcing (Wm^{-2})
LBL	30	-0.102
	70	-0.060
ISAM narrowband	30	-0.121
	70	-0.066

4 CONCLUSIONS

For the HSCT scenarios analyzed in IPCC (1999), our derived stratospheric adjusted radiative forcing for perturbations to ozone are within the range of the results presented in Chapter 6 (Prather et al., 1999) of that assessment. However, our evaluation of the radiative forcing for the water vapor perturbations from these scenarios suggests that the overall evaluation in Prather et al. (1999) may have overestimated the stratospheric adjusted radiative forcing for the water vapor changes derived from these scenarios. Additional studies are currently underway to better evaluate these differences. Results also indicate that the radiative forcing impact of the water vapor perturbation is much more significant than that due to ozone, which is consistent with the IPCC(1999) conclusions.

One of the advantages in the radiative transfer model we used in this study compared to those used in the IPCC assessment is that our radiative transfer model has higher altitude resolution near the tropopause and in the lower stratosphere. We also fully calculate the effects of seasonal variations on the derived radiative forcing, whereas one of the two models calculating the radiative forcing with stratospheric adjustment presented in IPCC (1999) used a similar approach to ours and the other used annual mean concentrations in determining the radiative forcing.

Zhong and Haigh (2003) have discussed how the typical broad-band radiation schemes underestimate the instantaneous shortwave radiative forcing due to increased stratospheric water vapor. The sensitivity analysis performed in this study indicates that the shortwave derivation for

water vapor in our radiative transfer model is not subject to this error discussed in Zhong and Haigh (2003).

REFERENCES

Baughcum, S. L., 2002: Informal Report Describing the Development of Parametric Emission Scenarios, NAS3-01140 Revolutionary Aero-Space Engine Research Task Order #5 prepared for NASA Glenn Research Center, Cleveland, pp 13.

Briegleb, B., 1992: Delta-Eddington approximation for solar radiation in the NCAR Community Climate Model. *J. Geophys. Res., 97,* 7603-7612.

Forster, P. M. deF., and K. P. Shine,2002: Assessing the climate impact of trends in stratospheric water vapour, *Geophys. Res. Lett.*, 29, doi: 10.1029/2001GL013909.

Isaksen, I., C. Jackman, S. L. Baughcum, F. Dentener, W. Grose, P. Kasibhatla, D. Kinnison, M. K. W. Ko, J. C. McConnell, G. Pitari, D. J. Wuebbles, T. Berntsen, M. Danilin, R. Eckman, E. Fleming, M. Gauss, V. Grewe, R, Harwood, D. Jacob, H. Kelder, J.-F. Muller, M. Prather, H. Rogers, R. Sausen, D. Stevenson, P. von Velthoven, M. van Weele, P. Vohralik, Y. Wang, and D. Weisenstein, 1999: Modeling the Chemical Composition of the Future Atmosphere. Chapter 4 in Intergovernmental Panel on Climate Change, *Aviation and the Global Atmosphere*. J. E. Penner, D. H. Lister, D. J. Griggs, D. J. Dokken, and M. McFarland (eds.), Cambridge University Press. Cambridge, UK.

Jain, A.K., B. P. Briegleb, K. Minschwaner, D. J. Wuebbles, 2000: Radiative forcings and global warming potentials of thirty-nine greenhouse gases. *J. Geophys. Res.*, 105, 20,773-20,790.

McDaniel, A. H., C. A. Cantrell, J. A. Davidson, R. E. Shetter, and J. G. Calvert, 1991: The temperature dependent infrared absorption cross-sections for chlorofluorocarbons: CFC-11, CFC-12, CFC-13, CFC-14, CFC-22, CFC-113, CFC-114, CFC-115. *J. Atmos. Chem*, 12, 211-227.

Ponater, M., S. Brinkop, R. Sausen, and U. Schumann, 1996: Simulating the global atmospheri cresponse to aircraft water vapour emissions and contrails – a first approach using a GCM. *Annales Geophysicae*, 14, 941-960.

Prather, M., R. Sausen, A. S. Grossman, J. M. Haywood, D. Rind, B. H. Subbaraya, P. Forster, A. Jain, M. Ponater, U. Schumann, W.-C. Wang, T. M. L. Wigley, and D. J. Wuebbles, 1999: Potential Climate Change from Aviation. Chapter 6 in Intergovernmental Panel on Climate Change, *Aviation and the Global Atmosphere*. J. E. Penner, D. H. Lister, D. J. Griggs, D. J. Dokken, and M. McFarland (eds.), Cambridge University Press. Cambridge, UK.

Rind, D., P. Lonergan, and K. Shah, climatic effects of water vapor release in the upper troposphere. *J. Geophys. Res*., 101, 29395-29406, 1996.

Rothman, L. S., et al., 1992: The HITRAN molecular database: Editions of 1991 and 1992. *J. Quant. Spectrosc. Radiat. Transfer, 48,* 469-507.

Seinfeld, J. H., Clouds, contrails, and climate. *Nature*, 391, 837-838, 1998.

Wei, C. -F., S.M.Larson, K.O. Patten and D.J. Wuebbles, 2001: Modeling of ozone reactions on aircraft-related soot in the upper troposphere and lower stratosphere. *Atmospheric Environment*, 35, 6167-6180.

Wuebbles, D.J., K. Patten, M.T. Johnson and R. Kotamarthi, 2001: New methodology for Ozone Depletion Potentials of short-lived compounds: n-Propyl bromide as an example. *J. Geophys. Res*., 106, 14,551-14,571.

Zhong, W., and J. D. Haigh, 2003: Shortwave radiative forcing by stratospheric water vapor. *Geophys. Res. Lett.*, 30, doi:10.1029/2002GL016042.

Sources of NOx at cruise altitudes: Implications for predictions of ozone and methane perturbations due to NOx from aircraft

T.K. Berntsen*, M. Gauss, I.S.A. Isaksen
Department of Geophysics, University of Oslo, Norway

V. Grewe, R. Sausen
Deutsches Zentrum für Luft- und Raumfahrt e.V. (DLR), Germany

G. Pitari, E. Mancini
University of L'Aquila (ULAQ), Italy

E. Meijer
Royal Dutch Meteorological Institute (KNMI), The Netherlands

D.Hauglustaine
Centre Nationale de la Recherche Scientifique (IPSL), France

Keywords: Aircraft emissions, Ozone, Methane, NOx emissions

ABSTRACT: The impact of NOx background levels in the upper troposphere on the predicted ozone and methane perturbations caused by NOx emissions from aircraft has been studied with five global chemical transport models (CTMs) within the EU-project TRADEOFF. The relative contribution from the different NOx sources to concentration levels at cruise altitudes varies significantly between the CTMs. The calculated ozone perturbations caused by NOx emitted by aircraft vary between 1 and 4 ppbv at northern mid-latitudes for July, due to differences in the vertical mixing in the CTMs, as well as the NOx background levels. The average reduction of the methane lifetime due to NOx from aircraft is 1.2 %/Tg(N)/yr with a range from 0.7 to 1.9. There is a tendency that the CTMs that give the largest ozone perturbations by aircraft (positive RF) give the smallest decrease in the lifetime of methane (negative RF).

1 INTRODUCTION

NOx emissions from aviation in the upper troposphere and lower stratosphere (UTLS) cause radiative forcing of climate through enhanced concentrations of ozone and reduced lifetime of methane. Assessments using global chemical tracer models (CTMs) have shown significant differences between the estimated impacts (e.g. IPCC, 1999). Due to the non-linear nature of the photochemistry of the atmosphere, the impact of additional NOx from aircraft is very dependent on the background concentrations of NOx. In this region of the atmosphere NOx can originate from a many sources, mainly from lightning, convective transport of NOx from surface sources, downward transport from the stratosphere (from N_2O oxidation), and from in–situ aircraft emissions. To improve our understanding of the possible environmental impacts of NOx emissions from aircraft, it is of key importance to be able to simulate the background NOx chemistry, which requires the calculation of the contributions of all other NOx sources.

Within the EU-project TRADEOFF we have intercompared calculations with 5 global CTMs of the contributions from the different sources to the NOx levels at cruise altitude**.** The total global NOx emissions were differentiated into the following 6 source categories: Fossil fuel combustion at the surface, biomass burning, biogenic emissions from soils, lightning, aircraft, oxidation of N_2O in the stratosphere and transport to the UTLS region. Based on a reference simulation using the emissions according to the OXCOMP intercomparison (IPCC, 2001; Prather et al., 2003; Gauss et

* *Corresponding author:* Terje Berntsen, Dept. of Geophysics, University of Oslo, P.O.Box 1022, Blindern , 0315 Oslo, Norway. Email: t.k.berntsen@cicero.uio.no

al., 2003), each CTM calculated the effects of a 10% perturbation (enhancement) of each source category (one at the time) on the chemical composition. From the results of the reference and each perturbation simulation we calculated the contributions of the total NOx emission of the considered source category, assuming that a 10% perturbation has a linear effect on the atmospheric composition. The 5 CTMs that participated in this exercise were: The TM3 model operated by KNMI (Dentener et al., 1999; Bregman et al., 2000), the OsloCTM2 model from University of Oslo (Kraabøl et al., 2002), the ULAQ model of the University of l'Aquila (Pitari et al., 1997), the LMDzINCA model from IPSL, and the ECHAM4/CHEM model run at DLR (Hein et al., 2001).

2 THE NO_x BUDGET

A rigorous evaluation of the models, by comparing the results with trace gas observations from all major research aircraft campaigns, commercial airlines, and ozone soundings in the period 1995-1998, has been reported elsewhere (Brunner et al., 2003). Here we focus on the relative contribution from the different NOx sources to the background NOx concentrations in the UTLS region. Figures 1 and 2 show the percentage contribution from lightning and fossil fuel combustion to zonally averaged NOx concentrations for July.

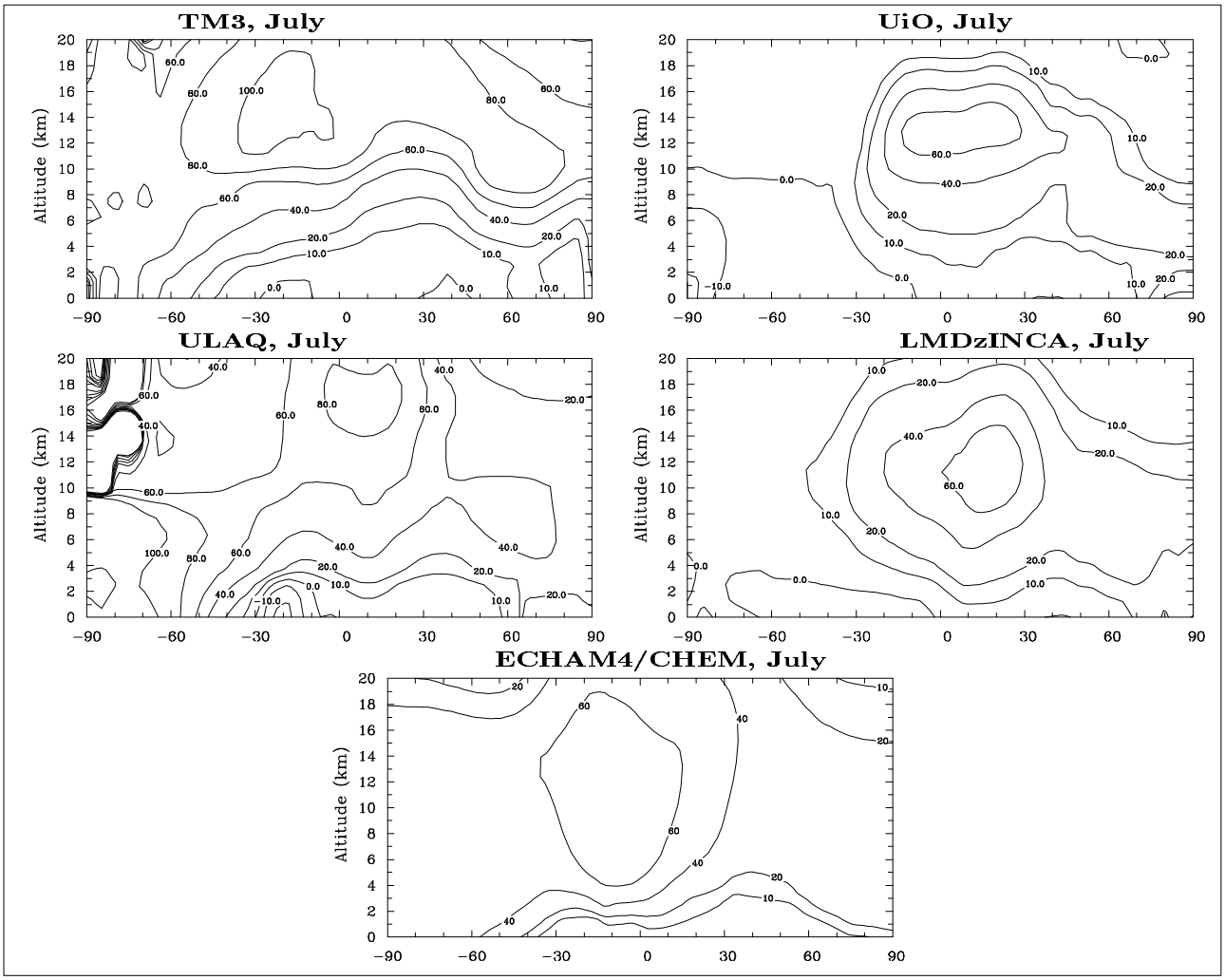

Figure 1. Contribution (%) to the zonally averaged background NOx levels by NOx from lightning (5 Tg(N)/yr in all models).

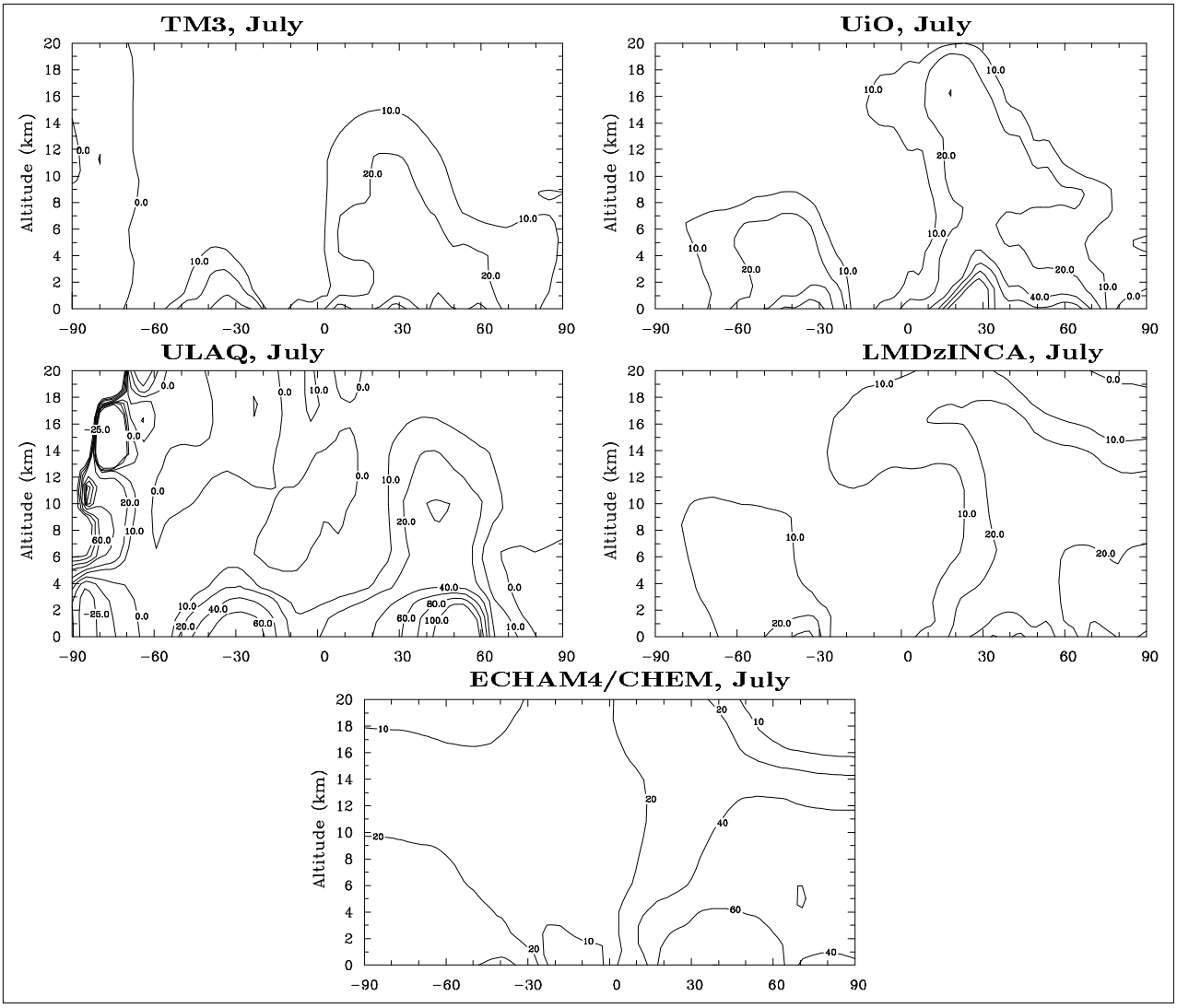

Figure 2. Contribution (%) to the zonally averaged background NOx levels by NOx from fossil fuel combustion from surface sources.

In the region with largest impact of aircraft NOx (10-12 km altitude, 45-65ºN) all CTM results for July show significant contributions from the other sources. The positioning and magnitude of the lightning emissions are linked to key parameters in the description of the convective processes (including generation of convective precipitation) in the models. The vertical lifting of NOx from ground sources depends mainly on the convective transport as the lifetime of NOx is to short for the advection to play a major role. In the TM3 model the impact of lightning extends northwards to 70ºN contributing to about 80% of the NOx levels, while in the other models the effect is mostly south of 40ºN, contribution about 30% in the aircraft region. The very high contributions in the tropical tropopause region in TM3 were recently corrected, but that correction does not affect the findings presented here. The contribution from ground based fossil fuel combustion is 20 and 45% in OsloCTM2, LMDzINCA and ECHAM4/CHEM, while in TM3 and the ULAQ models it is lower (10-20%) due to large impact of lightning in TM3 and less efficient convection in the ULAQ model. The impact of aircraft emissions itself are smallest during summer and constitutes a contribution of 10-15% in all models except in the ULAQ model where it is 50% due to less efficient vertical mixing by convection (cf. Rogers et al., 2002)

3 CHANGES IN OZONE AND METHANE LIFETIMES DUE TO NOx FROM AIRCRAFT

Figure 3 shows the ozone perturbations for July due to current subsonic aircraft emissions in the 5 CTMs. The estimate for current (2000) aircraft emissions of *0.59 Tg(N)/yr) of NOx* were used in all CTMs. Enhancements of the zonally averaged ozone concentrations in the free troposphere range from 1.3 to 5 ppbv between the 5 CTMs. All models, except the LMDzINCA model, show a maximum in the ozone perturbation in the polar regions of the northern hemisphere during July. The ULAQ model is the only one which shows a summer (July) maximum, while the other models give a maximum in late winter or spring. The summer maximum in the ULAQ model is probably related to the less efficient vertical mixing in this model by convection. This is illustrated in Figure 4 which is taken from a previous study (EU project AEROCHEM-II, Isaksen et al., (2000)) involving three of the CTMs used in TRADEOFF. The OsloCTM2 and ECHAM4/CHEM models give maximum increase in the tropospheric column of ozone at 35-45ºN in May, while the maximum in the ULAQ model is founding July over the North Pole. During summer increased convection at mid-latitudes tends to mix ozone produced at cruise altitude down to lower altitudes or even to the ground where it is lost more rapidly. Efficient vertical mixing, as indicated in the weak vertical gradient in the fossil fuel contribution to NOx (Figure 2), is probably the reason for the small ozone perturbation in LMDzINCA.

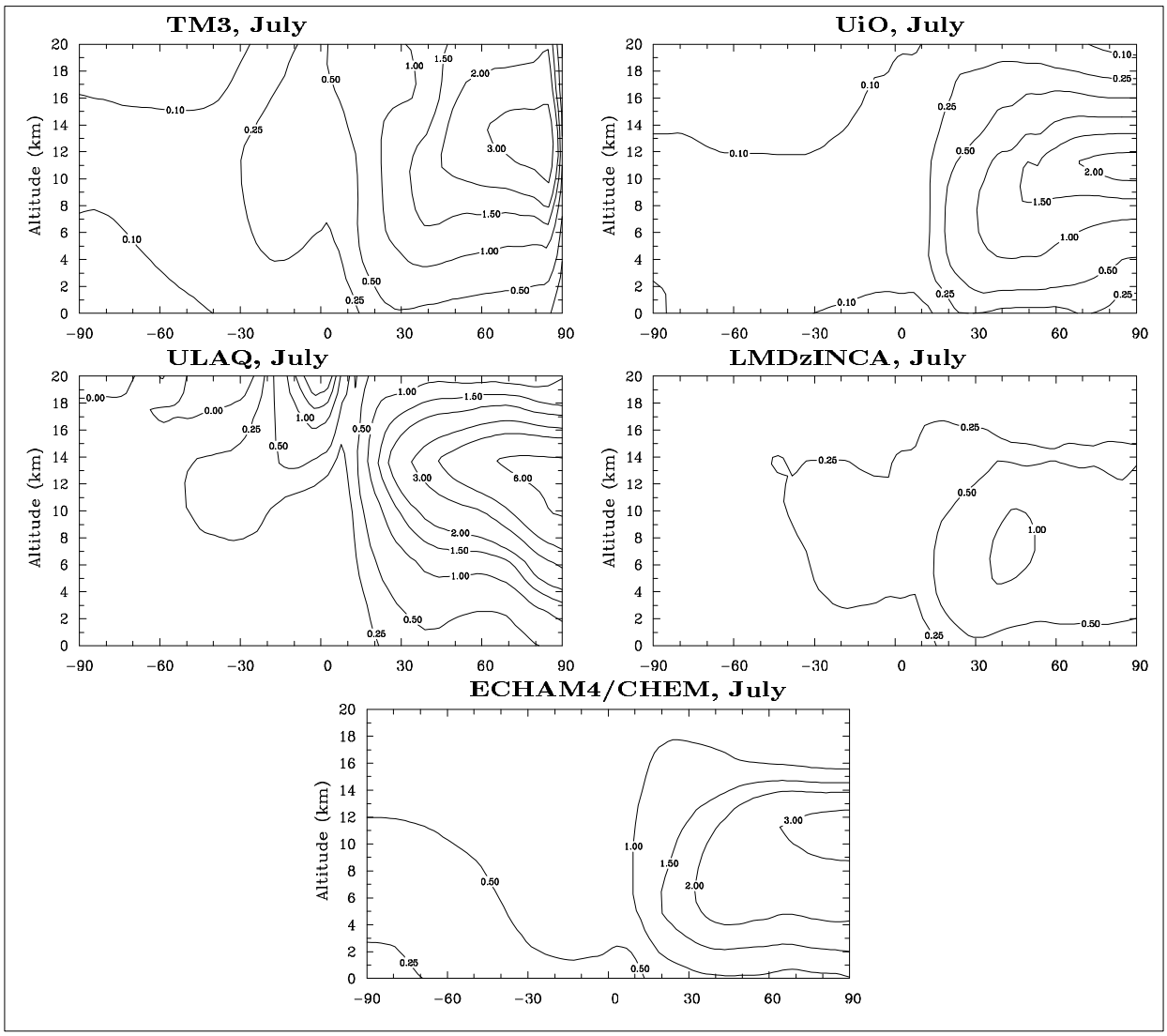

Figure 3. Zonally averaged ozone change (ppbv, July) due to aircraft emissions of NOx.

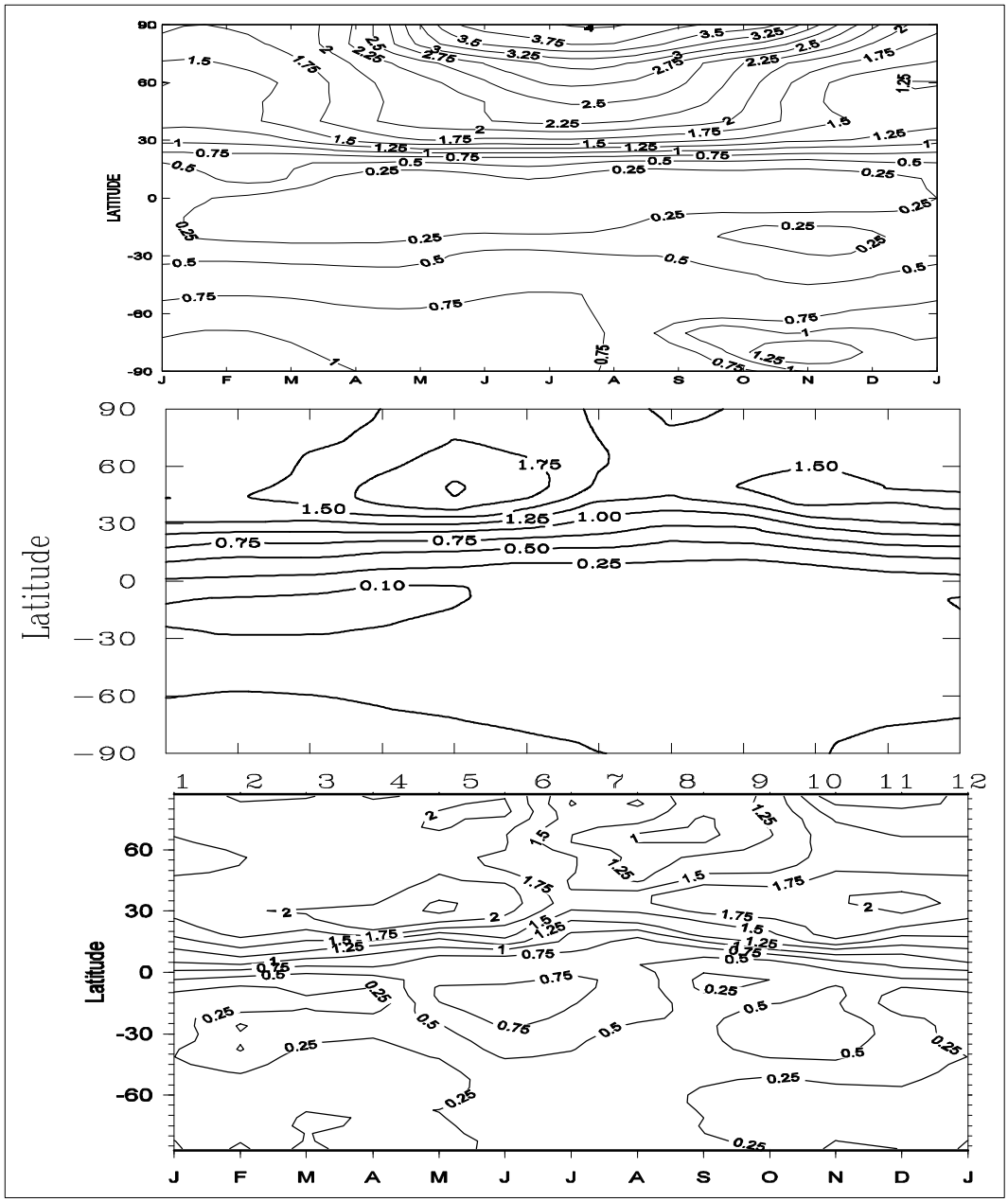

Figure 4. Zonally averaged tropospheric ozone column increase (in Dobson Units) due to 2015 aircraft emissions of NOx (1.08 Tg(N)/yr) from ULAQ (top), OsloCTM2 (middle) and ECHAM4/CHEM models (From AEROCHEM-II final report).

To study how differences in the calculated background NOx budget affect the calculated ozone perturbations, two additional model experiments with enhanced emissions from lighting and fossil fuel combustion by 30% were performed with the TM3 and UiO models. Simulations with and without aircraft emissions were performed with these enhanced NOx emissions from lightning and fossil fuels. Increasing the NOx emissions from fossil fuels by 30% reduced the maximum ozone perturbations due to aircraft by 150 pptv in both models. Increasing the NOx emissions from lightning by 30% reduced the maximum ozone perturbations due to aircraft by 600 pptv in TM3 and only 100 pptv in the UiO model. The latter experiment shows how the northerly shift in the NOx production by lightning in the TM3 model towards the main flight routes enhances the background NOx concentrations and thereby lowers ozone production efficiency of the additional NOx from aircraft.

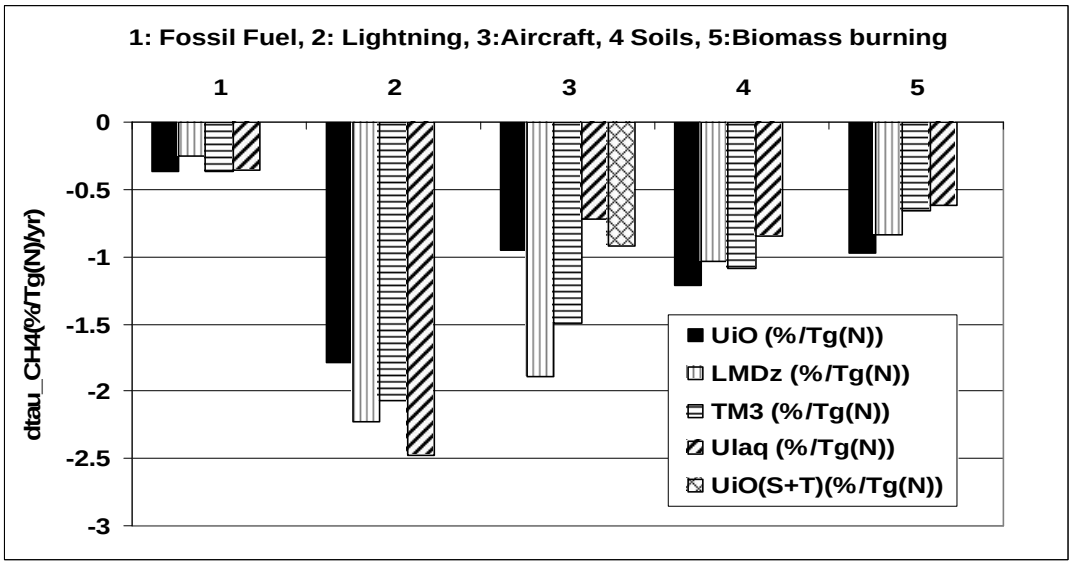

Figure 5. Sensitivity of the methane lifetime due to perturbations of various NOx sources. The figure shows the relative change in the lifetime of methane normalized to the perturbations (+10%) of each of the NOx sources. The OsloCTM2 model is denoted UiO in the figure. UiO (S+T) denotes the extended version of the UiO model including both the troposphere and stratosphere.

Emissions of NOx from aircraft also lead to changes in the lifetime of methane. Concentrations of the hydroxyl radiacl (OH) increase and thus the lifetime of methane in the atmosphere is reduced through:

- Increased ozone giving OH through $O_3 + h\nu \rightarrow O(^1D) + O_2$ and $O(^1D) + H_2O \rightarrow 2OH$
- $NO + HO_2 \rightarrow NO_2 + OH$
- Interaction with CO perturbations at cruise levels and transport of the signal to low altitudes and latitudes (IPCC, 1999)

The CTM results show consistently that per mass unit emission of NOx, lightning has the largest impact on the methane lifetime, and fossil fuel (FF) emissions have the least. Lightning occurs in regions with low background NOx levels and consequently the impact on OH is much larger than for fossil fuel emissions that occur mainly in high background NOx regions at mid-latitudes. The aircraft source has the second largest impact in the LMDzINCA and TM3 models, while in the OsloCTM2 and ULAQ models the impact of aircraft is about equal to the impact of NOx from soils and biomass burning. However, the difference between the models is significantly larger for aircraft, indicating that perturbations in the UTLS region are particularly difficult to model since there is such a close interaction between chemistry and transport in this region of the atmosphere. There is a tendency that the CTMs that give the largest ozone perturbations by aircraft (positive RF) give the smallest decrease in the lifetime of methane (negative RF). This is an important observation since the radiative impact is a net effect of a positive contribution from ozone and a negative contribution from methane. This can be explained by the fact that little vertical mixing keeps the pollutants (NOx and ozone) aloft, while the reduction of the lifetime of methane is believed to be caused by transport of a CO signal to lower altitudes.

4 CONCLUSIONS

The contribution to the tropospheric NOx contributions from 6 different NOx source categories has been studied with 5 global chemistry transport models. Although all models give a reasonable representation of the observed NOx concentrations in the UTLS region (Brunner et al., 2003) there are significant differences in the relative contribution from the different NOx sources in the this region of the atmosphere. This is particularly pronounced at northern mid-latitudes, which is most important with respect to the impacts of aircraft, due to the importance of convective lifting of the

large surface emissions from fossil fuel combustion. The calculated ozone perturbations caused by NOx emitted by aircraft vary between 1 and 4 ppbv at northern mid-latitudes for July, due to differences in the vertical mixing in the CTMs, as well as the NOx background levels. The average reduction of the methane lifetime due to NOx from aircraft is 1.2 %/Tg(N)/yr with a range from 0.7 to 1.9. An important finding is that there is a tendency that the CTMs that give the largest ozone perturbations by aircraft (causing positive RF) give the smallest decrease in the lifetime of methane (negative RF), probably due to less efficient vertical mixing in these models. Since the net RF caused by aircraft through ozone and methane perturbations is the difference between two numbers of similar magnitude, this impact of vertical mixing will give a much larger inter model variability in the net effect than in the ozone or methane effects separately.

ACKNOWLEDGEMENT

This work has been supported by the European Community grant (TRADEOFF, contract no. EVK2-1999-00030)

REFERENCES

Bregman B. et al., 2000: The N_2O and ozone relationship in the lowermost stratosphere: diagnostic for mixing processes as represented by a three dimensional model, *J. Geophys. Res, 105*, 17,279, 17,290.

Brunner, D., J. Staehelin, H.L. Rogers, M.O. Köhler, J.A. Pyle, D. Hauglustaine, L. Jourdain, T.K. Berntsen, M. Gauss, I.S.A. Isaksen. E. Meijer, P. van Velthoven, G. Pitari, E. Mancini, V. Grewe, and R. Sausen, 2003: An evaluation of the performance of chemistry transport models by comparison with research aircraft observations. Part 1: Concepts and overall model performance. *Atmos. Chem. Phys. Discuss. 3*, 2499-2545.

Dentener F., H. Feicter, and A Jueken, 1999: Simulations of the transport of Rn222 using on-line and off-line global models at different horizontal resolutions: a detailed comparison with measurements, *Tellus, 51*, 573-602.

Gauss, M., G. Myhre, G. Pitari, M. J. Prather, I. S. A. Isaksen, T. K. Berntsen, G. P. Brasseur, F. J. Dentener, R. G. Derwent, D. A. Hauglustaine, L. W. Horowitz, D. J. Jacob, M. Johnson, K. S. Law, L. J. Mickley, J.-F. Müller, P.-H. Plantevin, J. A. Pyle, H. L. Rogers, D. S. Stevenson, J. K. Sundet, M. van Weele, O. Wild, 2003: Radiative forcing in the 21st century due to ozone changes in the troposphere and the lower stratosphere, *.J. Geophys. Res., 108***,** 4292, doi:10.1029/2002JD002624.

Hein R., Dameris, M., Grewe, V., Schnadt, C., Steil, B., and Landgraf, J., 2001: Results of an interactively coupled atmospheric chemistry - general circulation model: Comparison with observations, *Ann. Geophysicae, 19*,435-457.

IPCC, 1999: Aviation and the global atmosphere, Ed. by J.E. Penner, D.H. Lister, D.J. Griggs, D.J. Dokken, and M. McFarland. Cambridge University Press, New York. pp. 373.

Isaksen I.S.A. (Ed.) 2000. AEROCHEM-II, Modelling of the impact on ozone and other chemical compounds in the atmosphere from airplane emissions, May 1998-April 1999, Final Report, Contract No. ENV4-CT97-0621.

Kraabøl A.G., F. Stordal, T. Berntsen, and J. Sundet. 2002: Impacts of NOx emissions from subsonic aircraft in a global 3-D CTM including plume processes. *J. Geophys. Res.*, 10.1029/2001JD001019.

Pitari G., B. Grassi, and G. Visconti, 1997: Results of a chemical transport model with interactive aerosol microphysics, *R.D. Bojkov and G. Visconti. Eds., XVIII Ozone symp. proc*., 759-763.

Prather, M., M. Gauss, T. Berntsen, I. Isaksen, J. Sundet, I. Bey, G. Brasseur, F. Dentener, R. Derwent, D. Stevenson; P.I. Grenfell, D. Lee; D. Hauglustaine, L. Horowitz, D. Jacob, L. Mickley, M. Lawrence, R. von Kuhlmann, J.-F. Muller, G. Pitari, H. Rogers, M. Johnson, J. Pyle, K. Law, M. van Weele, O. Wild, 2003: Fresh air in the 21st century?, *Geophys. Res. Lett*. **30(2),** 1100, 10.1029/2002GL016285.

Rogers, H., H. Teyssedre, G. Pitari, V. Grewe, P. van Velthoven, and J. Sundet, 2002: Model intercomparison of the transport of aircraft-like emissions from sub- and supersonic aircraft, *Met. Z., 11*, 151-161.